SUPPLEMENTARY INFORMATION

Spatially resolved gene expression profiling of tumor microenvironment reveals key steps of lung adenocarcinoma development

Yuma Takano, Jun Suzuki, Kotaro Nomura, Gento Fujii, Junko Zenkoh, Hitomi Kawai, Yuta Kuze, Yukie Kashima, Satoi Nagasawa, Yuka Nakamura, Motohiro Kojima, Katsuya Tsuchihara, Masahide Seki, Akinori Kanai, Daisuke Matsubara, Takashi Kohno, Masayuki Noguchi, Akihiro Nakaya, Masahiro Tsuboi, Genichiro Ishii, Yutaka Suzuki*, Ayako Suzuki*

*To whom correspondence should be addressed;
Yutaka Suzuki; Tel.: +81 4 7136 4076; Email: ysuzuki@edu.k.u-tokyo.ac.jp
Ayako Suzuki; Tel.: +81 4 7136 4076; Email: asuzuki@edu.k.u-tokyo.ac.jp

Contents:
Supplementary Figures S1–S17 (p. 2–91)
Supplementary Tables S1–S8 (p. 92–103)
Supplementary References (p. 104)

Supplementary Figures

Supplementary Figure S1

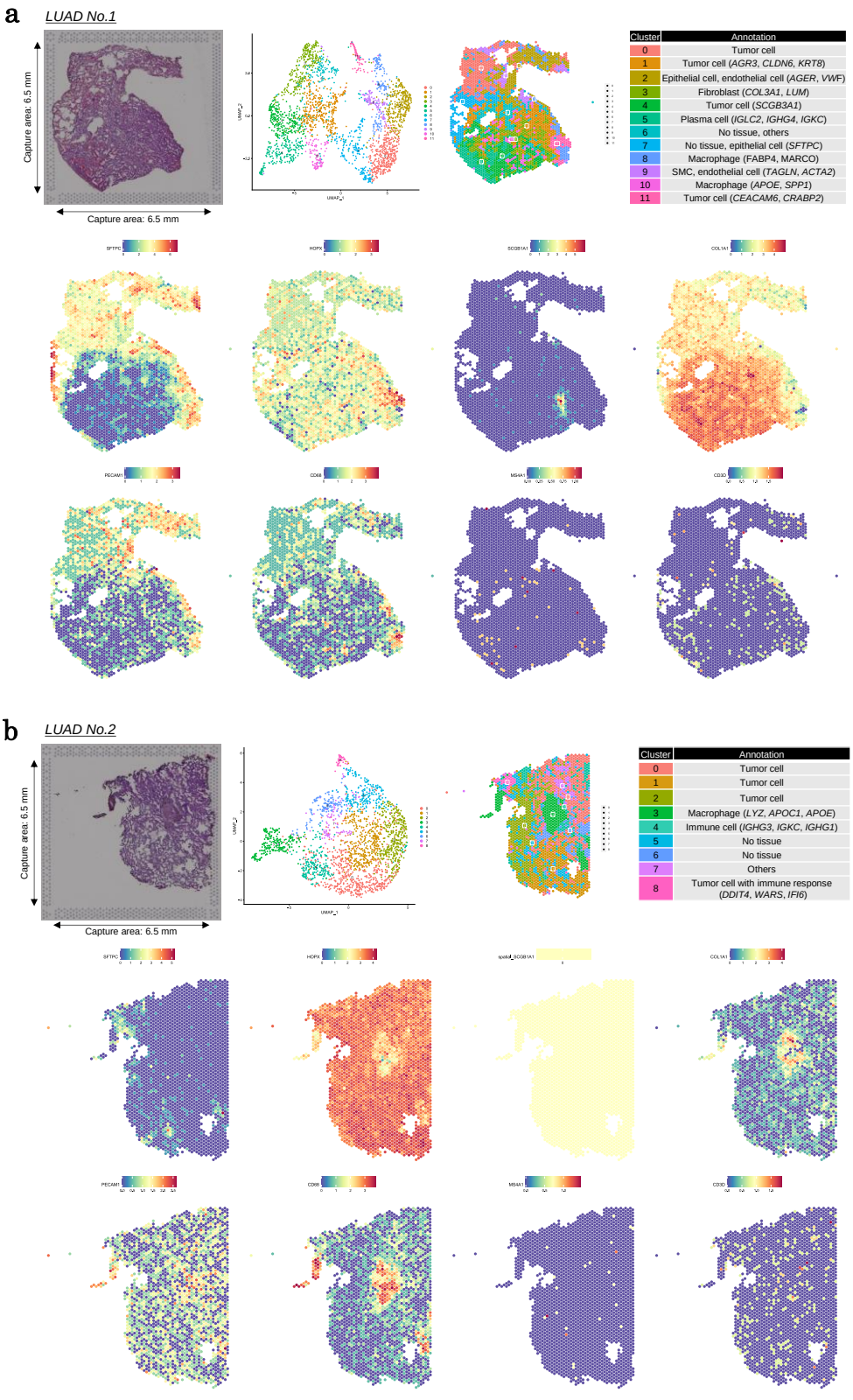

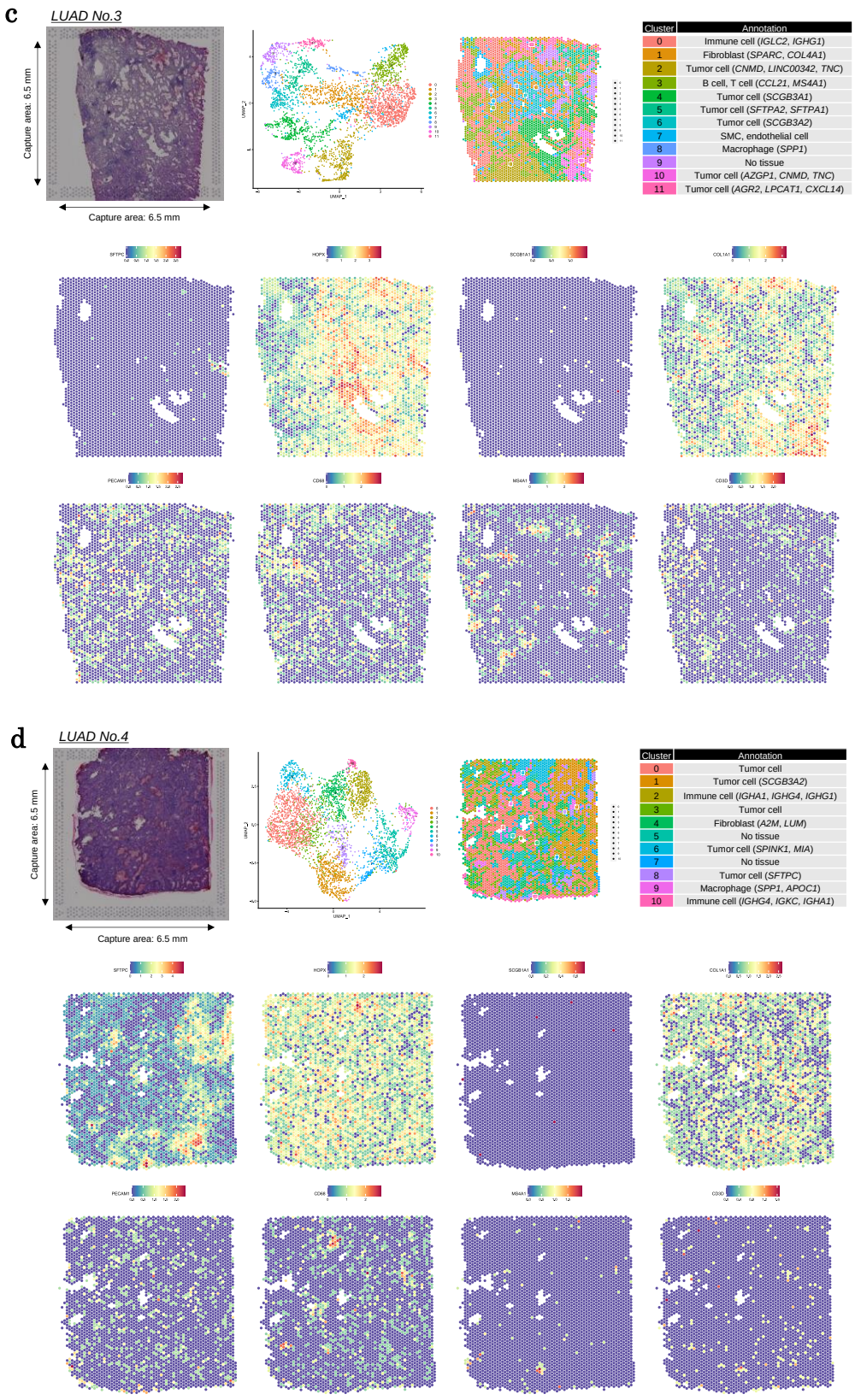
c
LUAD No.3
Capture area: 6.5 mm
Capture area: 6.5 mm
Cluster
Annotation
0 Immune cell (IGLC2, IGHG1)
1 Fibroblast (SPARC, COL4A1)
2 Tumor cell (CNMD, LINC00342, TNC)
3 B cell, T cell (CCL21, MS4A1)
4 Tumor cell (SCGB3A1)
5 Tumor cell (SFTPA2, SFTPA1)
6 Tumor cell (SCGB3A2)
7 SMC, endothelial cell
8 Macrophage (SPP1)
9 No tissue
10 Tumor cell (AZGP1, CNMD, TNC)
11 Tumor cell (AGR2, LPCAT1, CXCL14)
d
LUAD No.4
Capture area: 6.5 mm
Capture area: 6.5 mm
Cluster
Annotation
0 Tumor cell
1 Tumor cell (SCGB3A2)
2 Immune cell (IGHA1, IGHG4, IGHG1)
3 Tumor cell
4 Fibroblast (A2M, LUM)
5 No tissue
6 Tumor cell (SPINK1, MIA)
7 No tissue
8 Tumor cell (SFTPC)
9 Macrophage (SPP1, APOC1)
10 Immune cell (IGHG4, IGKC, IGHA1)

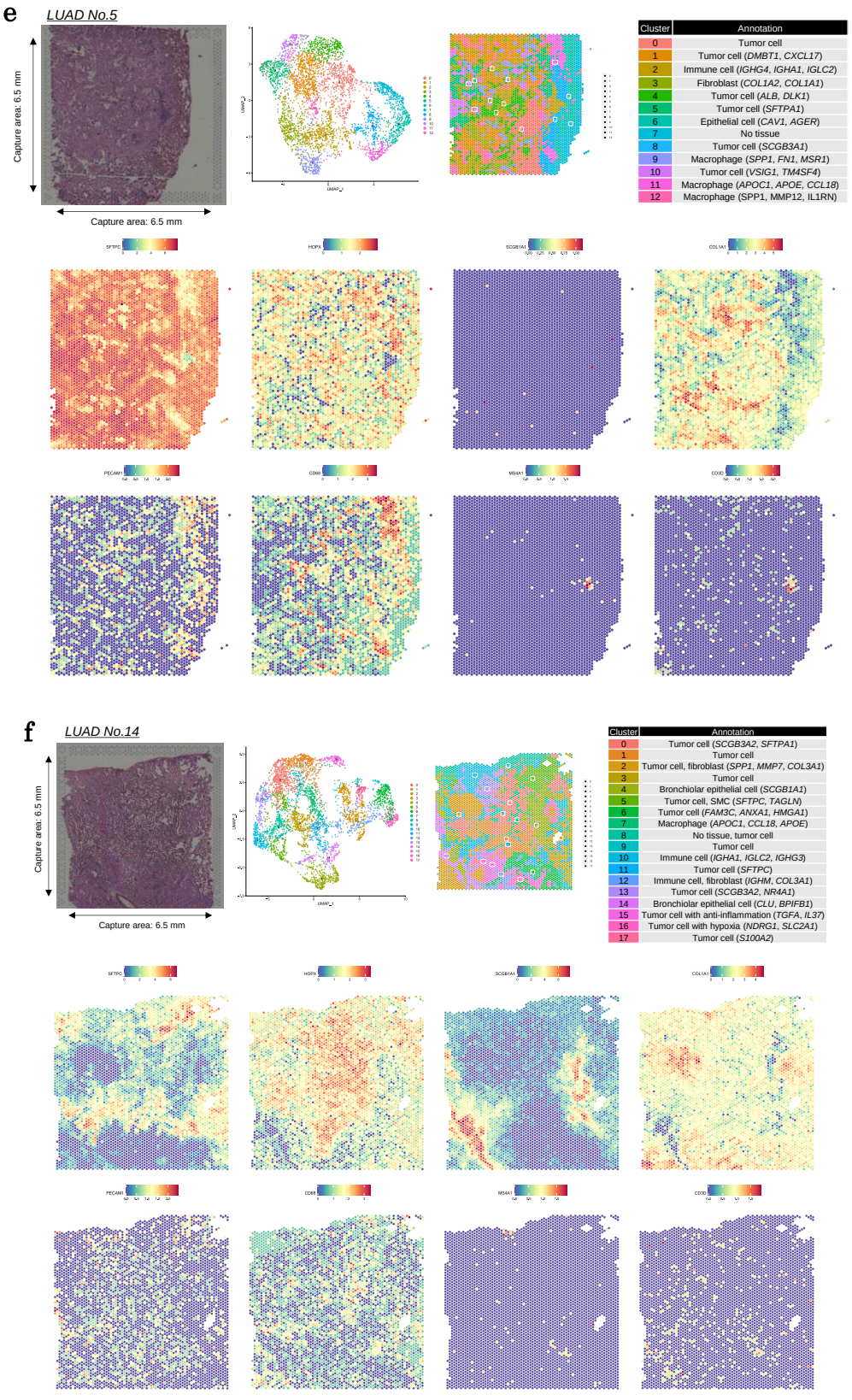
e
LUAD No.5
Capture area: 6.5 mm
Capture area: 6.5 mm
Cluster
Annotation
0 Tumor cell
1 Tumor cell (DMBT1, CXCL17)
2 Immune cell (IGHG4, IGHA1, IGLC2)
3 Fibroblast (COL1A2, COL1A1)
4 Tumor cell (ALB, DLK1)
5 Tumor cell (SFTPA1)
6 Epithelial cell (CAV1, AGER)
7 No tissue
8 Tumor cell (SCGB3A1)
9 Macrophage (SPP1, FN1, MSR1)
10 Tumor cell (VSIG1, TM4SF4)
11 Macrophage (APOC1, APOE, CCL18)
12 Macrophage (SPP1, MMP12, IL1RN)
f
LUAD No.14
Capture area: 6.5 mm
Capture area: 6.5 mm
Cluster
Annotation
0 Tumor cell (SCGB3A2, SFTPA1)
1 Tumor cell
2 Tumor cell, fibroblast (SPP1, MMP7, COL3A1)
3 Tumor cell
4 Bronchiolar epithelial cell (SCGB1A1)
5 Tumor cell, SMC (SFTPC, TAGLN)
6 Tumor cell (FAM3C, ANXA1, HMGA1)
7 Macrophage (APOC1, CCL18, APOE)
8 No tissue, tumor cell
9 Tumor cell
10 Immune cell (IGHA1, IGLC2, IGHG3)
11 Tumor cell (SFTPC)
12 Immune cell, fibroblast (IGHM, COL3A1)
13 Tumor cell (SCGB3A2, NR4A1)
14 Bronchiolar epithelial cell (CLU, BPIFB1)
15 Tumor cell with anti-inflammation (TGFA, IL37)
16 Tumor cell with hypoxia (NDRG1, SLC2A1)
17 Tumor cell (S100A2)

g *LUAD No.16*

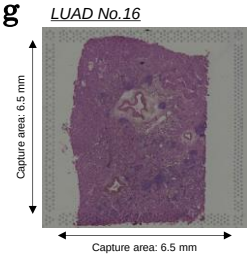

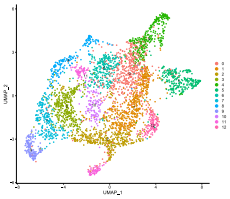

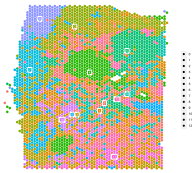

Cluster	Annotation
0	Tumor cell
1	Immune cell (*IGHG1*, *IGKC*, *IGHG4*)
2	Fibroblast (*COL3A1*, *LUM*, *SPARC*)
3	Tumor cell
4	SMC (*MALAT1*, *MYL9*, *ACTA2*)
5	Bronchiolar epithelial cell (*SCGB1A1*)
6	No tissue
7	Tumor cell (*MUC21*, *TFPI2*, *S100A6*)
8	Macrophage (*APOC1*, *APOE*, *LYZ*)
9	Tumor cell (*SFTPB*)
10	Tumor cell, fibroblast (*SPP1*)
11	Tumor cell (*SFTPA1*, *SFTPB*)
12	T cell, B cell (*CCL19*, *TRAC*, *TRBC2*)

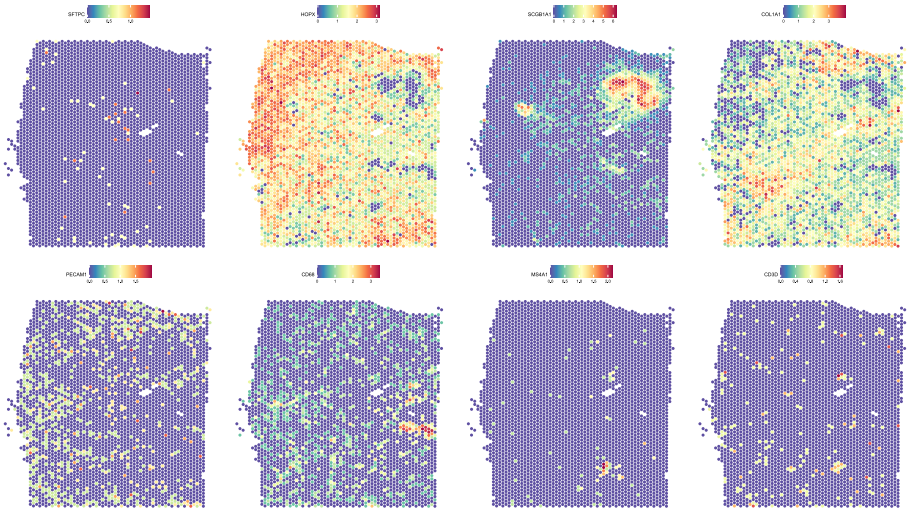

h *LUAD No.17*

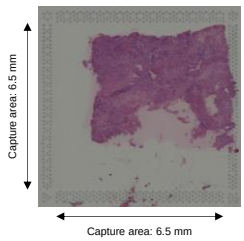

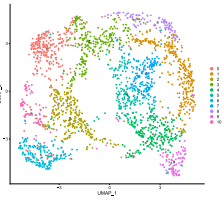

Cluster	Annotation
0	Tumor cell, no tissue
1	Fibroblast (*SFRP4*, *LUM*, *THBS1*)
2	Tumor cell (*SFTPA2*, *UPK3BL1*, *LCN2*)
3	Macrophage (*SPP1*, *MMP12*)
4	Immune cell (*IGHG4*, *IGHG3*)
5	Fibroblast (*MGP*, *A2M*)
6	Tumor cell (*SCGB3A2*, *SLC34A2*)
7	Fibroblast (*COL4A1*, *COL4A2*)
8	Fibroblast (*MMP11*, *COL11A1*)
9	Macrophage (*APOC1*, *APOE*)
10	Tumor cell (*S100A9*, *S100A8*)

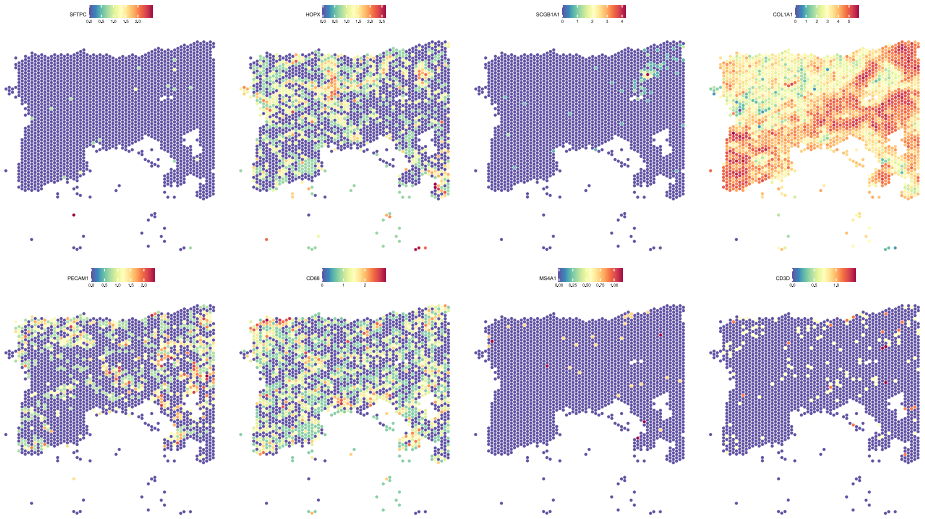

i *LUAD No.2 FFPE, A*

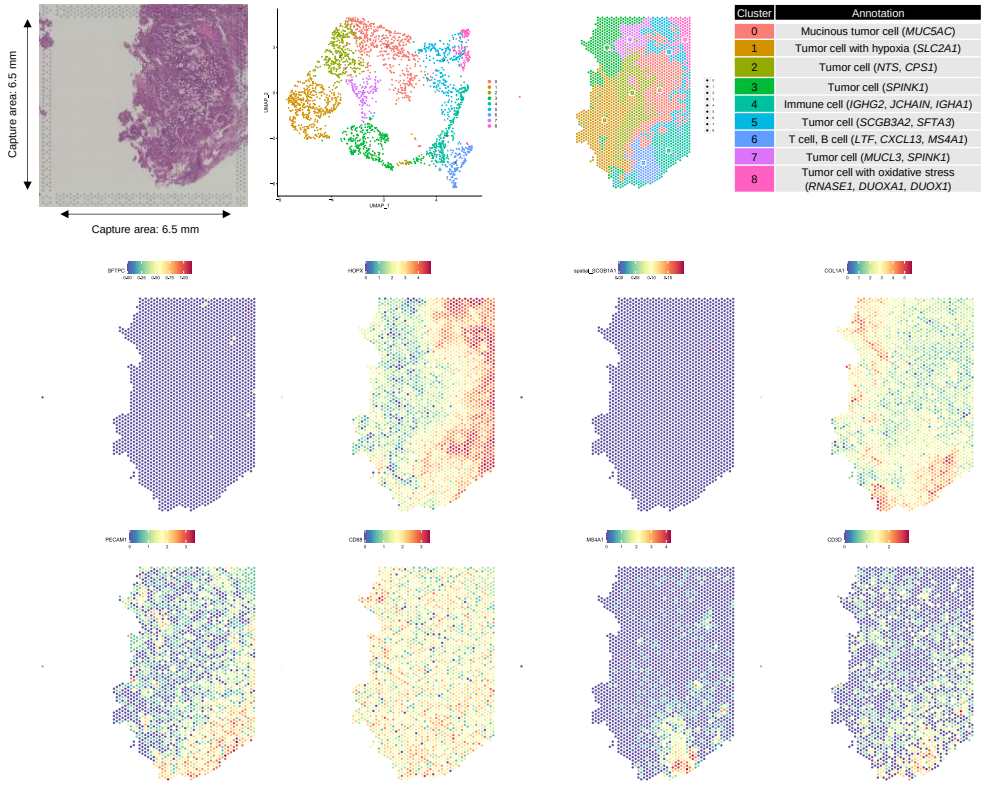

Cluster	Annotation
0	Mucinous tumor cell (*MUC5AC*)
1	Tumor cell with hypoxia (*SLC2A1*)
2	Tumor cell (*NTS*, *CPS1*)
3	Tumor cell (*SPINK1*)
4	Immune cell (*IGHG2*, *JCHAIN*, *IGHA1*)
5	Tumor cell (*SCGB3A2*, *SFTA3*)
6	T cell, B cell (*LTF*, *CXCL13*, *MS4A1*)
7	Tumor cell (*MUCL3*, *SPINK1*)
8	Tumor cell with oxidative stress (*RNASE1*, *DUOXA1*, *DUOX1*)

j *LUAD No.2 FFPE, B*

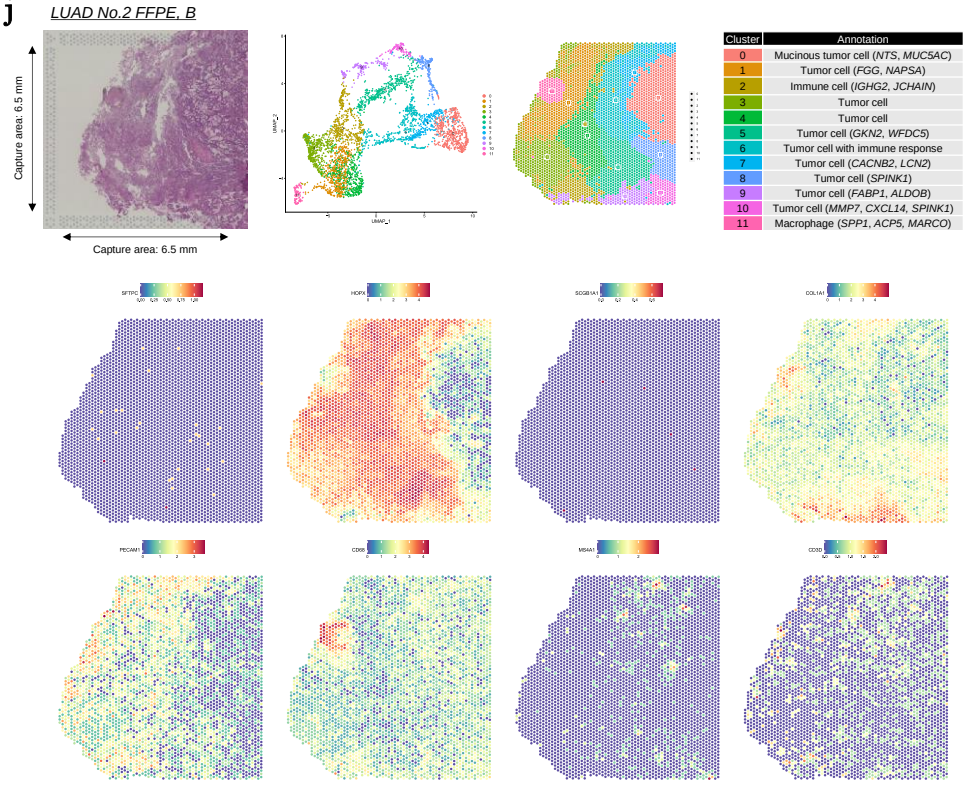

Cluster	Annotation
0	Mucinous tumor cell (*NTS*, *MUC5AC*)
1	Tumor cell (*FGG*, *NAPSA*)
2	Immune cell (*IGHG2*, *JCHAIN*)
3	Tumor cell
4	Tumor cell
5	Tumor cell (*GKN2*, *WFDC5*)
6	Tumor cell with immune response
7	Tumor cell (*CACNB2*, *LCN2*)
8	Tumor cell (*SPINK1*)
9	Tumor cell (*FABP1*, *ALDOB*)
10	Tumor cell (*MMP7*, *CXCL14*, *SPINK1*)
11	Macrophage (*SPP1*, *ACP5*, *MARCO*)

k *LUAD No.2 FFPE, C*

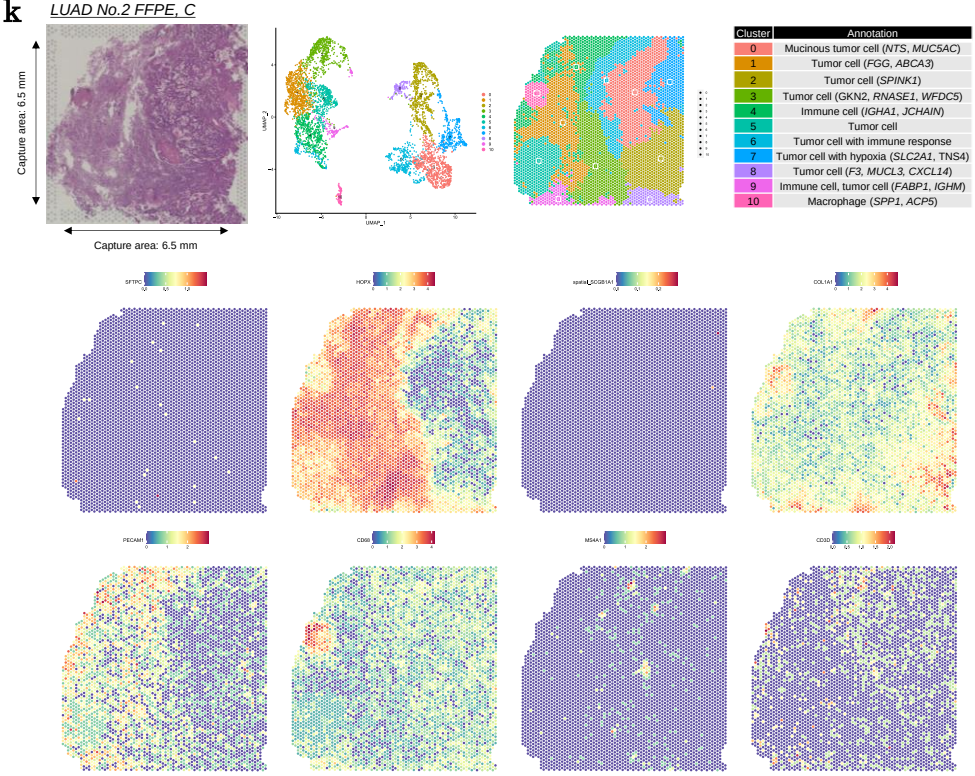

Cluster	Annotation
0	Mucinous tumor cell (*NTS*, *MUC5AC*)
1	Tumor cell (*FGG*, *ABCA3*)
2	Tumor cell (*SPINK1*)
3	Tumor cell (GKN2, *RNASE1*, *WFDC5*)
4	Immune cell (*IGHA1*, *JCHAIN*)
5	Tumor cell
6	Tumor cell with immune response
7	Tumor cell with hypoxia (*SLC2A1*, TNS4)
8	Tumor cell (*F3*, *MUCL3*, *CXCL14*)
9	Immune cell, tumor cell (*FABP1*, *IGHM*)
10	Macrophage (*SPP1*, *ACP5*)

l *LUAD No.2 FFPE, D*

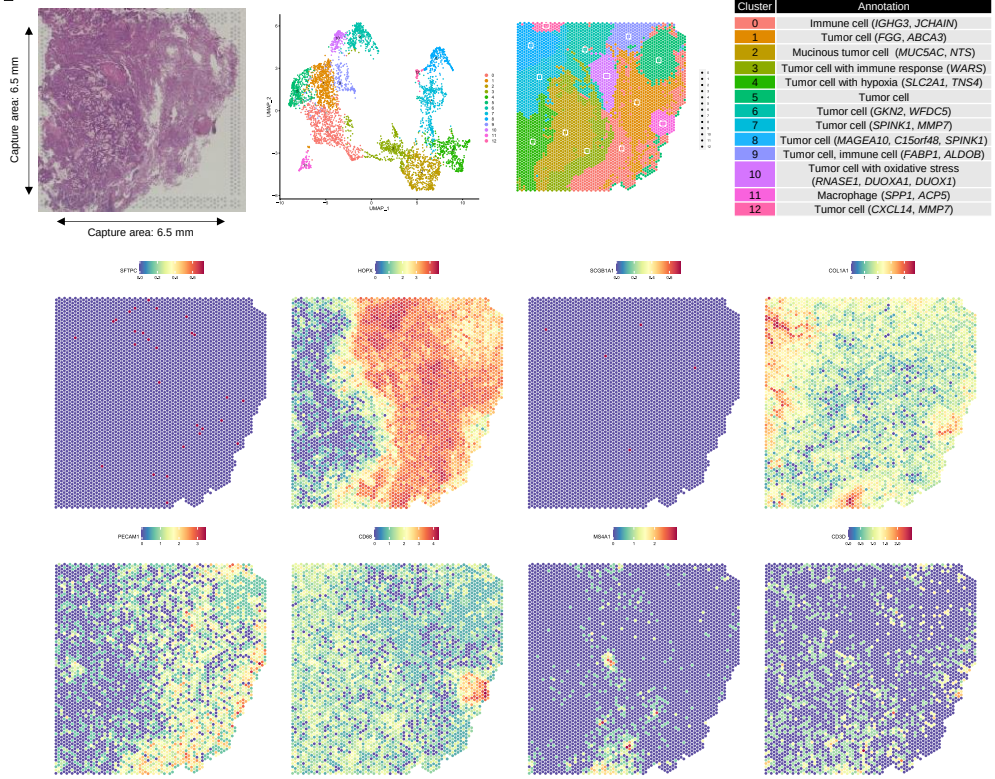

Cluster	Annotation
0	Immune cell (*IGHG3*, *JCHAIN*)
1	Tumor cell (*FGG*, *ABCA3*)
2	Mucinous tumor cell (*MUC5AC*, *NTS*)
3	Tumor cell with immune response (*WARS*)
4	Tumor cell with hypoxia (*SLC2A1*, *TNS4*)
5	Tumor cell
6	Tumor cell (*GKN2*, *WFDC5*)
7	Tumor cell (*SPINK1*, *MMP7*)
8	Tumor cell (*MAGEA10*, *C15orf48*, *SPINK1*)
9	Tumor cell, immune cell (*FABP1*, *ALDOB*)
10	Tumor cell with oxidative stress (*RNASE1*, *DUOXA1*, *DUOX1*)
11	Macrophage (*SPP1*, *ACP5*)
12	Tumor cell (*CXCL14*, *MMP7*)

m *LUAD No.3 FFPE, A*

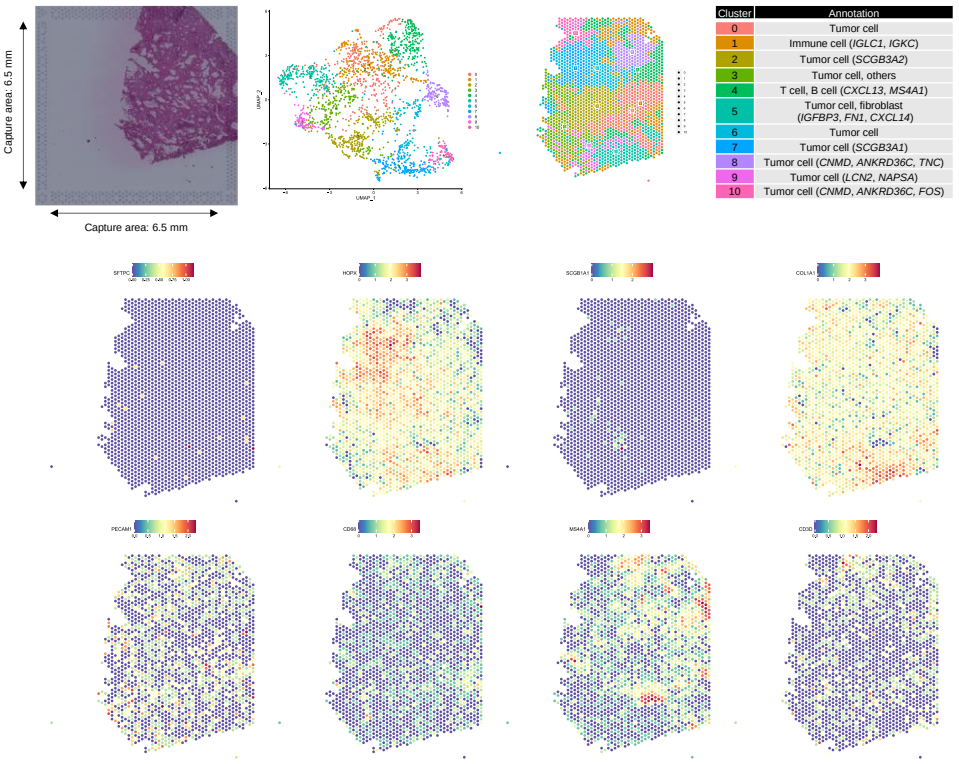

Cluster	Annotation
0	Tumor cell
1	Immune cell (*IGLC1*, *IGKC*)
2	Tumor cell (*SCGB3A2*)
3	Tumor cell, others
4	T cell, B cell (*CXCL13*, *MS4A1*)
5	Tumor cell, fibroblast (*IGFBP3*, *FN1*, *CXCL14*)
6	Tumor cell
7	Tumor cell (*SCGB3A1*)
8	Tumor cell (*CNMD*, *ANKRD36C*, *TNC*)
9	Tumor cell (*LCN2*, *NAPSA*)
10	Tumor cell (*CNMD*, *ANKRD36C*, *FOS*)

n *LUAD No.3 FFPE, B*

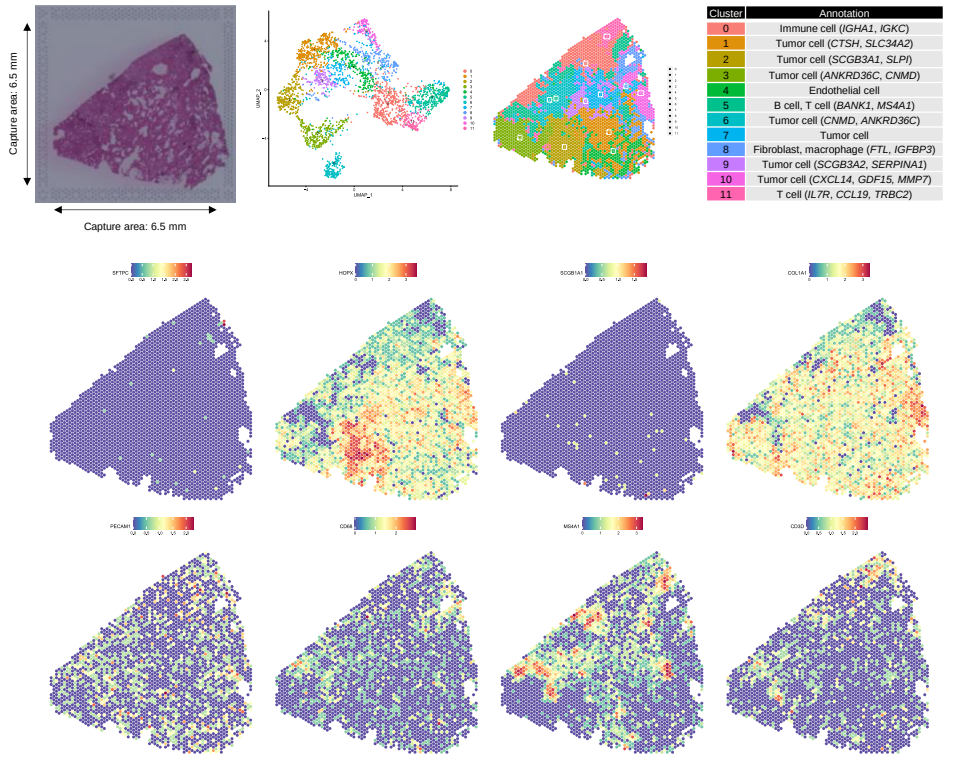

Cluster	Annotation
0	Immune cell (*IGHA1*, *IGKC*)
1	Tumor cell (*CTSH*, *SLC34A2*)
2	Tumor cell (*SCGB3A1*, *SLPI*)
3	Tumor cell (*ANKRD36C*, *CNMD*)
4	Endothelial cell
5	B cell, T cell (*BANK1*, *MS4A1*)
6	Tumor cell (*CNMD*, *ANKRD36C*)
7	Tumor cell
8	Fibroblast, macrophage (*FTL*, *IGFBP3*)
9	Tumor cell (*SCGB3A2*, *SERPINA1*)
10	Tumor cell (*CXCL14*, *GDF15*, *MMP7*)
11	T cell (*IL7R*, *CCL19*, *TRBC2*)

o *LUAD No.4 FFPE, C*

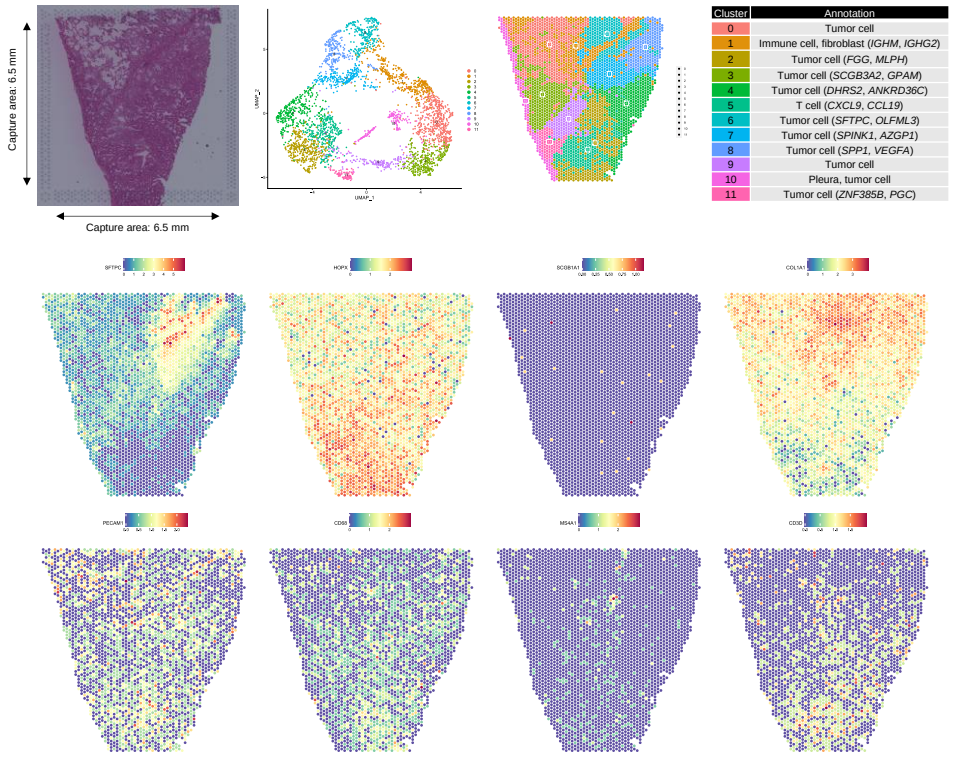

Cluster	Annotation
0	Tumor cell
1	Immune cell, fibroblast (*IGHM*, *IGHG2*)
2	Tumor cell (*FGG*, *MLPH*)
3	Tumor cell (*SCGB3A2*, *GPAM*)
4	Tumor cell (*DHRS2*, *ANKRD36C*)
5	T cell (*CXCL9*, *CCL19*)
6	Tumor cell (*SFTPC*, *OLFML3*)
7	Tumor cell (*SPINK1*, *AZGP1*)
8	Tumor cell (*SPP1*, *VEGFA*)
9	Tumor cell
10	Pleura, tumor cell
11	Tumor cell (*ZNF385B*, *PGC*)

p *LUAD No.4 FFPE, D*

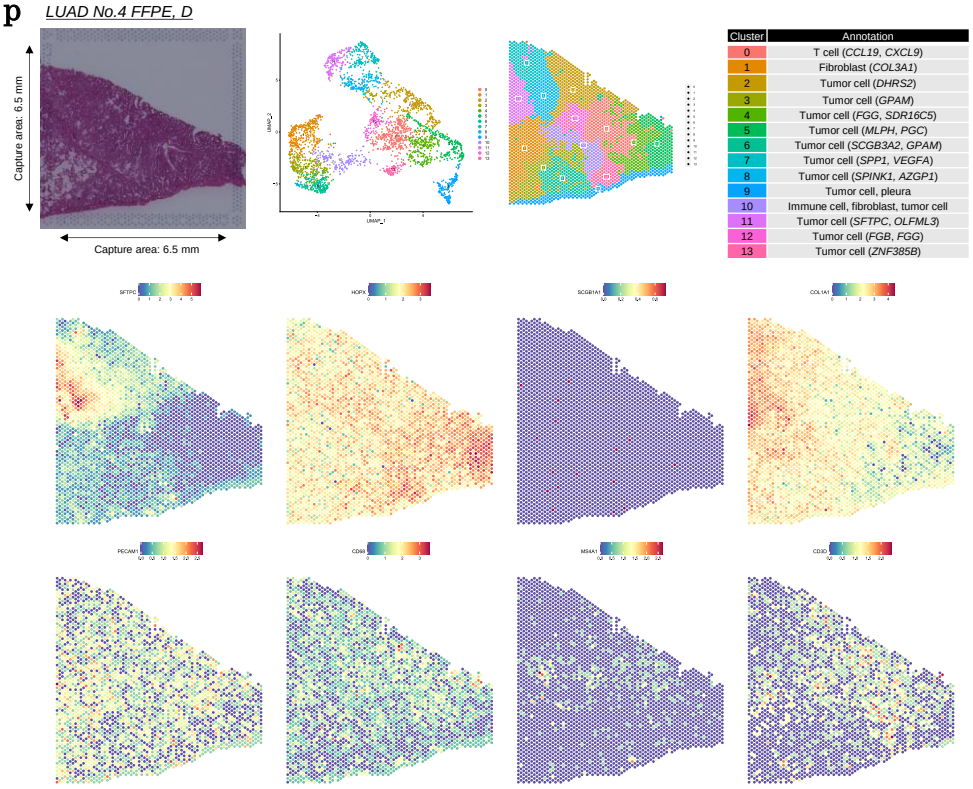

Cluster	Annotation
0	T cell (*CCL19*, *CXCL9*)
1	Fibroblast (*COL3A1*)
2	Tumor cell (*DHRS2*)
3	Tumor cell (*GPAM*)
4	Tumor cell (*FGG*, *SDR16C5*)
5	Tumor cell (*MLPH*, *PGC*)
6	Tumor cell (*SCGB3A2*, *GPAM*)
7	Tumor cell (*SPP1*, *VEGFA*)
8	Tumor cell (*SPINK1*, *AZGP1*)
9	Tumor cell, pleura
10	Immune cell, fibroblast, tumor cell
11	Tumor cell (*SFTPC*, *OLFML3*)
12	Tumor cell (*FGB*, *FGG*)
13	Tumor cell (*ZNF385B*)

Supplementary Figure S1 H&E images and results of clustering analysis of Visium data in eight invasive adenocarcinoma (IA) cases

(**a–h**) Visium analysis of fresh frozen (FF) samples from LUAD cases (No. 1–5, 14, 16, and 17). Upper panel: H&E image, clustering analysis results (UMAP and spatial plots), and annotation of each cluster are presented in the right, middle, and left panels, respectively. The capture area that is surrounded by the fiducial frame in the H&E image is 6.5 mm × 6.5 mm. Lower panel: expression patterns of representative cell type marker genes are shown in the spatial plot. (**i–l**) Visium analysis of formalin-fixed paraffin-embedded (FFPE) samples from LUAD No. 2; sections A–D are provided. The result of clustering analysis in LUAD No.2 FFPE section C is shown in **Figure 2**. (**m–p**) Visium analysis of FFPE samples from LUAD No. 3 and 4; sections A–D are presented. The result of clustering analysis from LUAD No. 3 FFPE section B is also shown in **Figure 3**.

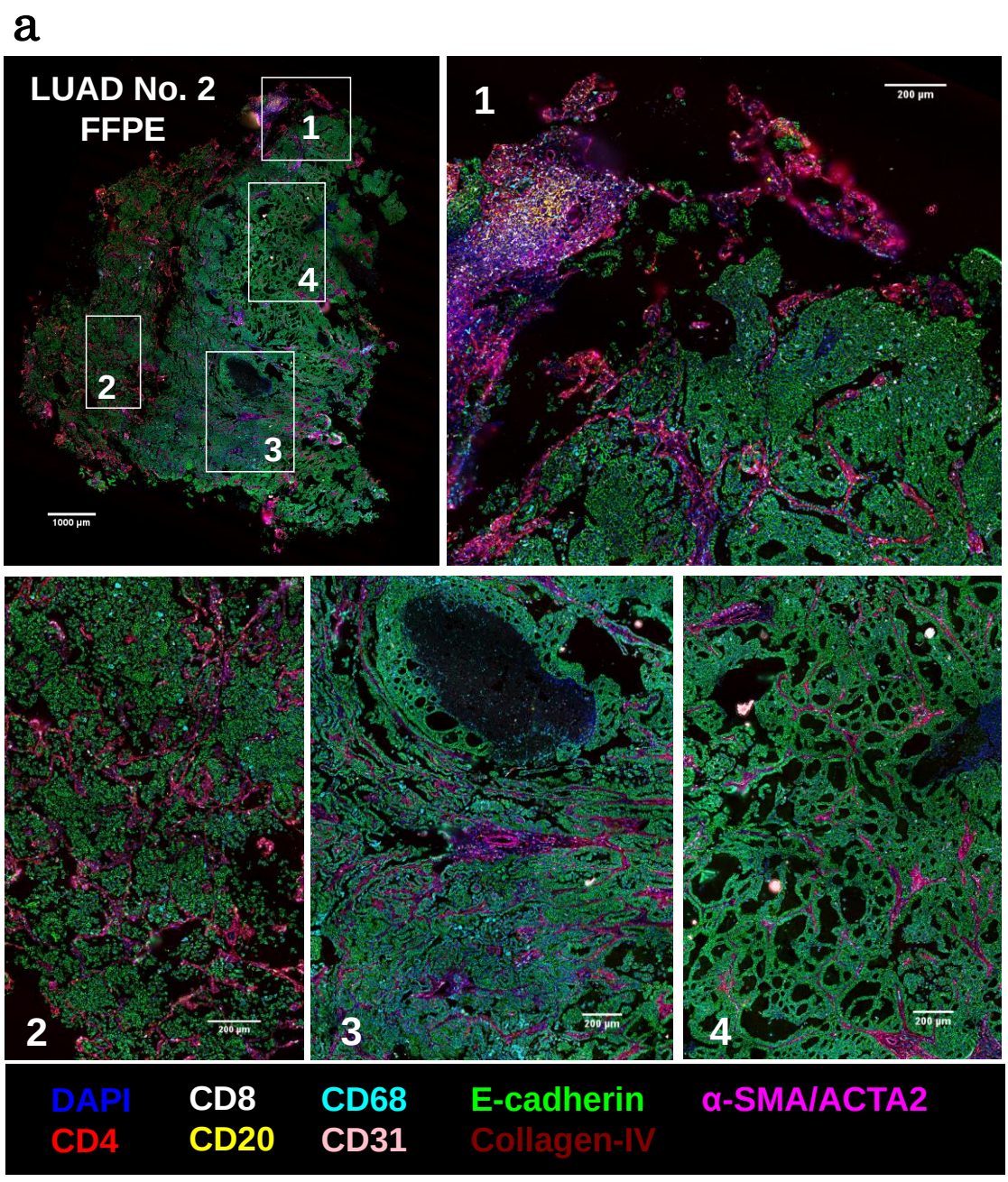
a
LUAD No. 2
FFPE
1
2
3
4
1000 µm
200 µm
DAPI
CD8
CD68
E-cadherin
α-SMA/ACTA2
CD4
CD20
CD31
Collagen-IV

Supplementary Figure S2

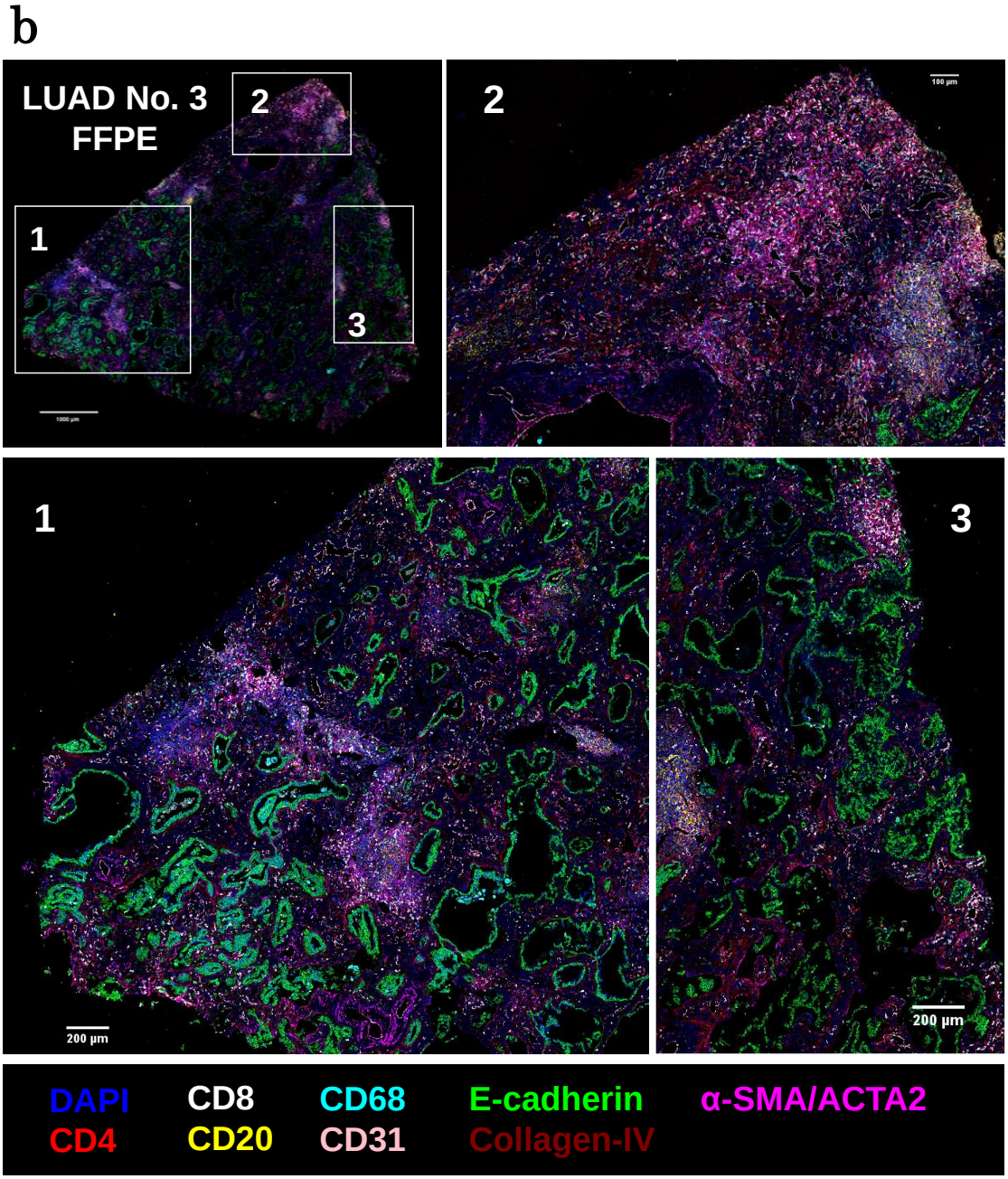

Supplementary Figure S2

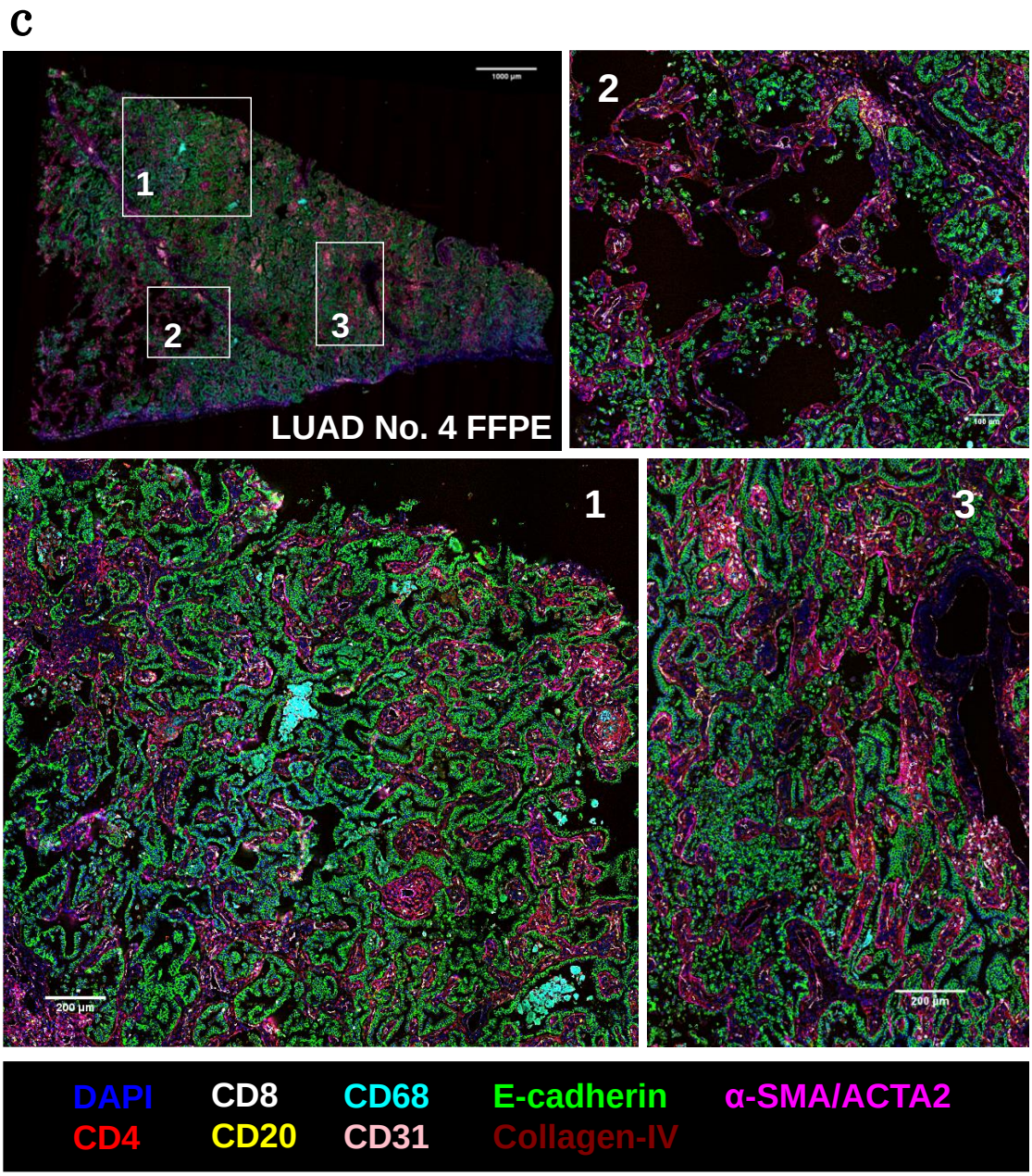

d

LUAD No. 2 FFPE (IA)

*Top 3 DEGs; log2FC > 0.5; log2FC > 2 in bold

Cluster	Annotation	Feature*
0	Proliferating tumor cell	HLA-A, Ki67, LIF
1	Proliferating tumor cell	Ki67, HLA-A
2	Tumor cell	NKX2-1, Pan-Cytokeratin
3	Stromal cell	**α-SMA**, **CD31**, CD44
4	Immune cell/Endothelial cell	**DC-LAMP**, **CXCL13**, **Podoplanin**
5	Tumor cell/Others	**PD-1**, Pan-Cytokeratin, NKX2-1
6	Tumor cell	NKX2-1, Pan-Cytokeratin
7	High IDO1 cell	IDO1, HLA-A
8	T cell/B cell	**CD45RO**, **CD8**, **CD4**
9	CD8+ T cell	**CD8**, CD45RO, CD3e
10	Immune cell	FOXP3, CD56
11	Macrophage/DC	CD11c, HLA-A, LIF
12	Tumor cell/Immune cell	**DC-LAMP**, NKX2-1, HLA-DPB1
13	Stromal cell/Immune cell	**Podoplanin**, **DC-LAMP**, **CD8**

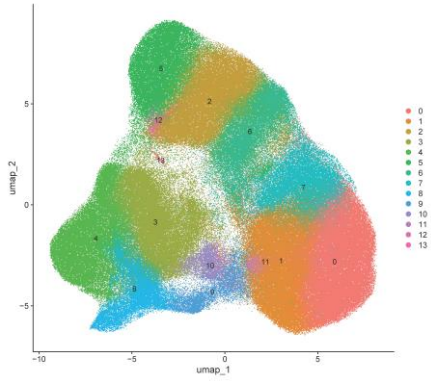

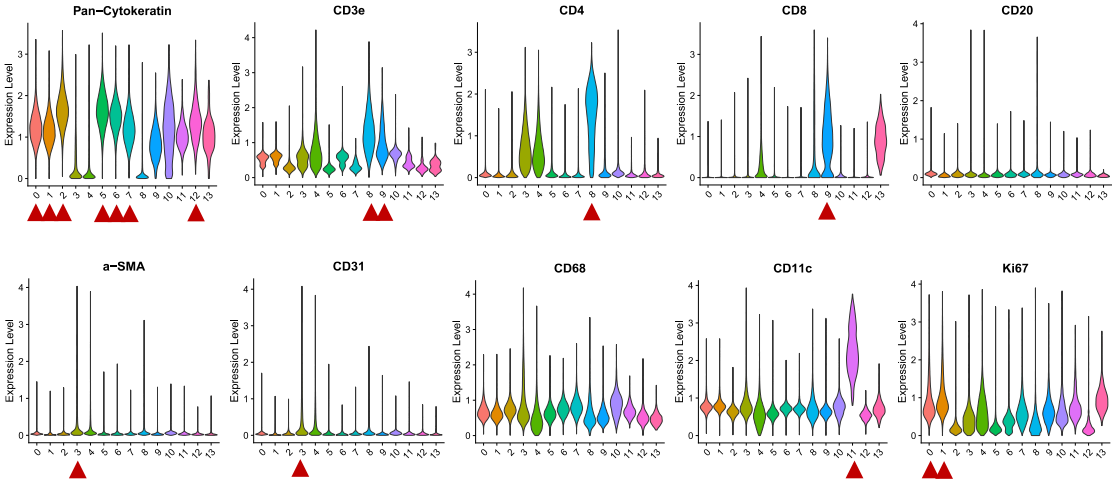

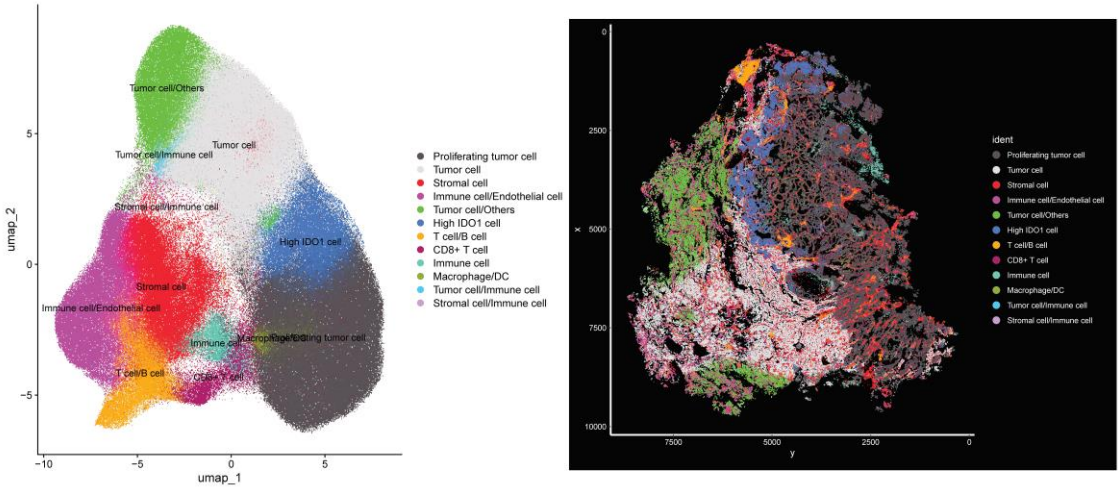

e

LUAD No. 3 FFPE (IA)

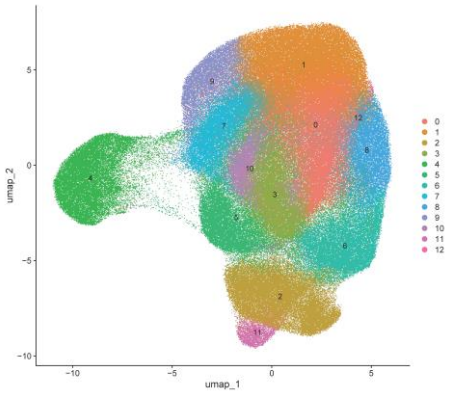

*Top 3 DEGs; log2FC > 0.5; log2FC > 2 in bold

Cluster	Annotation	Feature*
0	Stromal cell/Immune cell	DC-LAMP, PD-L1, Ki67
1	Stromal cell/Immune cell	---
2	T cell	**CD8**, **CD45RO**, CD4
3	Stromal cell/Immune cell	CD56, LIF, Podoplanin
4	Tumor cell	**Pan-Cytokeratin**, **E-Cadherin**, **NKX2-1**
5	Macrophage/DC	CD68, HLA-DPB1, CD11c
6	B cell	**CD20**, CXCL13, HLA-A
7	Fibroblast/SMC	**α-SMA**, Collagen-IV
8	B cell	**CXCL13**, CD20
9	High Galectin-3 cell	Galectin3, LAG3, DC-LAMP
10	Endothelial cell	**CD31**, HLA-A, Podoplanin
11	Treg	**FOXP3**, **CD45RO**, **Ki67**
12	Stromal cell/Immune cell	Podoplanin, PD-L1, DC-LAMP

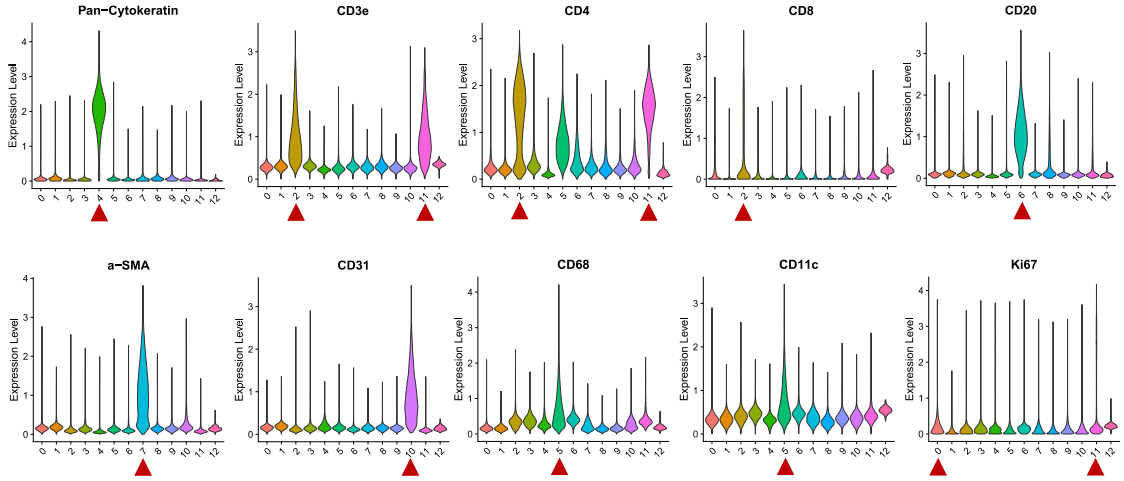

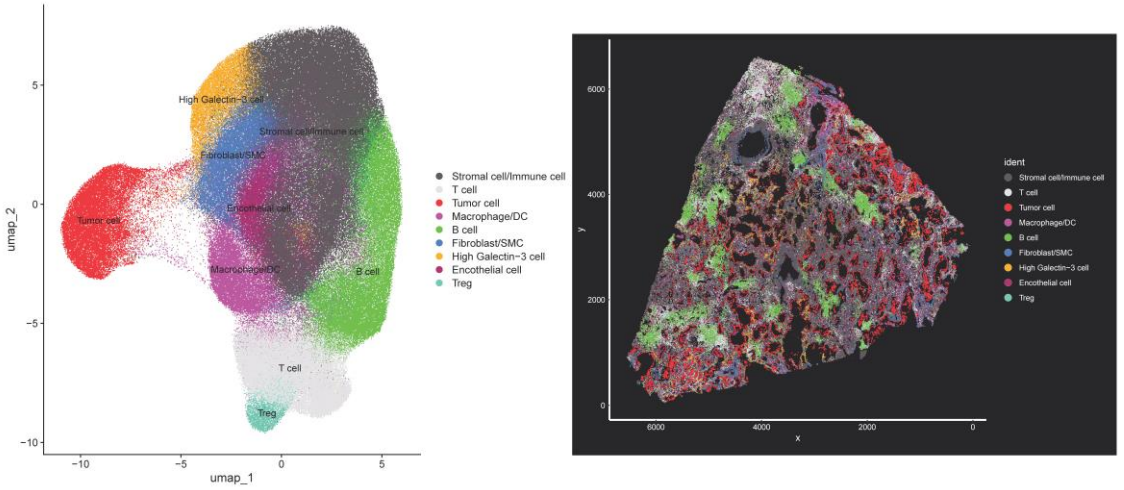

f

LUAD No. 4 FFPE (IA)

*Top 3 DEGs; log2FC > 0.5; log2FC > 2 in bold

Cluster	Annotation	Feature*
0	Tumor cell	Pan-Cytokeratin, NKX2-1, HLA-DPB1
1	Tumor cell	**NKX2-1**, Pan-Cytokeratin, E-Cadherin
2	Fibroblast/SMC	α-SMA
3	Immune cell	CD4, CD68, CD11c
4	T cell	**CD45RO**, **CD4**, CD3e
5	Fibroblast/SMC	**α-SMA**
6	Stromal cell/Immune cell	Podoplanin, CD8, Ki67
7	Endothelial cell	**CD31**, α-SMA, HLA-A
8	Tumor cell/Stromal cell	α-SMA, Pan-Cytokeratin, E-Cadherin
9	Proliferating tumor cell	**Ki67**, NKX2-1, Pan-Cytokeratin
10	B cell	**CD20**, HLA-A
11	Others	**CD8**, **Podoplanin**, **DC-LAMP**
12	Macrophage/DC	**CD68**, CD31, CD11c
13	DC/Immune cell	**DC-LAMP**, HLA-A, CD4
14	Tumor cell	TP53, NKX2-1, Pan-Cytokeratin
15	Stromal cell/Immune cell	Podoplanin, PD-L1, DC-LAMP

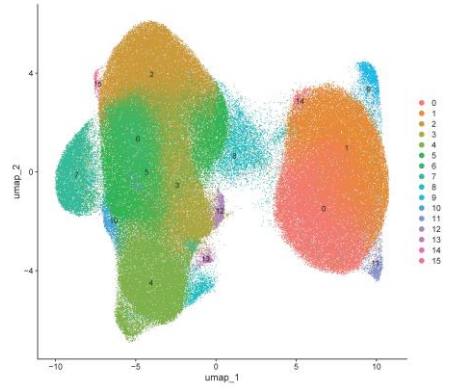

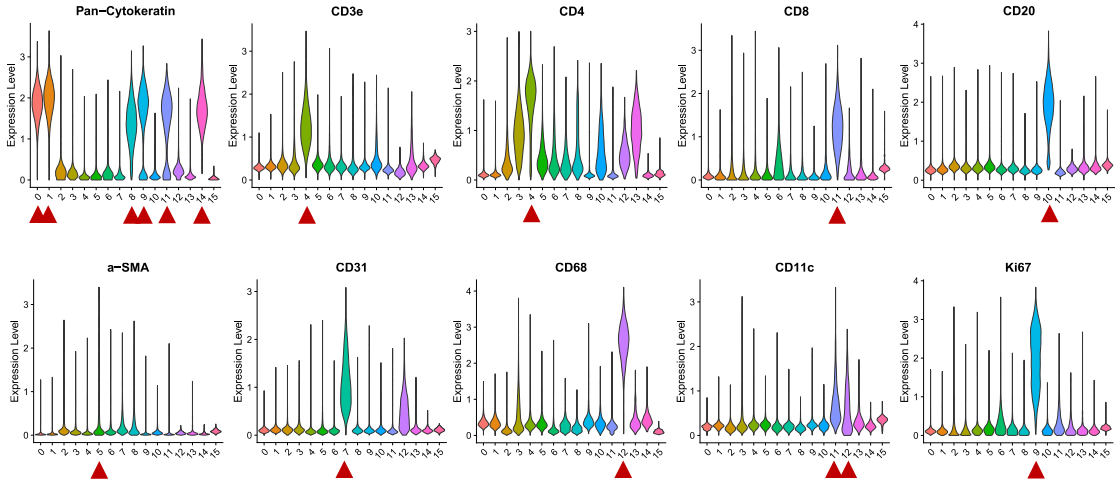

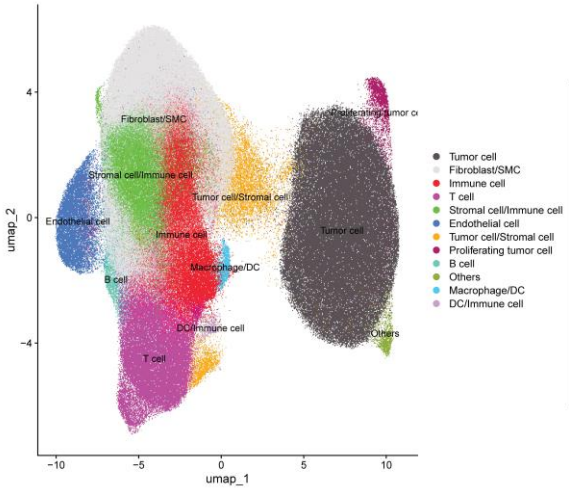

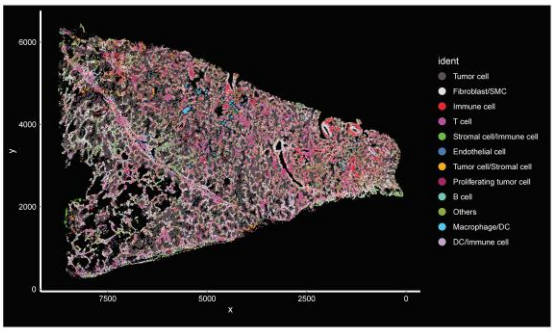

Supplementary Figure S2 Representative images and cell phenotyping results of PhenoCycler data in IA cases

(**a–c**) Representative images of PhenoCycler results in FFPE sections from LUAD No. 2–4. PhenoCycler signals of DAPI and eight proteins are shown. (**a**) The entire image and four ROIs are presented for LUAD No. 2 FFPE. ROI-1, a region containing lymphoid follicle and surrounding tumor cells. ROI-2, well- or moderately-differentiated tumor region. ROI-3, region with necrosis. ROI-4, mucinous tumor region. (**b**) The entire image and three ROIs are shown for LUAD No. 3 FFPE. ROI-1, a region with immune cell infiltration and surrounding tumor cells (around clusters 3, 5, and 6). ROI-2, T-cell-enriched region. ROI-3, tumor region with high expression levels of invasive genes (around cluster 10). (**c**) The entire image and three ROIs are presented for LUAD No. 4 FFPE. ROI-1, tumor region with high expression levels of invasive or hypoxic genes. ROI-2, normal-like differentiated tumor cells with lymphoid follicles and stroma. ROI-3, tumor region with stroma. (**d–f**) Clustering results and annotation of PhenoCycler data for cell phenotyping in LUAD No. 2–4 FFPE. The top panel displays a UMAP plot of the clustering results as well as a table with cell phenotype annotation for each cluster. The table includes the differentially expressed proteins of each cluster (top 3 with log2FC > 0.5; proteins with log2FC > 2 are bold). Violin plots of representative cell type markers are shown in middle panel. The UMAP and spatial plot with cell phenotyping data are shown in the bottom panel. All images and plots were flipped to match the orientation of Visium.

Supplementary Figure S3

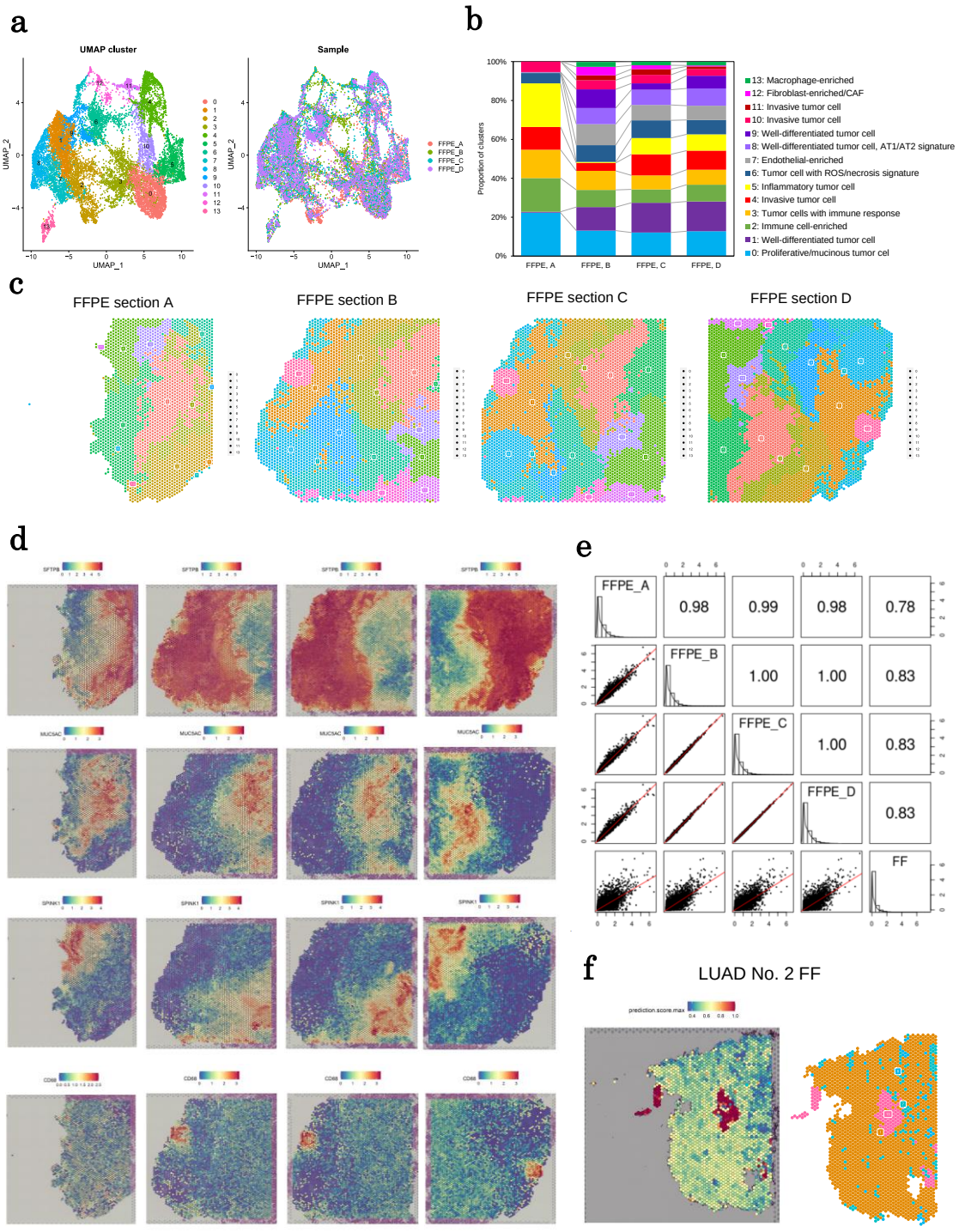

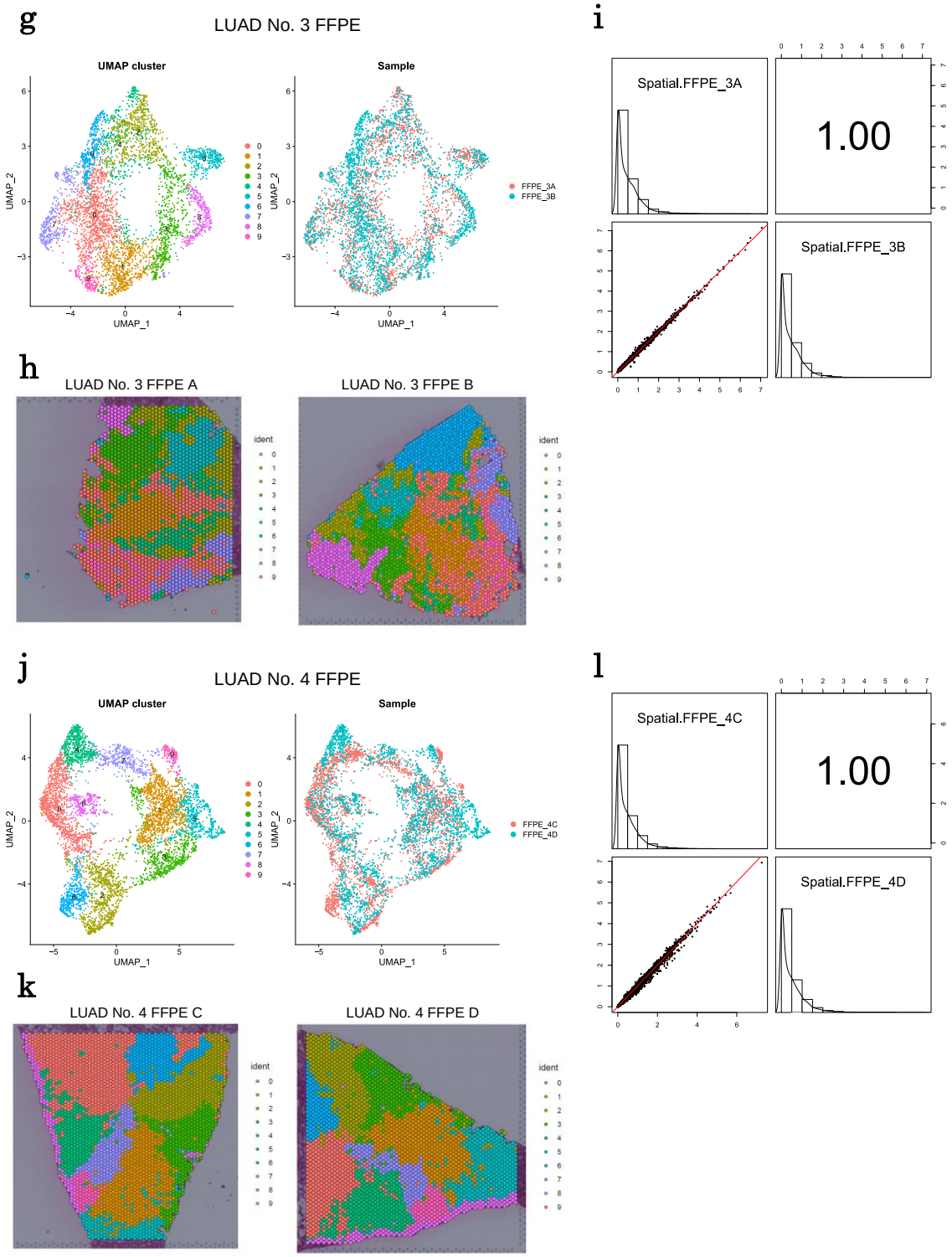
g
LUAD No. 3 FFPE
UMAP cluster
Sample
UMAP_1
UMAP_2
FFPE_3A
FFPE_3B
h
LUAD No. 3 FFPE A
LUAD No. 3 FFPE B
ident
i
Spatial.FFPE_3A
1.00
Spatial.FFPE_3B
j
LUAD No. 4 FFPE
FFPE_4C
FFPE_4D
k
LUAD No. 4 FFPE C
LUAD No. 4 FFPE D
l
Spatial.FFPE_4C
1.00
Spatial.FFPE_4D

Supplementary Figure S3 Integration and comparison of multiple sections in LUAD No. 2–4

(**a**) The integration of Visium data from four FFPE sections of LUAD No. 2. The clusters and sections are represented by UMAP plots in the left and right panels, respectively. Four FFPE sections are serial sections. (**b**) The percentage of clusters in each FFPE section of LUAD No. 2. (**c**) Spatial plots of clusters in each FFPE section of LUAD No. 2. (**d**) Expression patterns of representative cell type markers in the spatial plots of the four FFPE sections of LUAD No. 2. *SFTPB*, well-differentiated tumor cells; *MUC5AC*, mucinous tumor cells; *SPINK1*, invasive tumor cells; and *CD68*, macrophages. (**e**) Comparison of gene expression levels between FF and FFPE specimens from LUAD No. 2. (**f**) Projecting cluster annotation onto Visium FF results from LUAD No. 2. The scores and results of the projection are presented in the upper and lower panels, respectively. (**g**) Integration of Visium data from two FFPE sections of LUAD No. 3. The clusters and sections are represented by UMAP plots in the left and right panels, respectively. (**h**) Spatial plots of clusters in each FFPE section of LUAD No. 3. (**i**) Comparison of gene expression levels between sections of LUAD No. 3. (**j**) Integration of Visium data from two FFPE sections of LUAD No. 4. The clusters and sections are represented by UMAP plots in the left and right panels, respectively. (**k**) Spatial plots of clusters in each FFPE section of LUAD No. 4. (**l**) Comparison of gene expression levels between sections of LUAD No. 4. Source data are provided as a Source Data file for **b**.

Note:

Before proceeding with the analysis, we determined the extent to which the obtained data was compatible with the FF and FFPE Visium platforms. Each platform has unique advantages. For example, the pathological images on the FFPE platform are clearer than those on the FF platform. The FF platform can identify new transcripts or isoforms, including noncoding RNAs. The FF platform is better suited for many experimental validation analyses, including extensive transcriptome, epigenome, and genome analyses on locally dissected samples.

For comparison, we chose four consecutive FFPE sections and one FF section from LUAD No. 2. The histopathological images and H&E staining patterns were clearer in FFPE than in FF sections, allowing for more precise pathological inspection. In **Supplementary Figure S4a**, several pathological features, including well- or moderately-differentiated tumor regions, necrotic regions, mucinous-rich acinar or cribriform regions, and papillary regions with CAFs, are clearly represented in FFPE sections. For

this LUAD No. 2 specimen, we evaluated the gene expression profiles. Data from each FFPE section were highly reproducible (Pearson's correlation: 0.98–1.00). A comparison of FF and FFPE results from different parts of the same specimen revealed a reasonably high correlation between the platforms (Pearson's correlation: 0.78–0.83). In addition, we investigated whether FFPE and FF data could be combined. We found that FFPE and FF data could be combined using the label transfer method. In fact, when clustering was performed using mixed data, the FF and FFPE clusters were reasonably merged. Specifically, the number of detected genes in a given sequencing depth was higher in FFPE spatial transcriptome sequencing, partly owing to the procedure's inability to capture targets other than preset mRNAs, such as noncoding RNAs and mRNA-like technical noise products. Finally, all spatial expression pattern data from representative protein-coding genes obtained through FF and FFPE Visium analyses could be treated similarly.

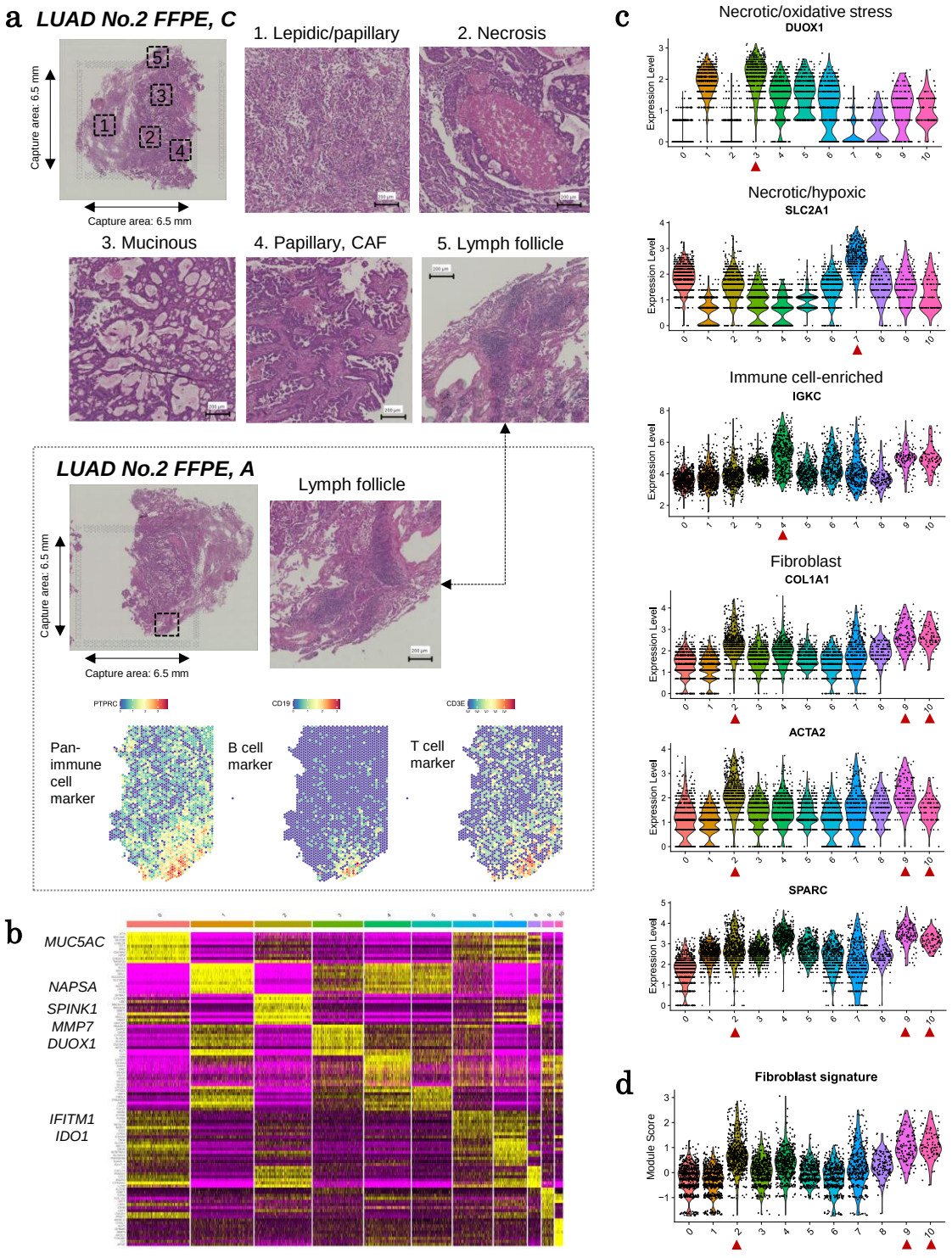
a
LUAD No.2 FFPE, C
1. Lepidic/papillary
2. Necrosis
3. Mucinous
4. Papillary, CAF
5. Lymph follicle
Capture area: 6.5 mm
Capture area: 6.5 mm
LUAD No.2 FFPE, A
Lymph follicle
Capture area: 6.5 mm
Capture area: 6.5 mm
PTPRC
CD19
CD3E
Pan-immune cell marker
B cell marker
T cell marker
b
MUC5AC
NAPSA
SPINK1
MMP7
DUOX1
IFITM1
IDO1
c
Necrotic/oxidative stress
DUOX1
Necrotic/hypoxic
SLC2A1
Immune cell-enriched
IGKC
Fibroblast
COL1A1
ACTA2
SPARC
Expression Level
d
Fibroblast signature
Module Score

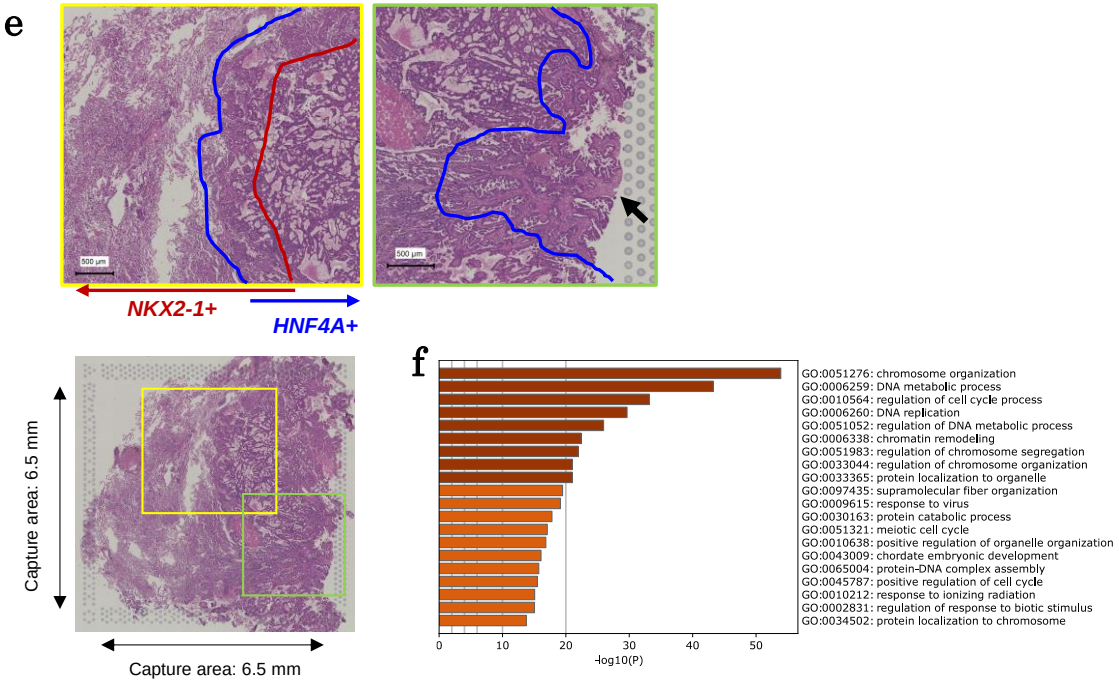

Supplementary Figure S4 Characterization of LUAD No. 2 FFPE

(**a**) Histological images of representative regions from LUAD No. 2 FFPE section C. The immune cell-rich region (5. Lymph Follicle) is partially out of frame in section C, so the H&E image of the adjacent section A was used, and expressions of representative immune cell markers were evaluated in this region. (**b**) Heatmap showing the expression patterns of differentially expressed genes (DEGs) in each cluster. The names of representative genes are highlighted in the margin. (**c**) Violin plots of expression levels in each cluster for representative genes. The cluster(s) with higher expressions of these genes are highlighted in red triangles in the margin. (**d**) Violin plots showing the expression signatures of three fibroblast markers. Module scores were calculated using the Seurat AddModuleScore function to show their average expression signature. (**e**) Upper left, H&E image of the boundary region between *NKX2-1*-positive well-differentiated tumor cells and *HNF4A*-positive mucinous tumor cells (around cluster 6), as defined in **Figure 2c**. Upper right, H&E image of the invasive tumor region (around cluster 3), as defined in **Figure 2g**. CAFs were enriched in this region (black arrow). Lower, the regions of the upper panels are indicated by yellow and yellow-green frames, respectively. (**f**) Gene Ontology enrichment analysis of DEGs in cluster 2. Source data are provided as a Source Data file for **f**.

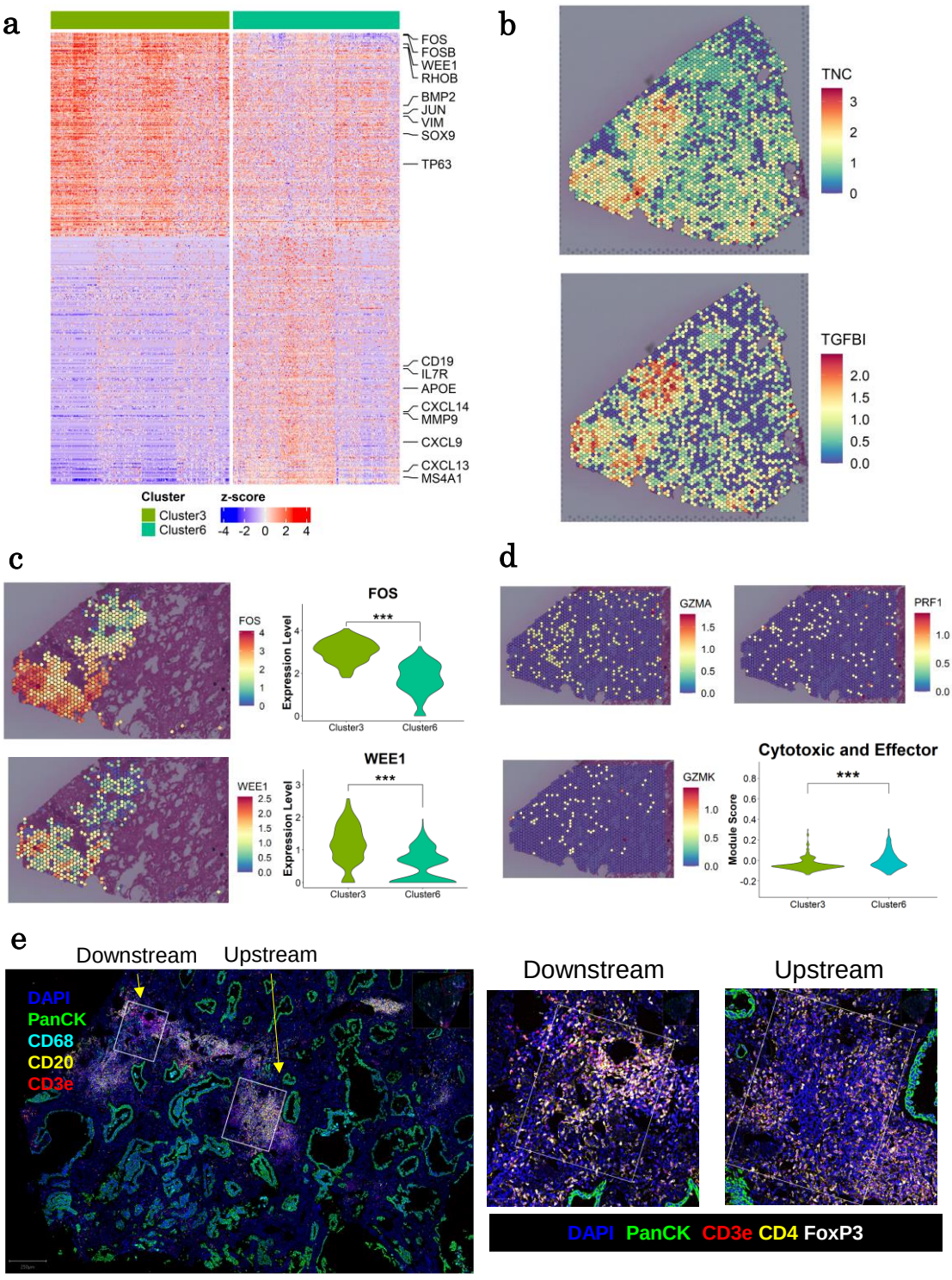
a
FOS
FOSB
WEE1
RHOB
BMP2
JUN
VIM
SOX9
TP63
CD19
IL7R
APOE
CXCL14
MMP9
CXCL9
CXCL13
MS4A1
Cluster
Cluster3
Cluster6
z-score
-4 -2 0 2 4
b
TNC
3
2
1
0
TGFBI
2.0
1.5
1.0
0.5
0.0
c
FOS
***
Expression Level
Cluster3
Cluster6
WEE1
***
d
GZMA
PRF1
GZMK
Cytotoxic and Effector
***
Module Score
e
Downstream
Upstream
DAPI
PanCK
CD68
CD20
CD3e
DAPI PanCK CD3e CD4 FoxP3

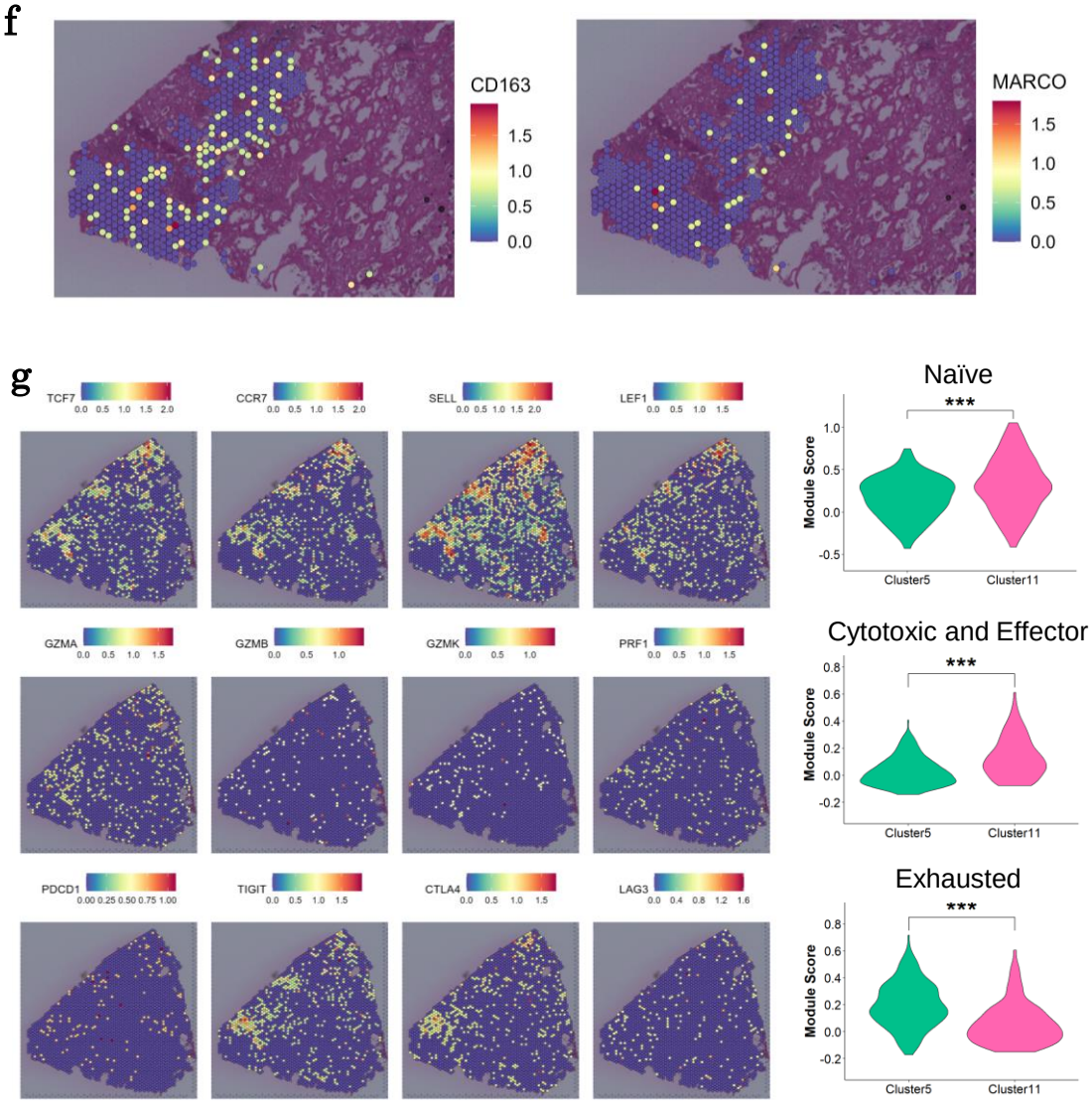
f
CD163
1.5
1.0
0.5
0.0
MARCO
1.5
1.0
0.5
0.0
g
TCF7
CCR7
SELL
LEF1
GZMA
GZMB
GZMK
PRF1
PDCD1
TIGIT
CTLA4
LAG3
Naïve
***
Module Score
Cluster5
Cluster11
Cytotoxic and Effector
***
Module Score
Cluster5
Cluster11
Exhausted
***
Module Score
Cluster5
Cluster11
h
Sender SPP1 signal
Receiver SPP1 signal

Supplementary Figure S5 Characterization of LUAD No. 3 FFPE

(**a**) DEGs between clusters 3 and 6 of LUAD No. 3 FFPE section B. Representative DEGs associated with EMT and immune cell markers are shown in the margin. The heatmap was visualized by ComplexHeatmap[1]. (**b**) The expression patterns of *TNC* and *TGFBI* are shown in the left and right panels, respectively, for LUAD No. 3 FFPE section B. (**c**) A comparison of the expression patterns of proliferation markers *FOS* and *WEE1* in clusters 3 and 6. Spatial and violin plots are shown on the left and right, respectively. *P*-values were determined using the Wilcoxon rank sum test. ***P< 1e−4. (**d**) Comparison of the expression patterns of the cytotoxic and effector immune cell markers *GZMA*, *GZMK*, and *PRF1* between clusters 3 and 6. Spatial and violin plots are shown on the left and right, respectively. *P*-values were determined using the Wilcoxon rank sum test. ***P < 1e−4. (**e**) Result of multiplexed immunostaining PhenoCycler with DAPI and representative cell markers. The region surrounding clusters 3, 5, and 6 is shown in the left panel. For cluster 5 with flow of immune cell infiltration, the right panels zoom in on the two subregions (downstream and upstream). (**f**) Expression of *CD163* (M2 macrophages) and *MARCO* (alveolar macrophages) in clusters 3 and 6. (**g**) Spatial expression patterns of naïve, cytotoxic or effector, and exhausted immune cell markers. The left and right panels show spatial and violin plots for comparing clusters 5 and 11. (**h**) An example of the results of ligand–receptor interaction analysis. The sender and receiver signals for SPP1 signaling (database: CellChat[2]) are shown.

a

1) Mask image generation

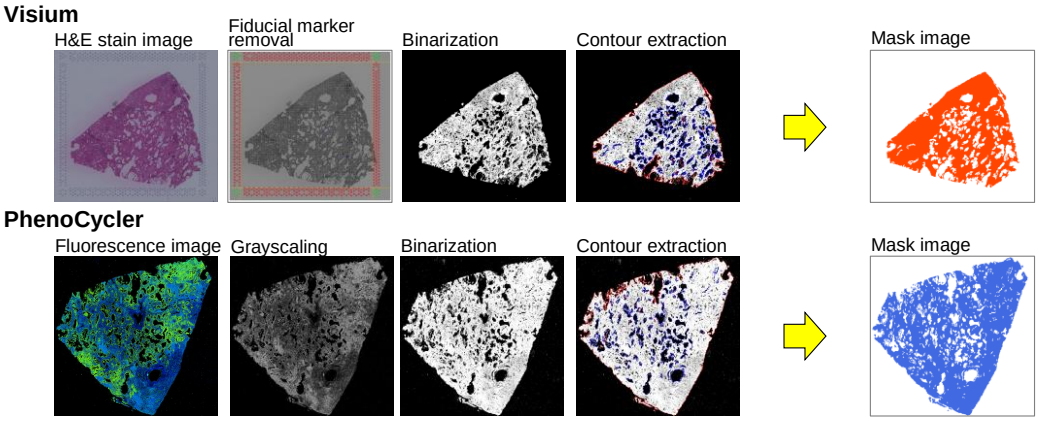

2) Mask image alignment

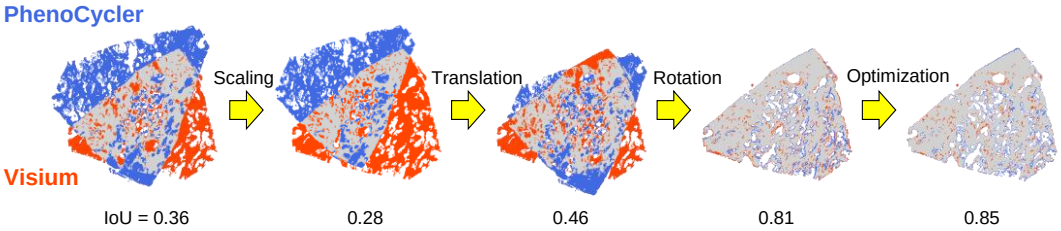

3) Coordinate transformation

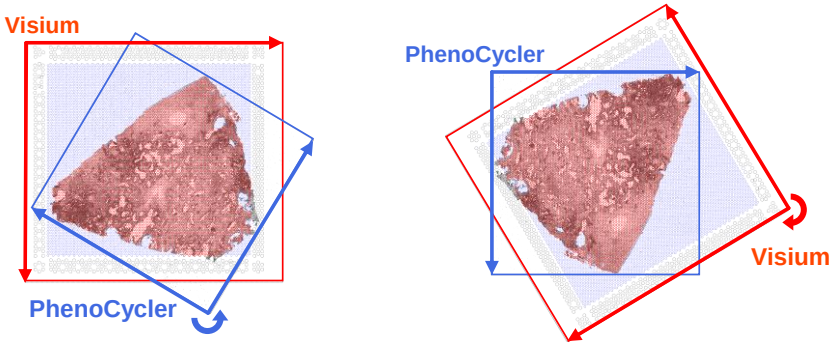

4) Mapping

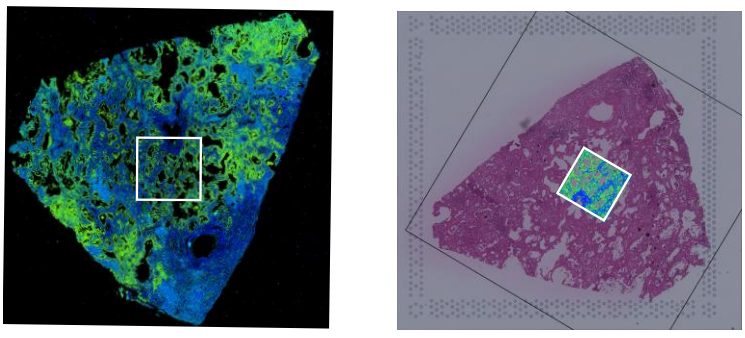

b

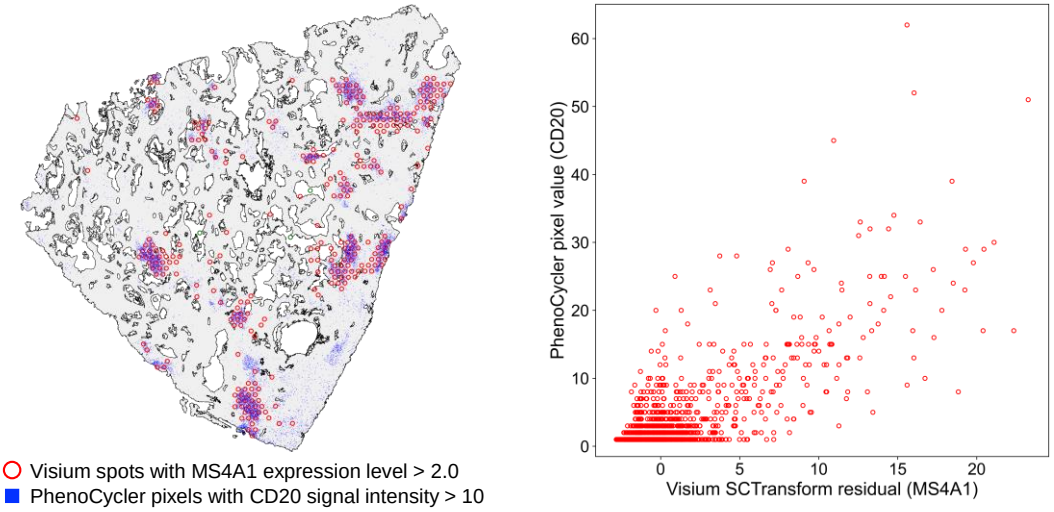
Visium spots with MS4A1 expression level > 2.0
PhenoCycler pixels with CD20 signal intensity > 10
PhenoCycler pixel value (CD20)
Visium SCTransform residual (MS4A1)
0
10
20
30
40
50
60
0
5
10
15
20

c

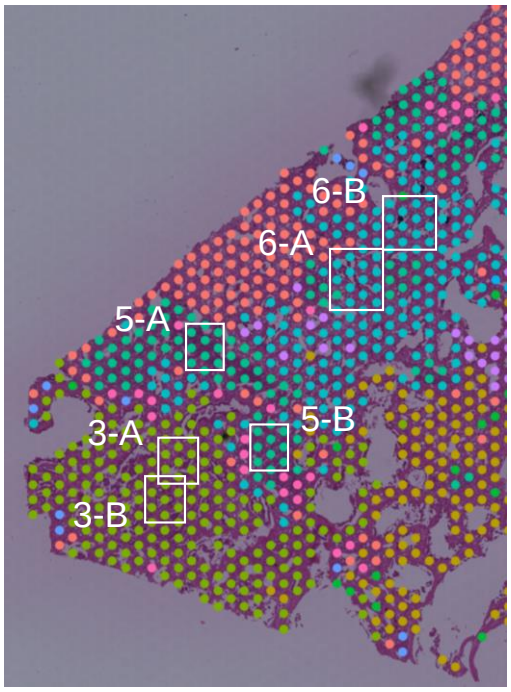
6-B
6-A
5-A
5-B
3-A
3-B

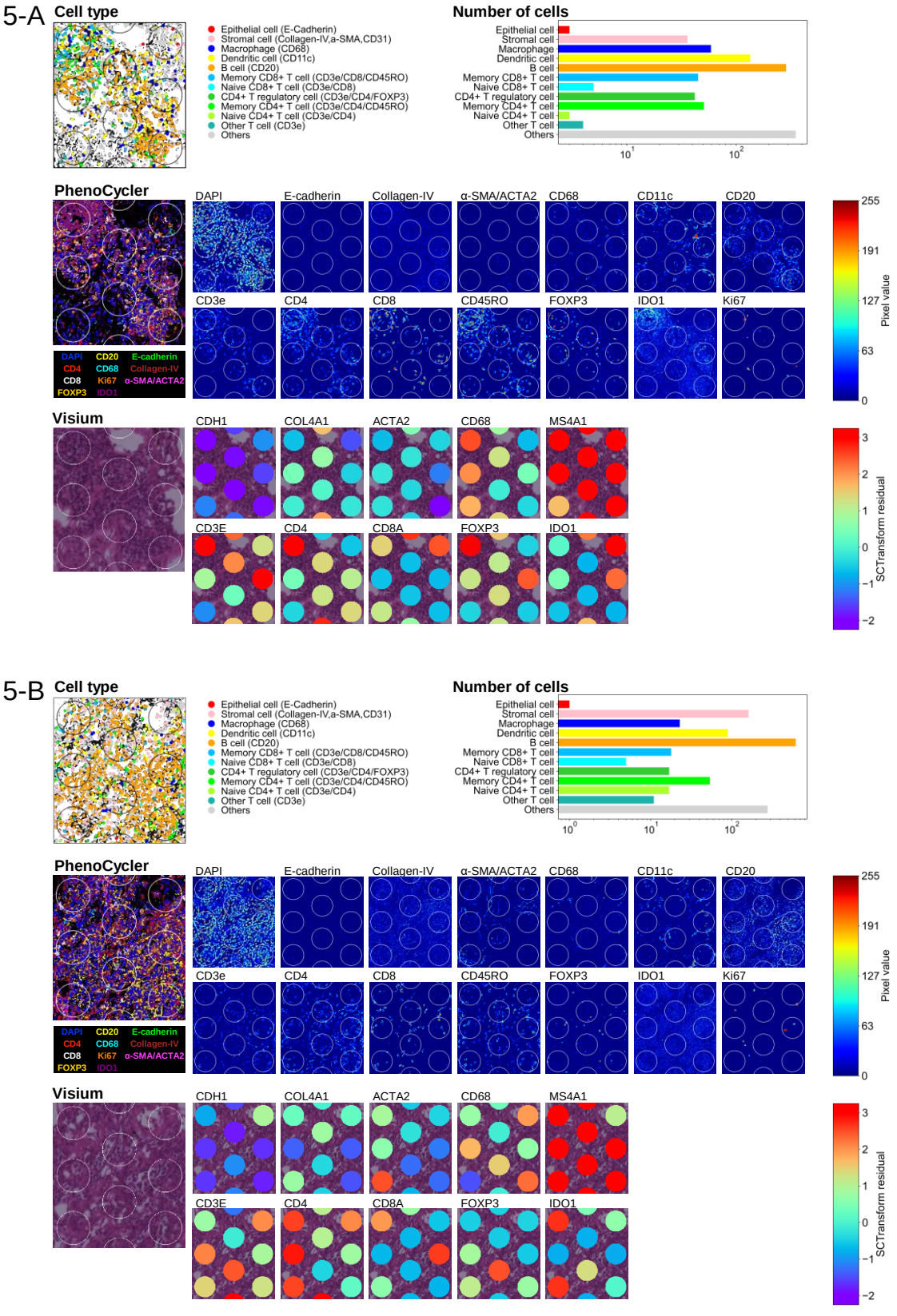
5-A
Cell type
Epithelial cell (E-Cadherin)
Stromal cell (Collagen-IV,a-SMA,CD31)
Macrophage (CD68)
Dendritic cell (CD11c)
B cell (CD20)
Memory CD8+ T cell (CD3e/CD8/CD45RO)
Naive CD8+ T cell (CD3e/CD8)
CD4+ T regulatory cell (CD3e/CD4/FOXP3)
Memory CD4+ T cell (CD3e/CD4/CD45RO)
Naive CD4+ T cell (CD3e/CD4)
Other T cell (CD3e)
Others
Number of cells
PhenoCycler
DAPI
E-cadherin
Collagen-IV
α-SMA/ACTA2
CD68
CD11c
CD20
CD3e
CD4
CD8
CD45RO
FOXP3
IDO1
Ki67
Pixel value
Visium
CDH1
COL4A1
ACTA2
CD68
MS4A1
CD3E
CD4
CD8A
FOXP3
IDO1
SCTransform residual
5-B
Cell type
Number of cells
PhenoCycler
Visium
SCTransform residual

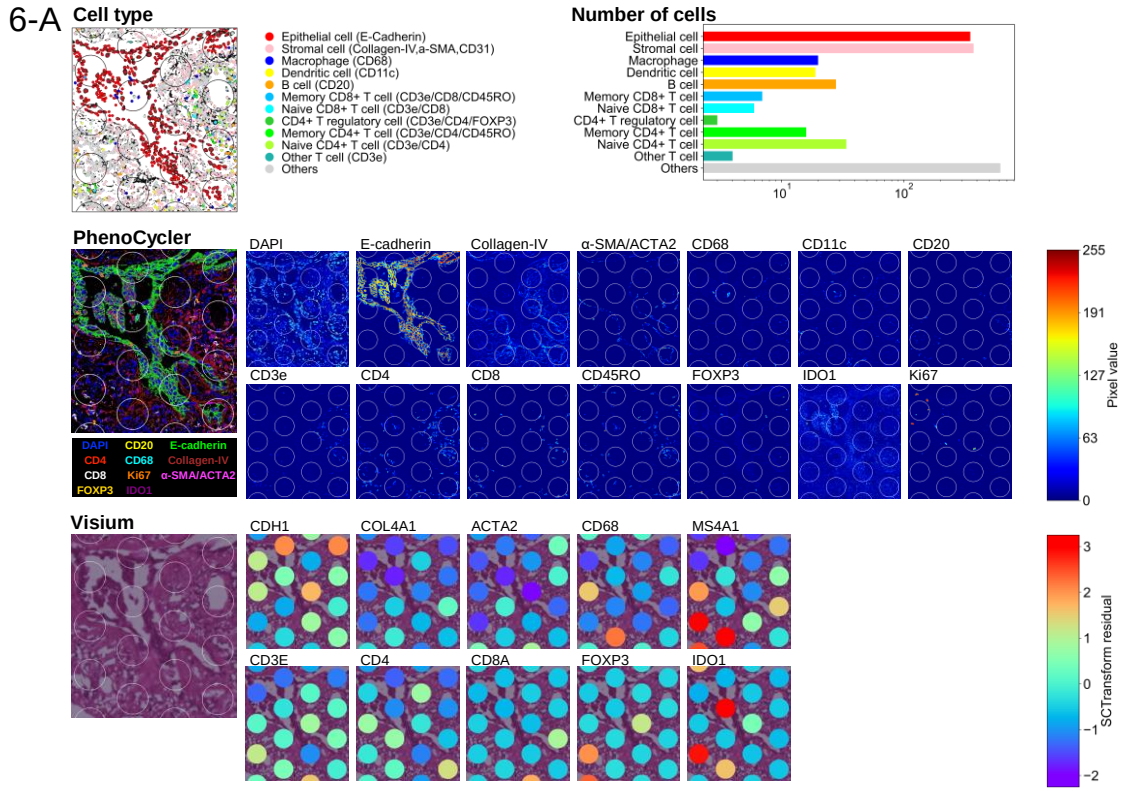
6-A
Cell type
Epithelial cell (E-Cadherin)
Stromal cell (Collagen-IV,a-SMA,CD31)
Macrophage (CD68)
Dendritic cell (CD11c)
B cell (CD20)
Memory CD8+ T cell (CD3e/CD8/CD45RO)
Naive CD8+ T cell (CD3e/CD8)
CD4+ T regulatory cell (CD3e/CD4/FOXP3)
Memory CD4+ T cell (CD3e/CD4/CD45RO)
Naive CD4+ T cell (CD3e/CD4)
Other T cell (CD3e)
Others
Number of cells
PhenoCycler
DAPI
E-cadherin
Collagen-IV
α-SMA/ACTA2
CD68
CD11c
CD20
CD3e
CD4
CD8
CD45RO
FOXP3
IDO1
Ki67
Pixel value
Visium
CDH1
COL4A1
ACTA2
CD68
MS4A1
CD3E
CD4
CD8A
FOXP3
IDO1
SCTransform residual

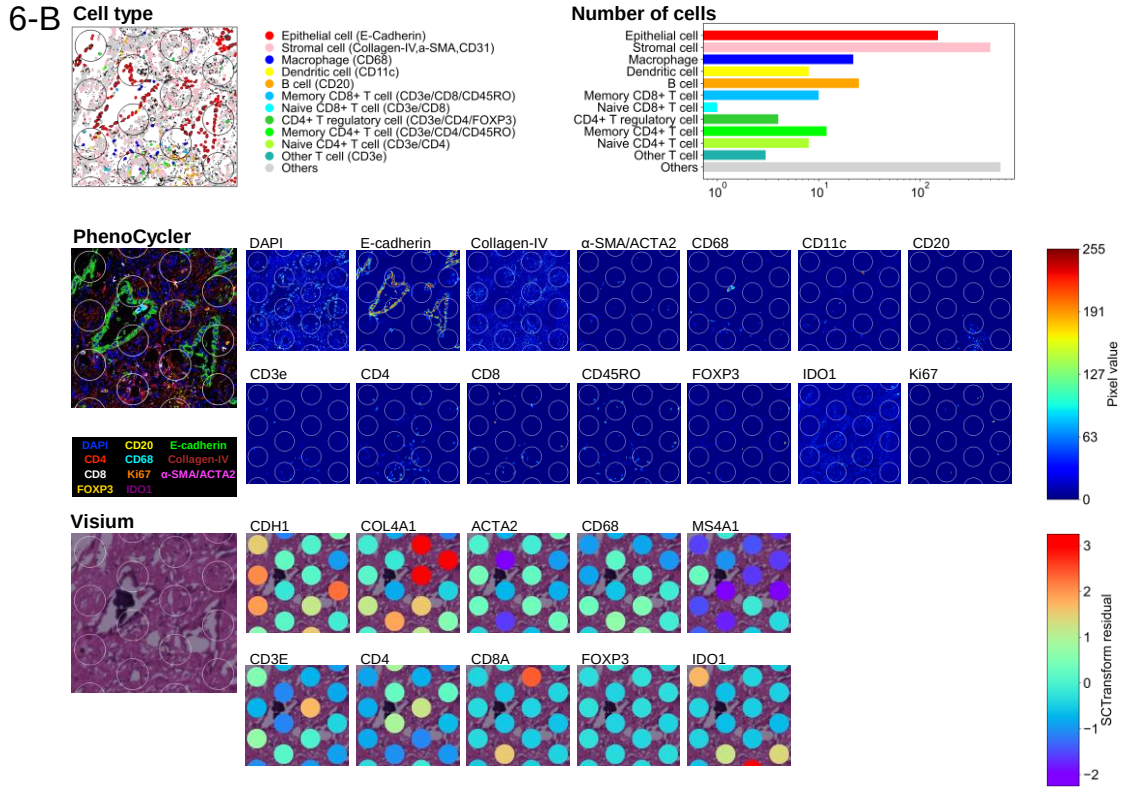
6-B
Cell type
Epithelial cell (E-Cadherin)
Stromal cell (Collagen-IV,a-SMA,CD31)
Macrophage (CD68)
Dendritic cell (CD11c)
B cell (CD20)
Memory CD8+ T cell (CD3e/CD8/CD45RO)
Naive CD8+ T cell (CD3e/CD8)
CD4+ T regulatory cell (CD3e/CD4/FOXP3)
Memory CD4+ T cell (CD3e/CD4/CD45RO)
Naive CD4+ T cell (CD3e/CD4)
Other T cell (CD3e)
Others
Number of cells
PhenoCycler
DAPI
E-cadherin
Collagen-IV
α-SMA/ACTA2
CD68
CD11c
CD20
CD3e
CD4
CD8
CD45RO
FOXP3
IDO1
Ki67
Pixel value
Visium
CDH1
COL4A1
ACTA2
CD68
MS4A1
CD3E
CD4
CD8A
FOXP3
IDO1
SCTransform residual

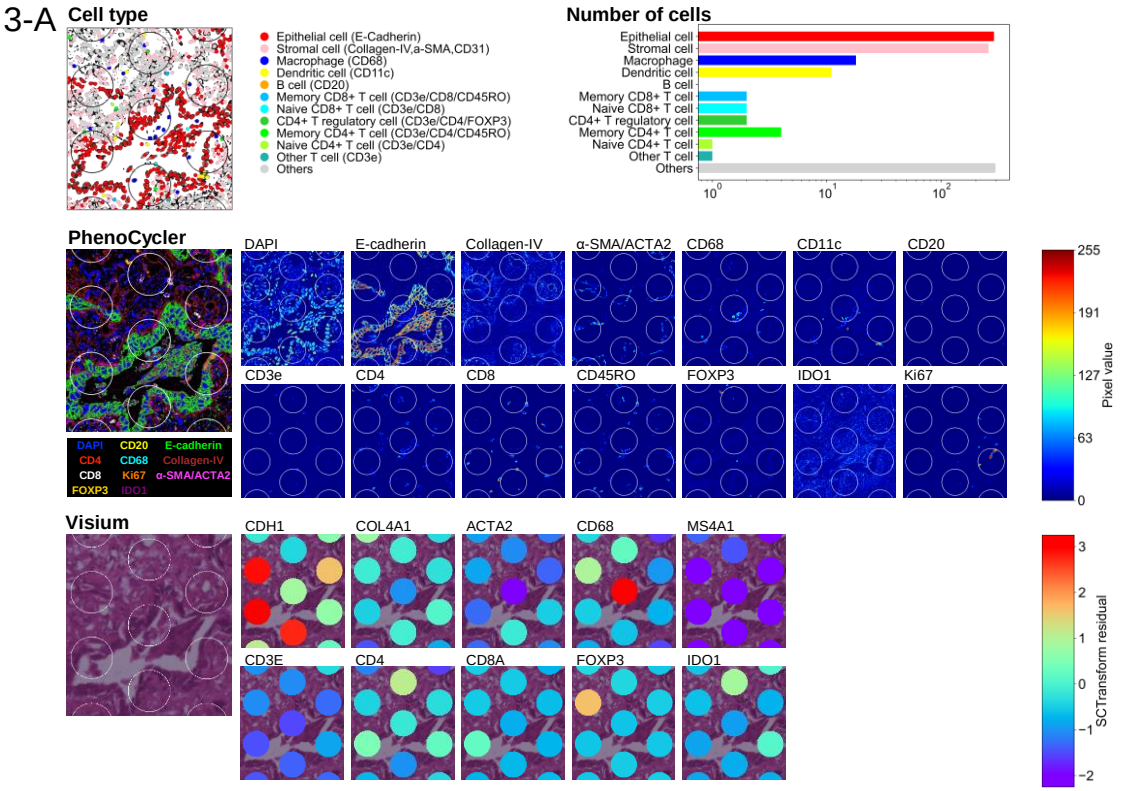
3-A
Cell type
Epithelial cell (E-Cadherin)
Stromal cell (Collagen-IV,a-SMA,CD31)
Macrophage (CD68)
Dendritic cell (CD11c)
B cell (CD20)
Memory CD8+ T cell (CD3e/CD8/CD45RO)
Naive CD8+ T cell (CD3e/CD8)
CD4+ T regulatory cell (CD3e/CD4/FOXP3)
Memory CD4+ T cell (CD3e/CD4/CD45RO)
Naive CD4+ T cell (CD3e/CD4)
Other T cell (CD3e)
Others
Number of cells
PhenoCycler
DAPI
E-cadherin
Collagen-IV
α-SMA/ACTA2
CD68
CD11c
CD20
CD3e
CD4
CD8
CD45RO
FOXP3
IDO1
Ki67
Pixel value
Visium
CDH1
COL4A1
ACTA2
CD68
MS4A1
CD3E
CD4
CD8A
FOXP3
IDO1
SCTransform residual

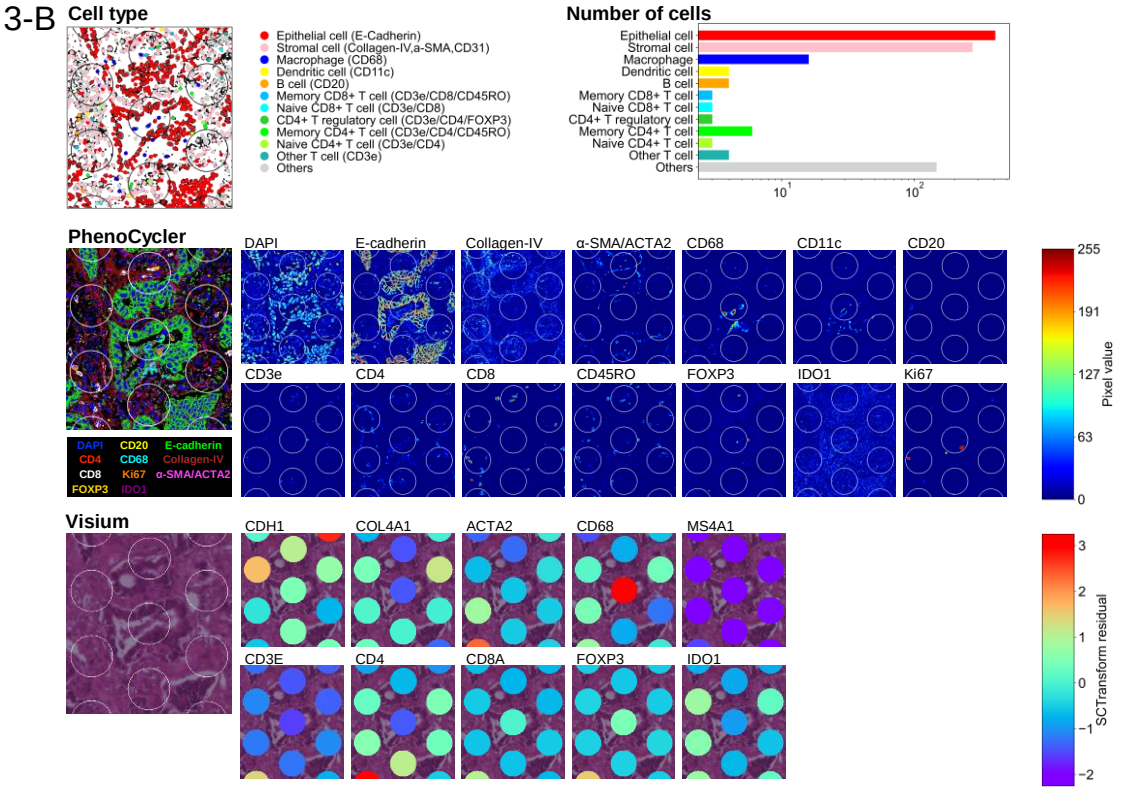
3-B
Cell type
Epithelial cell (E-Cadherin)
Stromal cell (Collagen-IV,a-SMA,CD31)
Macrophage (CD68)
Dendritic cell (CD11c)
B cell (CD20)
Memory CD8+ T cell (CD3e/CD8/CD45RO)
Naive CD8+ T cell (CD3e/CD8)
CD4+ T regulatory cell (CD3e/CD4/FOXP3)
Memory CD4+ T cell (CD3e/CD4/CD45RO)
Naive CD4+ T cell (CD3e/CD4)
Other T cell (CD3e)
Others
Number of cells
PhenoCycler
DAPI
E-cadherin
Collagen-IV
α-SMA/ACTA2
CD68
CD11c
CD20
CD3e
CD4
CD8
CD45RO
FOXP3
IDO1
Ki67
Pixel value
Visium
CDH1
COL4A1
ACTA2
CD68
MS4A1
CD3E
CD4
CD8A
FOXP3
IDO1
SCTransform residual

Supplementary Figure S6 Workflow and results for the integration of Visium and PhenoCycler image data

(**a**) Procedure for integrating Visium and PhenoCycler data. 1) The Visium H&E stained image and PhenoCycler fluorescence image were binarized to generate mask images using contour extraction. 2) Mask images of Visium (red) and PhenoCycler (blue) were scaled, translated, and rotated to maximize overlap based on their intersection over union (IoU), which is defined as (Visium ∩ PhenoCycler)/(Visium ∪ PhenoCycler). Using an exhaustive grid search in the vicinity of the above-stated solution, IoU was optimized to generate the final transformations. In the case of LUAD No. 3 FFPE (section B), IoU improved from 0.36 to 0.85, indicating adequate alignment quality for integrating the spatial datasets of various resolutions and orientations. 3) A mathematical function representing the transformations used in image alignment was developed to reciprocally associate pixel positions in Visium and PhenoCycler images. 4) Signals in Visium and PhenoCycler images were positionally integrated together using the mathematical function and its inverse. The pixels in a region of interest (ROI), represented by a white square in the PhenoCycler image (left panel), were mapped into the corresponding square in the Visium image (right panel) using the mathematical function generated by image alignment. (**b**) Expression patterns of MS4A1/CD20 (B cell marker) in Visium and PhenoCycler in LUAD No. 3 FFPE (section B). Left panel shows the positional relationship between Visium spots and PhenoCycler pixels with high signal levels. Spots with high *MS4A1* expression (>2.0) are shown as red circles, while pixels with high fluorescence level of the CD20 antibody (>10) are shown as blue dots. Right panel shows a comparison of MS4A1/CD20 expression levels in Visium and PhenoCycler. Each marker denotes a Visium spot. The horizontal axis shows the gene expression level of *MS4A1* determined by the residual of the SCTransform normalization of Visium count data. The vertical axis shows the expression level of the CD20 antibody, as measured by the average of non-zero fluorescence signals in the circular region of the PhenoCycler data to which the Visium spot corresponds. (**c**) ROIs for LUAD No. 3 FFPE (section B). For ROIs in clusters 3 and 6 (3-A, 3-B, 6-A, and 6-B) and cluster 5 (5-A and 5-B) (**Fig. 3e**), the types of cells and their frequencies detected using PhenoCycler fluorescence data are schematically presented. The fluorescence intensities of individual antibodies with PhenoCycler were compared to the positions of the circular regions of Visium spots. Superimposed images of the selected antibodies' fluorescence intensities were generated. The expression levels of the genes analyzed by Visium spots were plotted against the H&E staining image to investigate the relationships between Visium and PhenoCycler

expression levels.

Note:
We demonstrated that the integration of Visium and PhenoCycler data could be used to identify and validate cell types, particularly immune cells, which are sometimes difficult to decipher using Visium data due to low spatial resolution and differences in RNA and protein expression. For immune cell cluster 5 in LUAD No. 3 FFPE section B, we confirmed that B cells dominated while CD4+ Tregs were enriched in the downstream ROI (5-A) (also discussed in **Supplementary Figure S5**). For cluster 6, we confirmed infiltration of immune cells, including T and B cells. For cluster 3, where TAM-like alveolar macrophages were detected in Visium, we also found macrophages next to tumor cells in PhenoCycler data.

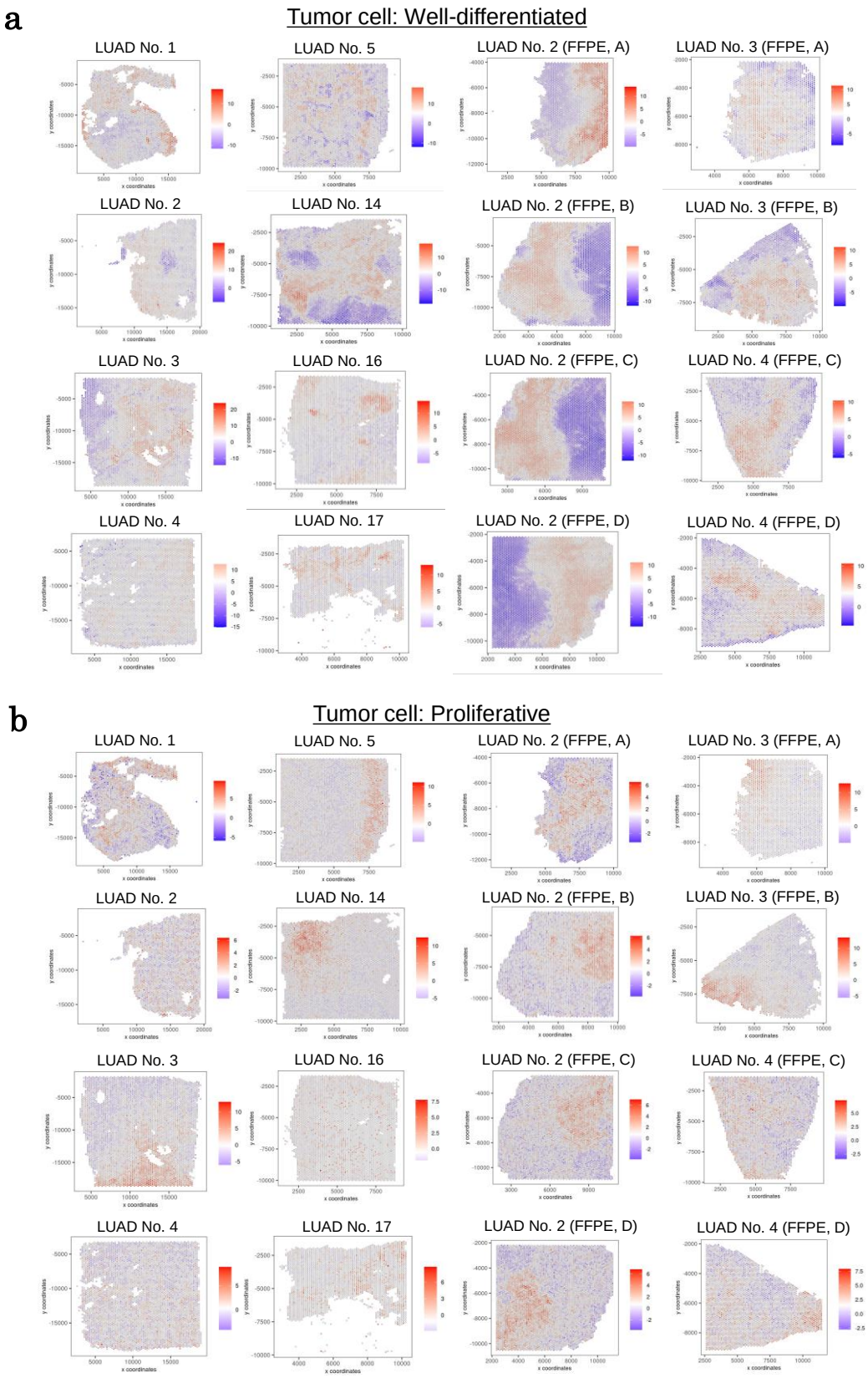
a
Tumor cell: Well-differentiated
LUAD No. 1
LUAD No. 5
LUAD No. 2 (FFPE, A)
LUAD No. 3 (FFPE, A)
LUAD No. 2
LUAD No. 14
LUAD No. 2 (FFPE, B)
LUAD No. 3 (FFPE, B)
LUAD No. 3
LUAD No. 16
LUAD No. 2 (FFPE, C)
LUAD No. 4 (FFPE, C)
LUAD No. 4
LUAD No. 17
LUAD No. 2 (FFPE, D)
LUAD No. 4 (FFPE, D)
b
Tumor cell: Proliferative
LUAD No. 1
LUAD No. 5
LUAD No. 2 (FFPE, A)
LUAD No. 3 (FFPE, A)
LUAD No. 2
LUAD No. 14
LUAD No. 2 (FFPE, B)
LUAD No. 3 (FFPE, B)
LUAD No. 3
LUAD No. 16
LUAD No. 2 (FFPE, C)
LUAD No. 4 (FFPE, C)
LUAD No. 4
LUAD No. 17
LUAD No. 2 (FFPE, D)
LUAD No. 4 (FFPE, D)

c

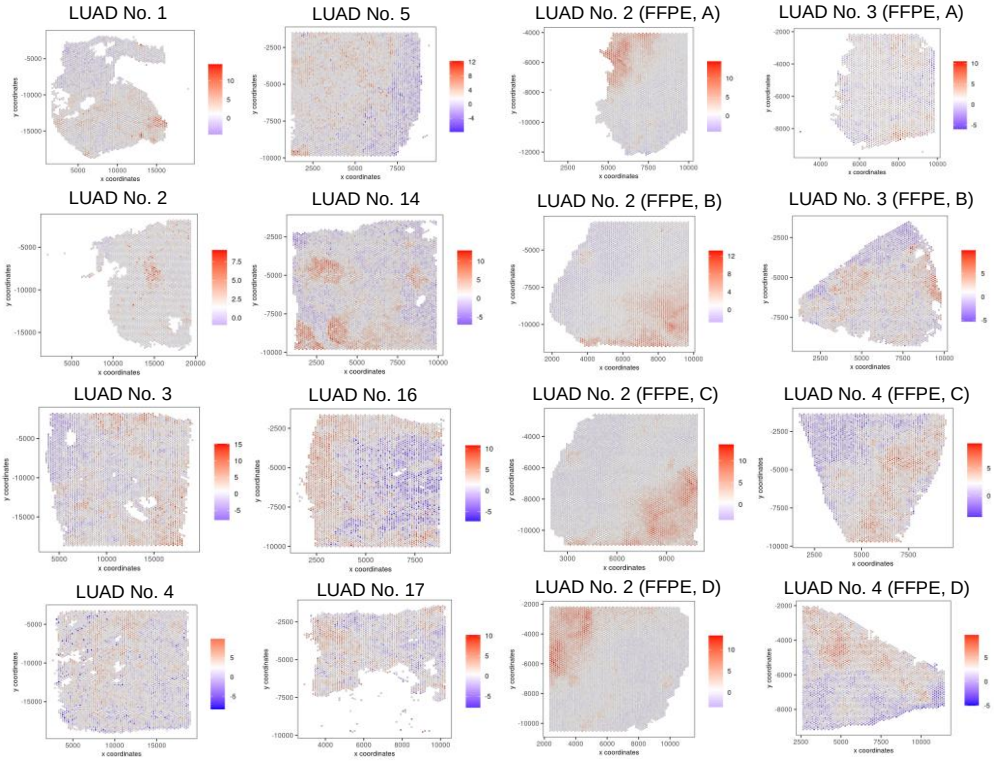
Tumor cell: Invasive
LUAD No. 1
LUAD No. 5
LUAD No. 2 (FFPE, A)
LUAD No. 3 (FFPE, A)
LUAD No. 2
LUAD No. 14
LUAD No. 2 (FFPE, B)
LUAD No. 3 (FFPE, B)
LUAD No. 3
LUAD No. 16
LUAD No. 2 (FFPE, C)
LUAD No. 4 (FFPE, C)
LUAD No. 4
LUAD No. 17
LUAD No. 2 (FFPE, D)
LUAD No. 4 (FFPE, D)

d

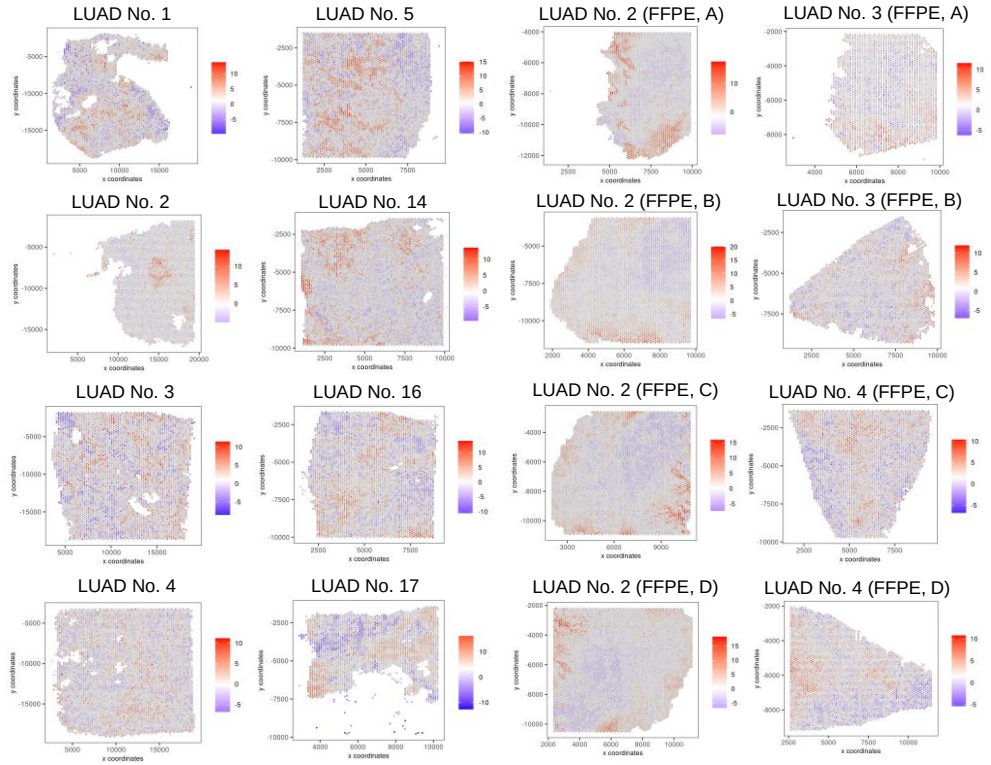
Microenvironment: Fibroblast/CAF
LUAD No. 1
LUAD No. 5
LUAD No. 2 (FFPE, A)
LUAD No. 3 (FFPE, A)
LUAD No. 2
LUAD No. 14
LUAD No. 2 (FFPE, B)
LUAD No. 3 (FFPE, B)
LUAD No. 3
LUAD No. 16
LUAD No. 2 (FFPE, C)
LUAD No. 4 (FFPE, C)
LUAD No. 4
LUAD No. 17
LUAD No. 2 (FFPE, D)
LUAD No. 4 (FFPE, D)

e

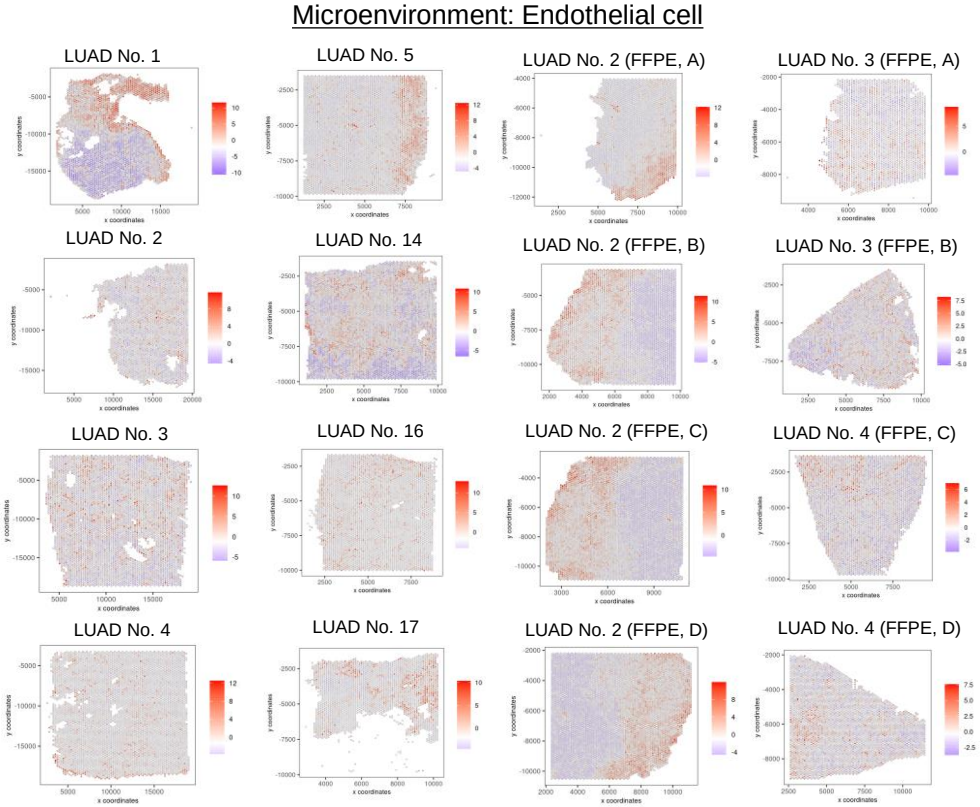
Microenvironment: Endothelial cell
LUAD No. 1
LUAD No. 5
LUAD No. 2 (FFPE, A)
LUAD No. 3 (FFPE, A)
LUAD No. 2
LUAD No. 14
LUAD No. 2 (FFPE, B)
LUAD No. 3 (FFPE, B)
LUAD No. 3
LUAD No. 16
LUAD No. 2 (FFPE, C)
LUAD No. 4 (FFPE, C)
LUAD No. 4
LUAD No. 17
LUAD No. 2 (FFPE, D)
LUAD No. 4 (FFPE, D)

f

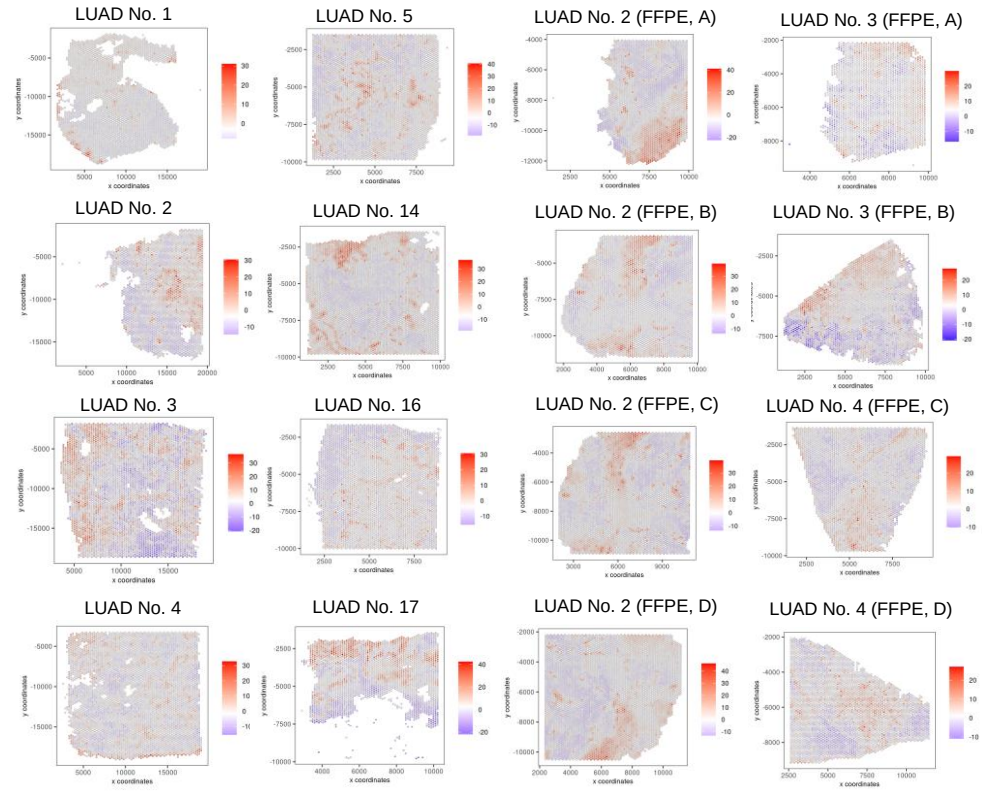
Microenvironment: Immune cell (Plasma cell)
LUAD No. 1
LUAD No. 5
LUAD No. 2 (FFPE, A)
LUAD No. 3 (FFPE, A)
LUAD No. 2
LUAD No. 14
LUAD No. 2 (FFPE, B)
LUAD No. 3 (FFPE, B)
LUAD No. 3
LUAD No. 16
LUAD No. 2 (FFPE, C)
LUAD No. 4 (FFPE, C)
LUAD No. 4
LUAD No. 17
LUAD No. 2 (FFPE, D)
LUAD No. 4 (FFPE, D)

g

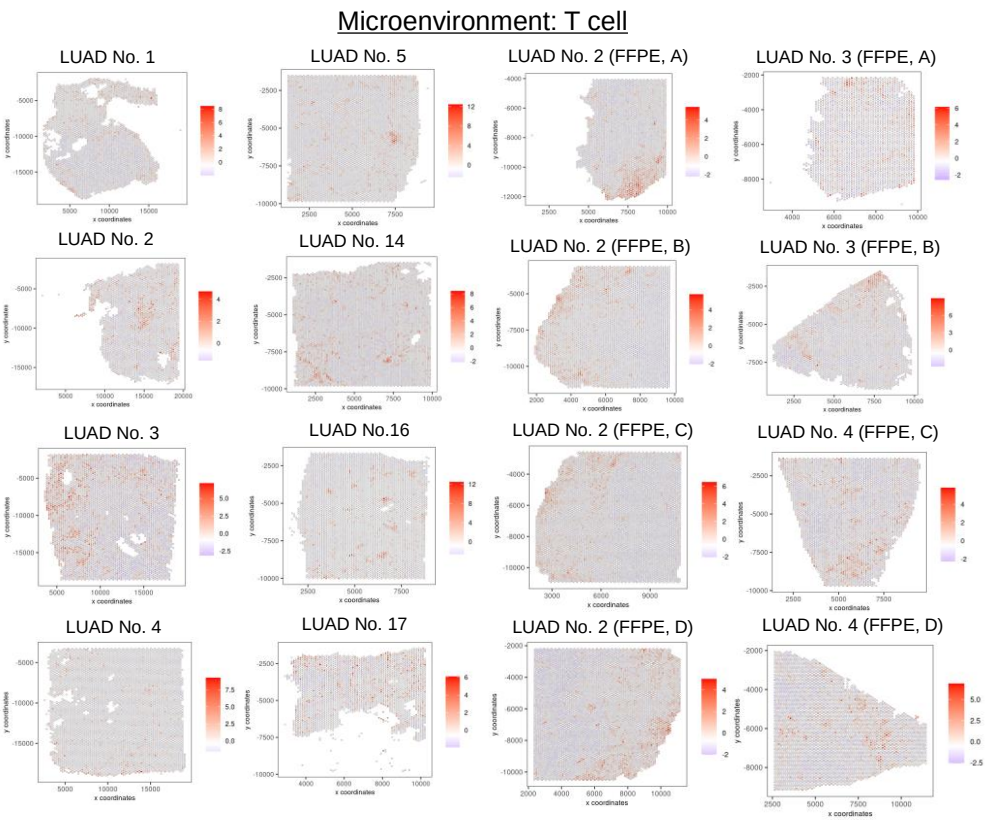
Microenvironment: T cell
LUAD No. 1
LUAD No. 5
LUAD No. 2 (FFPE, A)
LUAD No. 3 (FFPE, A)
LUAD No. 2
LUAD No. 14
LUAD No. 2 (FFPE, B)
LUAD No. 3 (FFPE, B)
LUAD No. 3
LUAD No.16
LUAD No. 2 (FFPE, C)
LUAD No. 4 (FFPE, C)
LUAD No. 4
LUAD No. 17
LUAD No. 2 (FFPE, D)
LUAD No. 4 (FFPE, D)

h

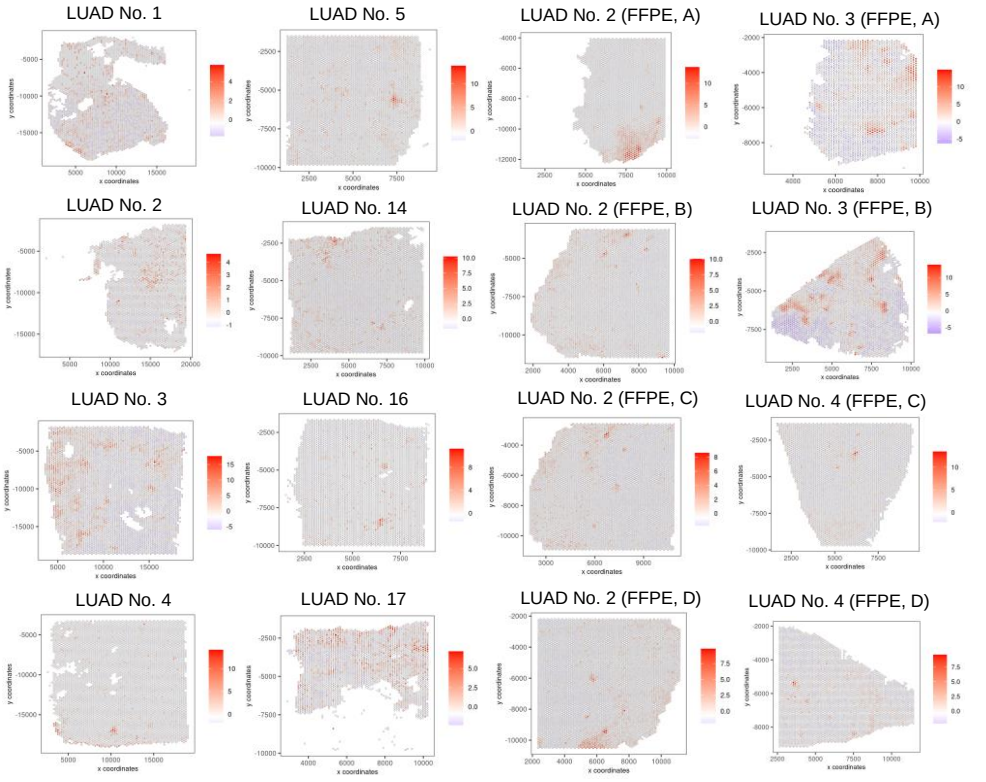
Microenvironment: B cell
LUAD No. 1
LUAD No. 5
LUAD No. 2 (FFPE, A)
LUAD No. 3 (FFPE, A)
LUAD No. 2
LUAD No. 14
LUAD No. 2 (FFPE, B)
LUAD No. 3 (FFPE, B)
LUAD No. 3
LUAD No. 16
LUAD No. 2 (FFPE, C)
LUAD No. 4 (FFPE, C)
LUAD No. 4
LUAD No. 17
LUAD No. 2 (FFPE, D)
LUAD No. 4 (FFPE, D)

i

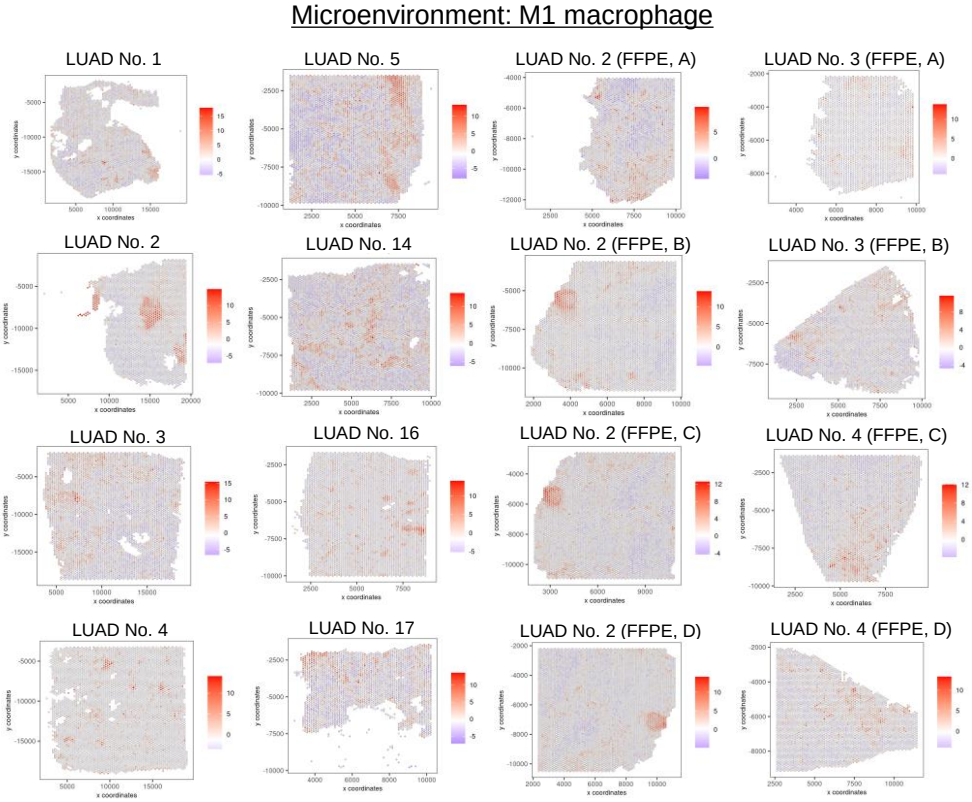
Microenvironment: M1 macrophage
LUAD No. 1
LUAD No. 5
LUAD No. 2 (FFPE, A)
LUAD No. 3 (FFPE, A)
LUAD No. 2
LUAD No. 14
LUAD No. 2 (FFPE, B)
LUAD No. 3 (FFPE, B)
LUAD No. 3
LUAD No. 16
LUAD No. 2 (FFPE, C)
LUAD No. 4 (FFPE, C)
LUAD No. 4
LUAD No. 17
LUAD No. 2 (FFPE, D)
LUAD No. 4 (FFPE, D)

j

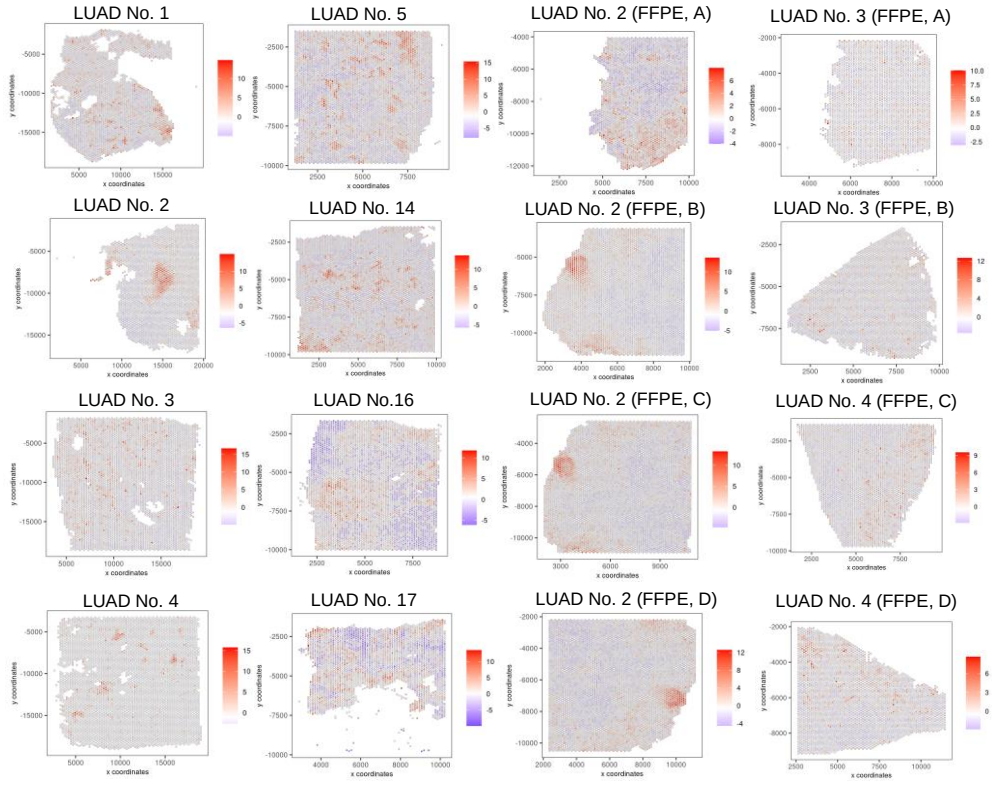
Microenvironment: M2 macrophage
LUAD No. 1
LUAD No. 5
LUAD No. 2 (FFPE, A)
LUAD No. 3 (FFPE, A)
LUAD No. 2
LUAD No. 14
LUAD No. 2 (FFPE, B)
LUAD No. 3 (FFPE, B)
LUAD No. 3
LUAD No.16
LUAD No. 2 (FFPE, C)
LUAD No. 4 (FFPE, C)
LUAD No. 4
LUAD No. 17
LUAD No. 2 (FFPE, D)
LUAD No. 4 (FFPE, D)

Supplementary Figure S7 TME scoring in all IA sections or cases

Results of tumor microenvironment (TME) scoring using PAGE analysis by Giotto[3]. The spatial distributions of scores for well-differentiated, proliferative, and invasive tumor cells are shown in panels **a**, **b**, and **c**, respectively. For non-tumor cells, the spatial distributions of the scores are represented by **d**–**j**.

a

Step 1. Manually determining paths considering Monocle 3 results and spatial information

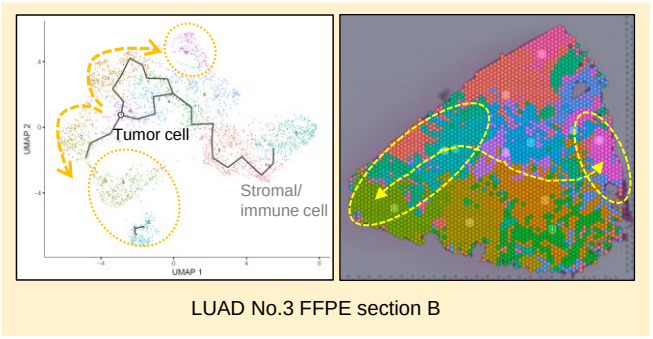

LUAD No.3 FFPE section B

Step 2. Drawing trajectories by projecting the paths to the spatial plot by SPATA2

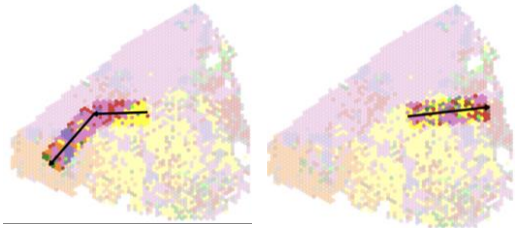

Trajectory #1 (Path-1) Trajectory #2 (Path-2)

LUAD No.3 FFPE section B

Step 3. Plotting TME scores along with the trajectory

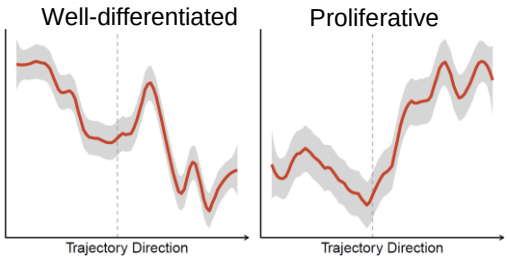

Step 4. Detecting regions where TME scores dramatically changed

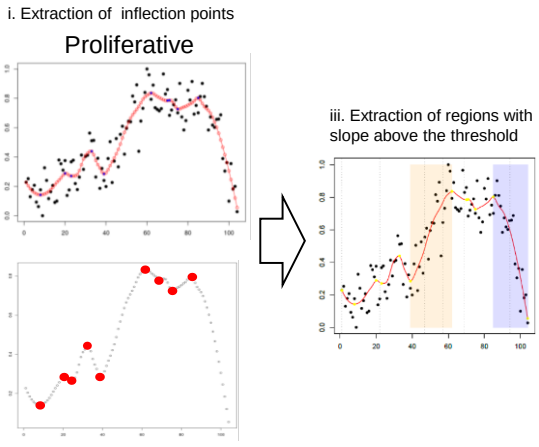

LUAD No.2 FFPE section C

Step 5. Evaluating association between TMEs

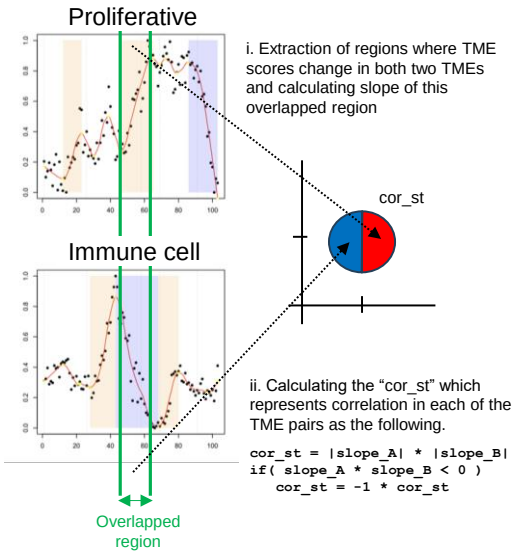

b

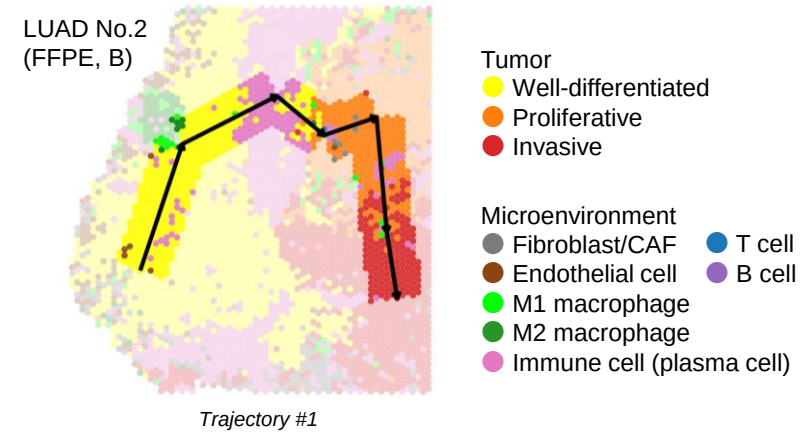

Trajectory #1

c

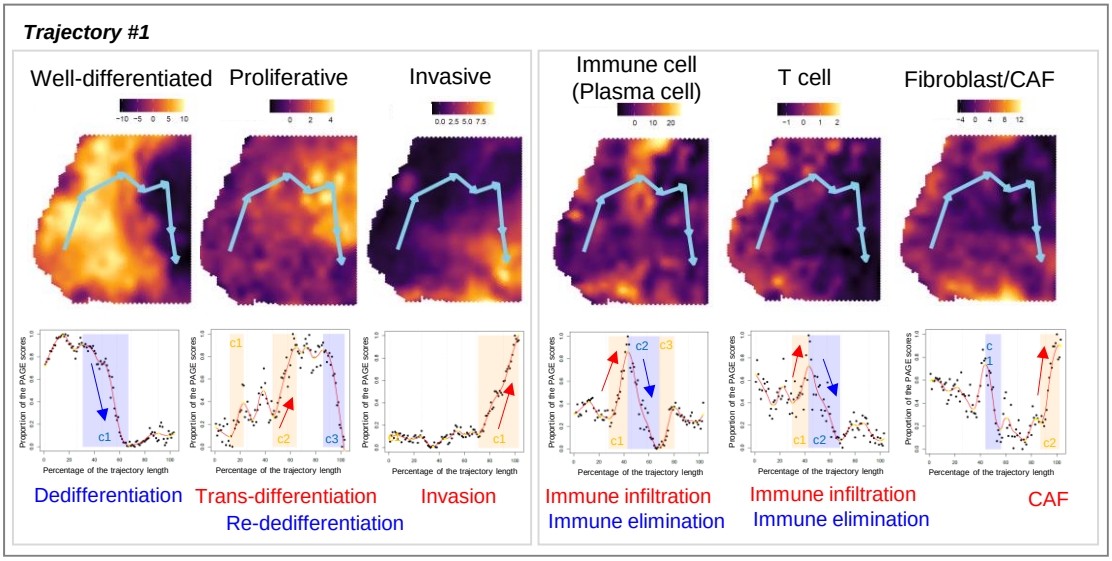

d

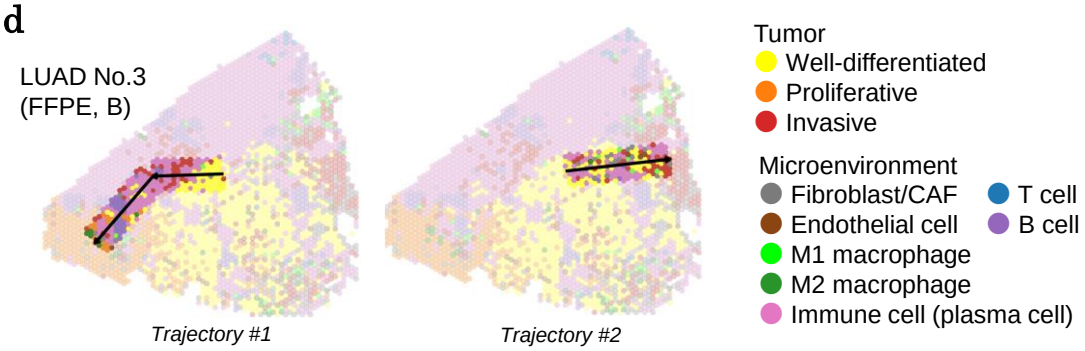
LUAD No.3
(FFPE, B)
Trajectory #1
Trajectory #2
Tumor
Well-differentiated
Proliferative
Invasive
Microenvironment
Fibroblast/CAF
Endothelial cell
M1 macrophage
M2 macrophage
Immune cell (plasma cell)
T cell
B cell

e

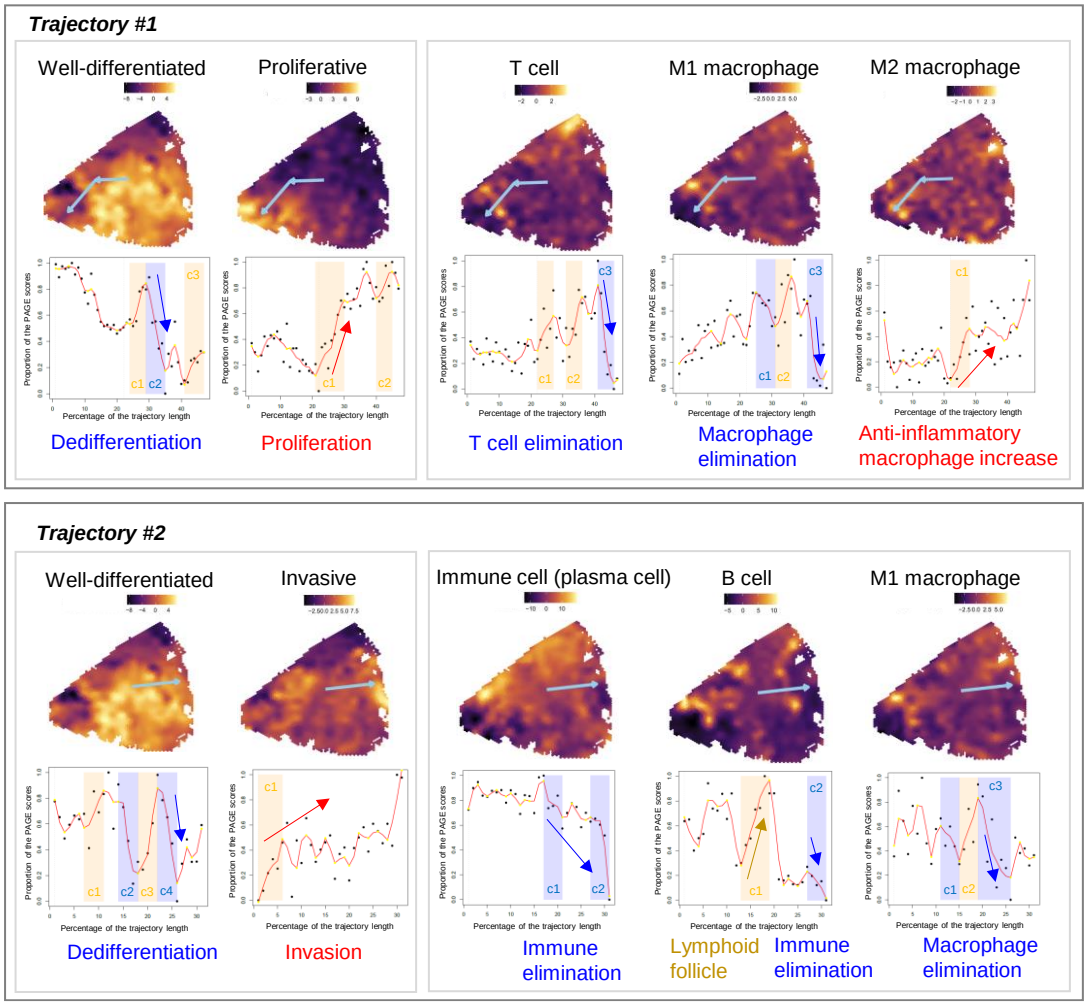
Trajectory #1
Well-differentiated
Proliferative
T cell
M1 macrophage
M2 macrophage
Dedifferentiation
Proliferation
T cell elimination
Macrophage elimination
Anti-inflammatory macrophage increase
Trajectory #2
Well-differentiated
Invasive
Immune cell (plasma cell)
B cell
M1 macrophage
Dedifferentiation
Invasion
Immune elimination
Lymphoid follicle
Immune elimination
Macrophage elimination

f

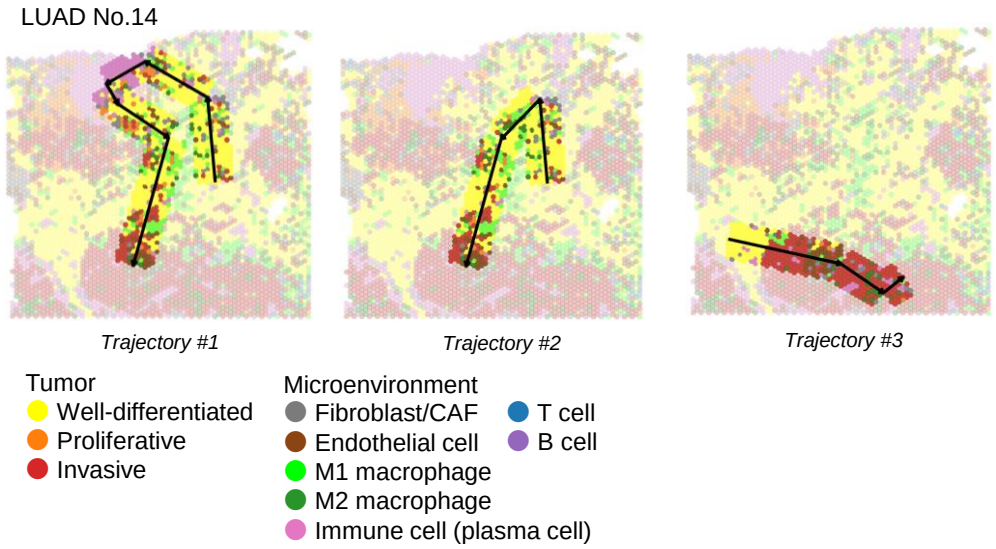
LUAD No.14
Trajectory #1
Trajectory #2
Trajectory #3
Tumor
Well-differentiated
Proliferative
Invasive
Microenvironment
Fibroblast/CAF
Endothelial cell
M1 macrophage
M2 macrophage
Immune cell (plasma cell)
T cell
B cell

g

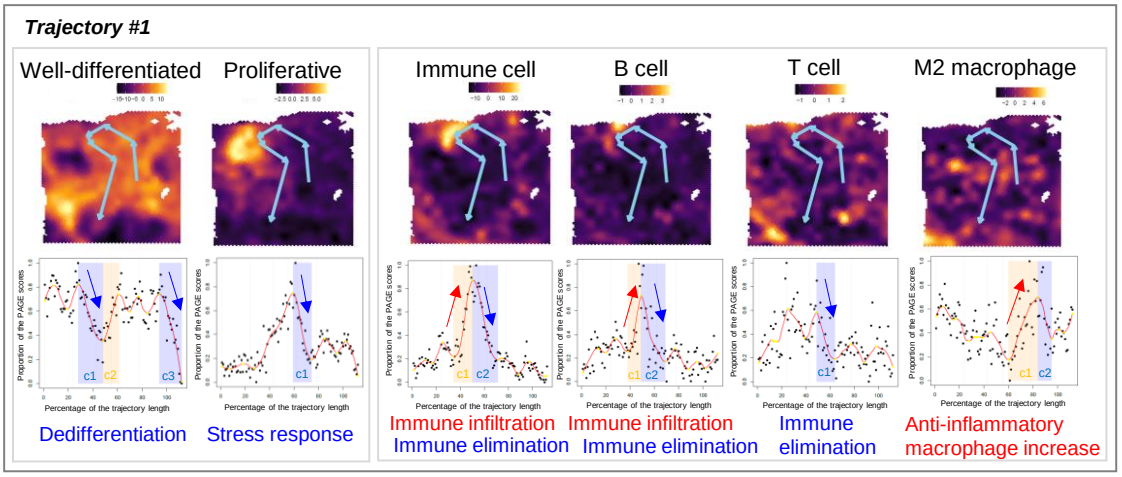
Trajectory #1
Well-differentiated
Proliferative
Immune cell
B cell
T cell
M2 macrophage
Dedifferentiation
Stress response
Immune infiltration
Immune elimination
Immune infiltration
Immune elimination
Immune elimination
Anti-inflammatory macrophage increase

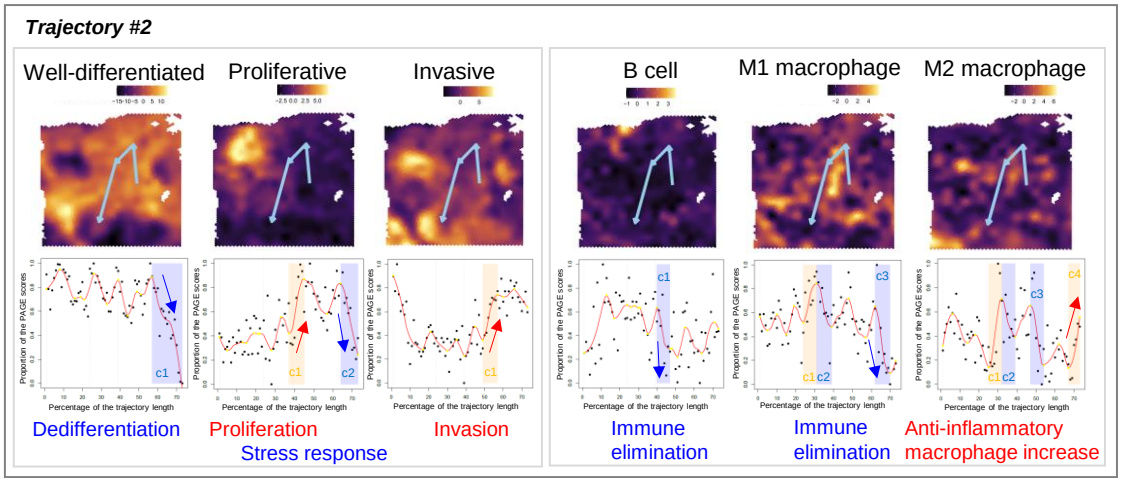
Trajectory #2
Well-differentiated
Proliferative
Invasive
B cell
M1 macrophage
M2 macrophage
Dedifferentiation
Proliferation
Stress response
Invasion
Immune elimination
Immune elimination
Anti-inflammatory macrophage increase

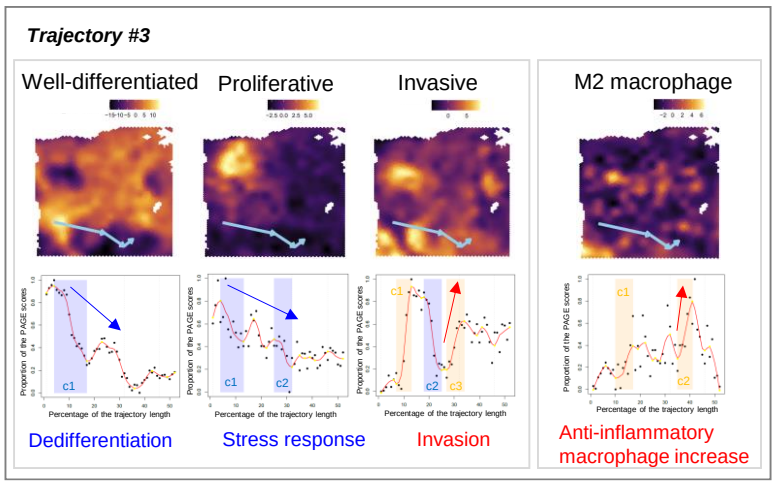

h

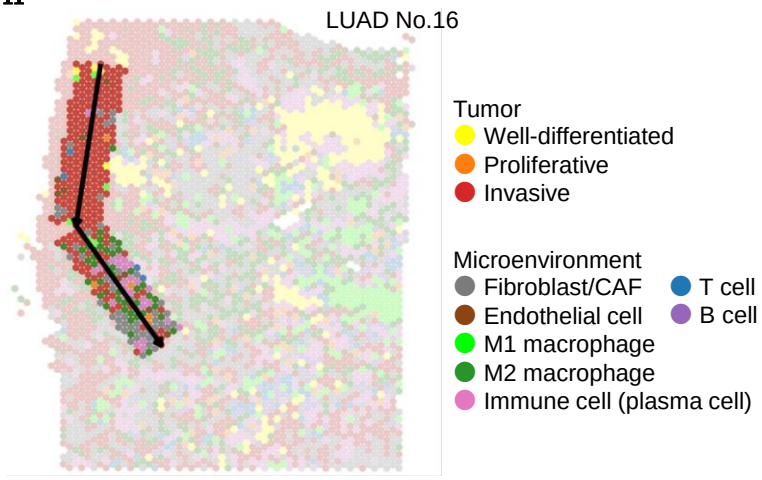

Trajectory #1

i

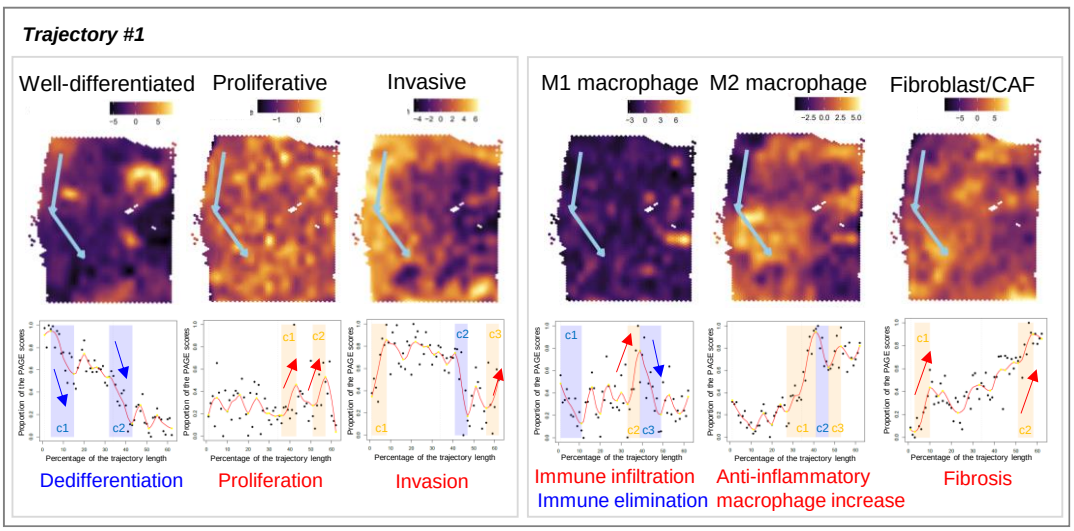

j

LUAD No.2 (FFPE, B)
Trajectory #1

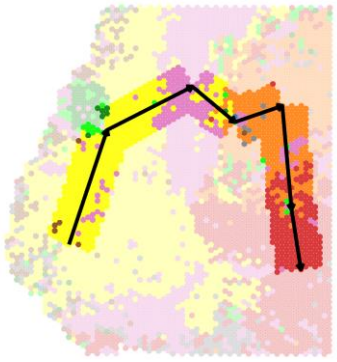

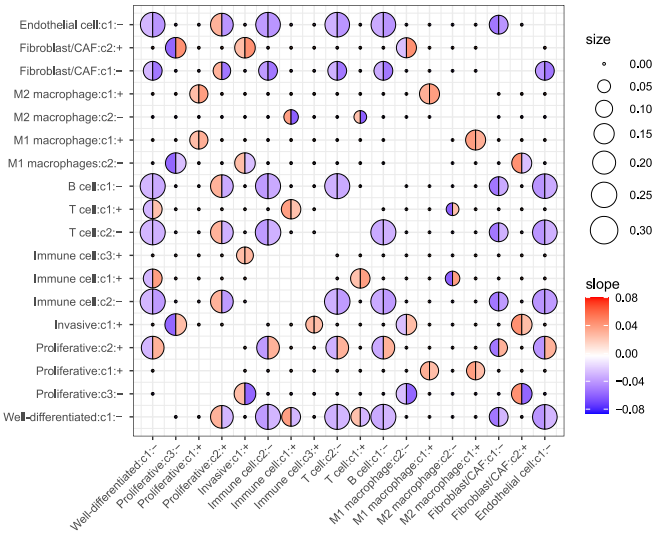

LUAD No.3 (FFPE, B)
Trajectory #1

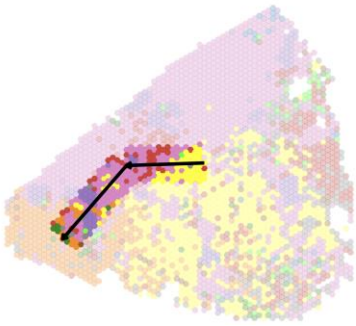

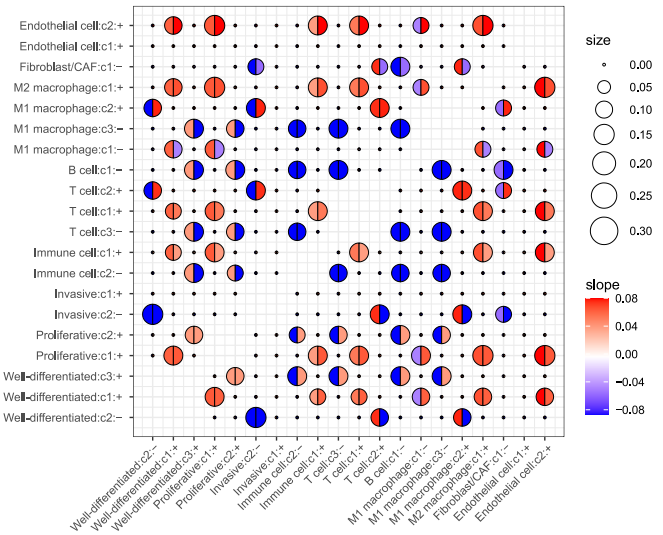

LUAD No.3 (FFPE, B)
Trajectory #2

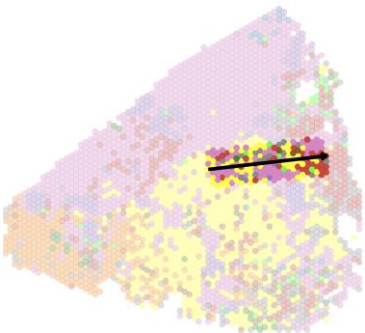

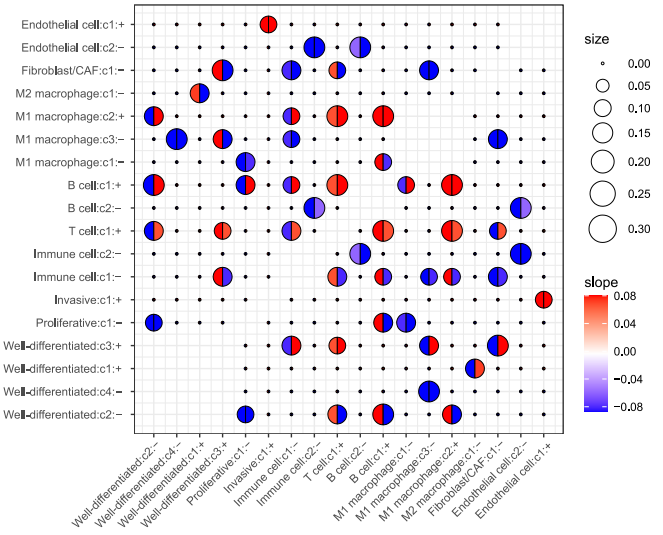

LUAD No.14
Trajectory #1

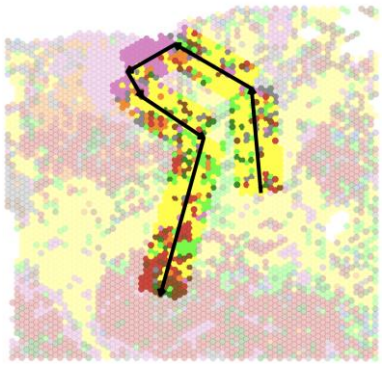

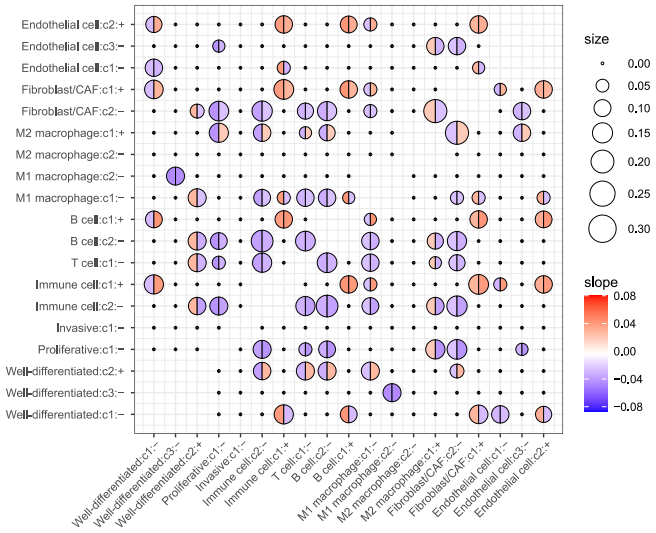

LUAD No.14
Trajectory #2

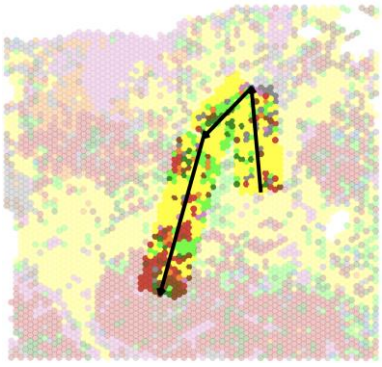

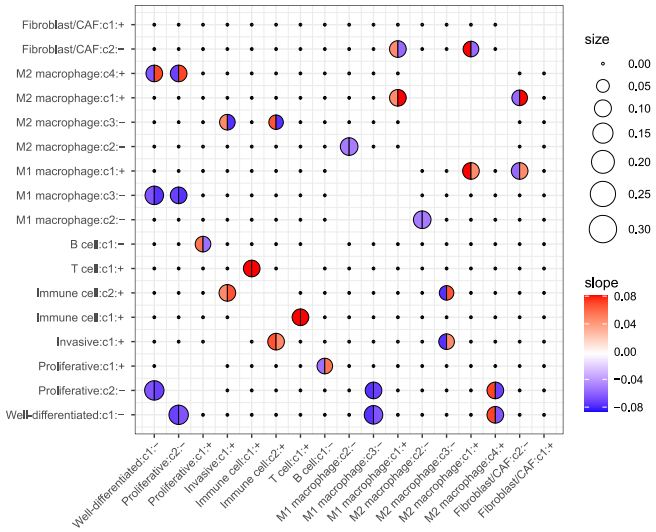

LUAD No.14
Trajectory #3

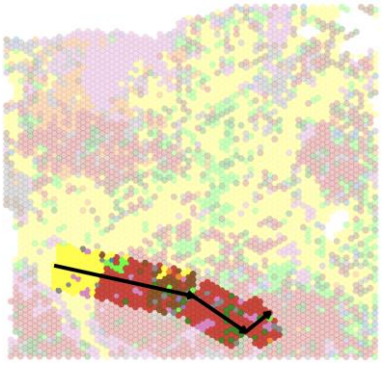

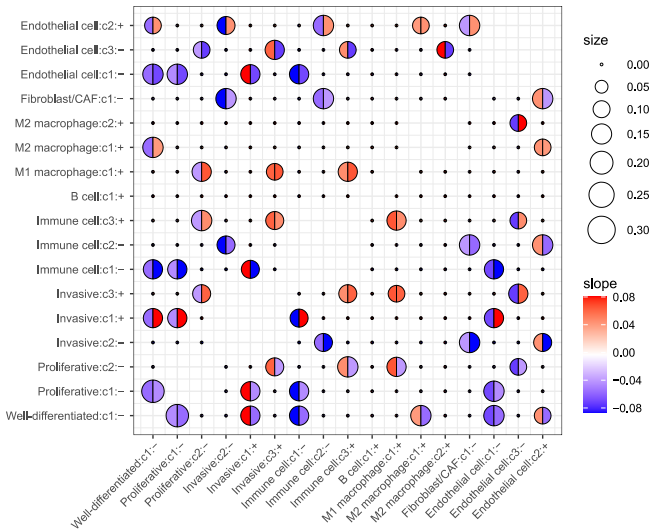

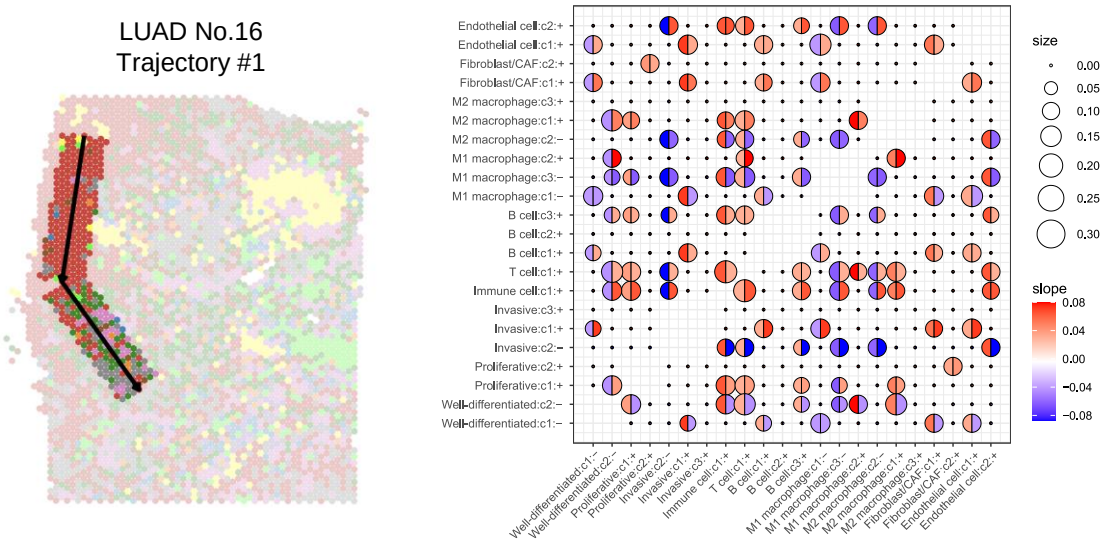

Supplementary Figure S8 Evaluation of changes of TME scores in IA cases

(**a**) A workflow for TME scoring to evaluate TME changes in IA cases. (**b**, **c**) TME scores and spatial transcriptome trajectory in LUAD No. 2 FFPE section B. (**b**) The most dominant TMEs in each spot were colored according to the color legend. (**c**) The spatial distribution of the scores is shown in each TME (top). The changes in the TME score and the trajectory are shown on dot plots (bottom). Smoothened lines are shown in red. (**d**, **e**) TME scores and two spatial transcriptome trajectories in LUAD No. 3 FFPE section B are presented as in **b** and **c**. (**f**, **g**) TME scores and three spatial transcriptome trajectories in LUAD No. 14 FF are shown as in **b** and **c**. (**h**, **i**) TME scores and spatial transcriptome trajectory in LUAD No. 16 FF as shown in **b** and **c**. (**j**) Relationships between each TME pair. Source data are provided as a Source Data file for **j**.

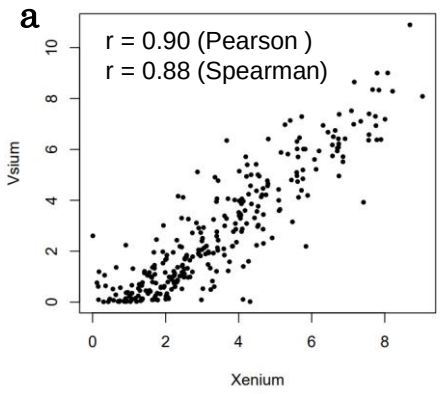

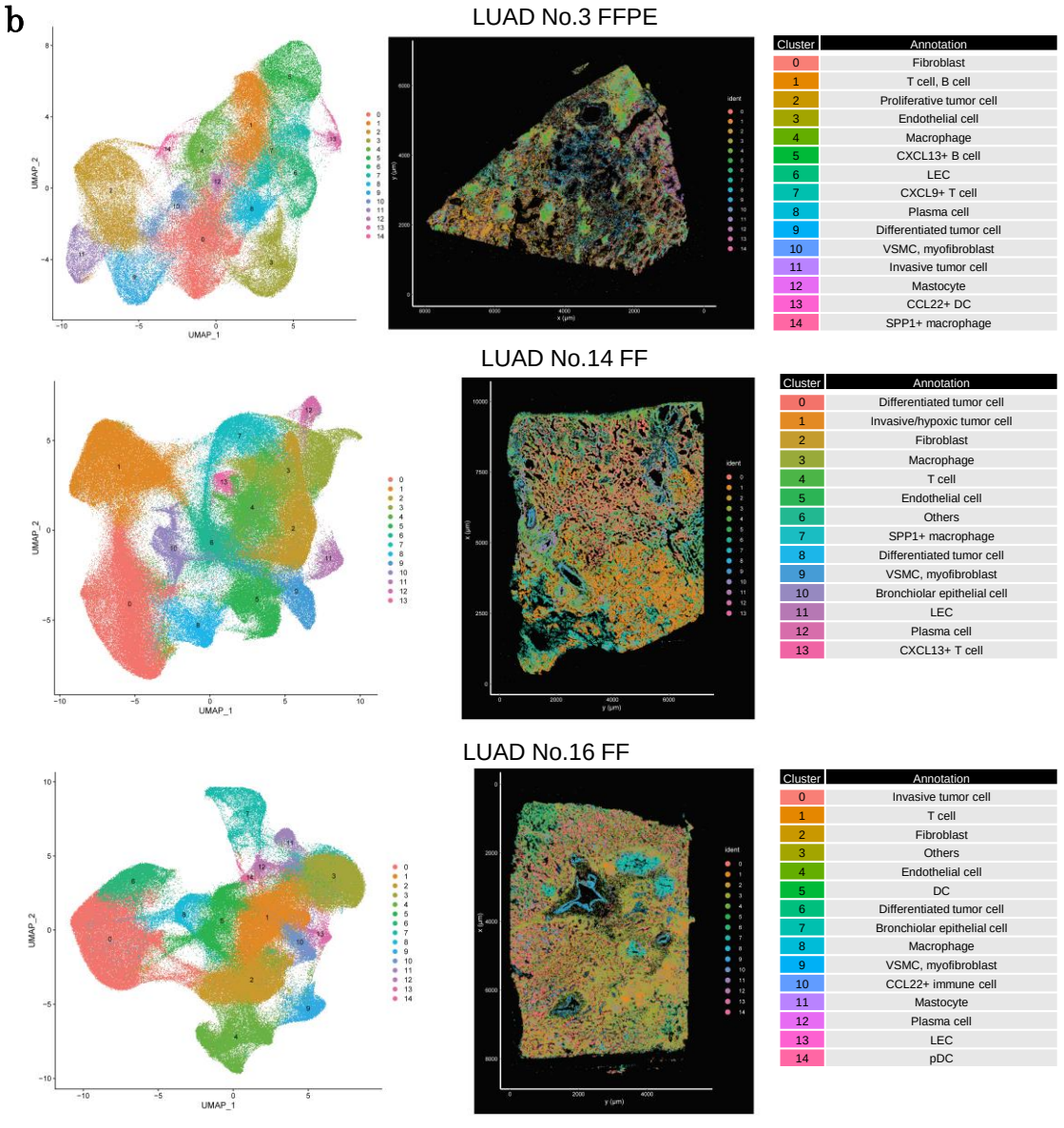

Cluster	Annotation
0	Fibroblast
1	T cell, B cell
2	Proliferative tumor cell
3	Endothelial cell
4	Macrophage
5	CXCL13+ B cell
6	LEC
7	CXCL9+ T cell
8	Plasma cell
9	Differentiated tumor cell
10	VSMC, myofibroblast
11	Invasive tumor cell
12	Mastocyte
13	CCL22+ DC
14	SPP1+ macrophage

Cluster	Annotation
0	Differentiated tumor cell
1	Invasive/hypoxic tumor cell
2	Fibroblast
3	Macrophage
4	T cell
5	Endothelial cell
6	Others
7	SPP1+ macrophage
8	Differentiated tumor cell
9	VSMC, myofibroblast
10	Bronchiolar epithelial cell
11	LEC
12	Plasma cell
13	CXCL13+ T cell

Cluster	Annotation
0	Invasive tumor cell
1	T cell
2	Fibroblast
3	Others
4	Endothelial cell
5	DC
6	Differentiated tumor cell
7	Bronchiolar epithelial cell
8	Macrophage
9	VSMC, myofibroblast
10	CCL22+ immune cell
11	Mastocyte
12	Plasma cell
13	LEC
14	pDC

LUAD No.17 FF

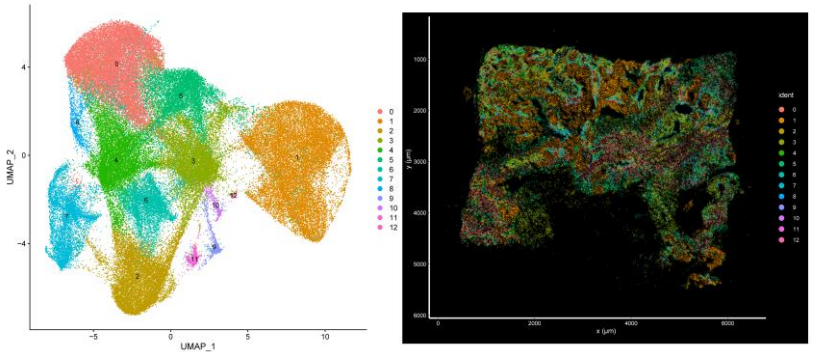

Cluster	Annotation
0	Fibroblast
1	Tumor cell
2	Plasma cell
3	Others
4	DC, macrophage
5	SPP1+ macrophage
6	T cell
7	Endothelial cell
8	IDO1+ fibroblast
9	LEC
10	Mastocyte
11	CXCL13+ T cell
12	Invasive tumor cell

c

LUAD No. 3 (FFPE, A)

LUAD No. 3 (FFPE, B)

Cell types (clusters of Xenium) in LUAD No. 3 FFPE

0	Fibroblast
1	T cell, B cell
2	Proliferative tumor cell
3	Endothelial cell
4	Macrophage
5	CXCL13+ B cell
6	LEC
7	CXCL9+ T cell
8	Plasma cell
9	Differentiated tumor cell
10	VSMC, myofibroblast
11	Invasive tumor cell
12	Mastocyte
13	CCL22+ DC
14	SPP1+ macrophage

LUAD No. 14 (FF)

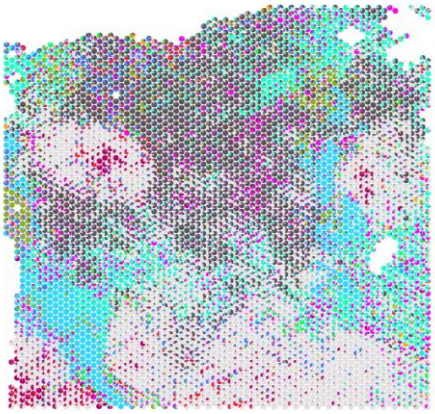

Cell types (clusters of Xenium) in LUAD No. 14 FF

0	Differentiated tumor cell
1	Invasive/hypoxic tumor cell
2	Fibroblast
3	Macrophage
4	T cell
5	Endothelial cell
6	Others
7	SPP1+ macrophage
8	Differentiated tumor cell
9	VSMC, myofibroblast
10	Bronchiolar epithelial cell
11	LEC
12	Plasma cell
13	CXCL13+ T cell

LUAD No. 16 (FF)

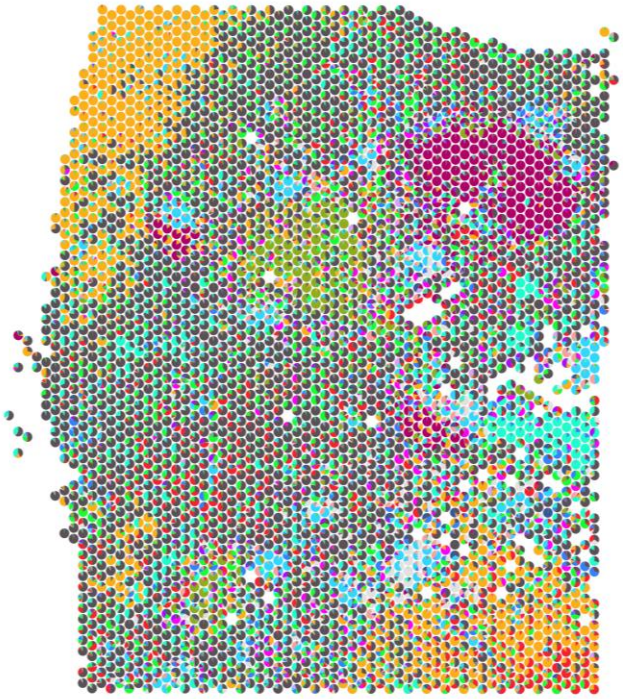

Cell types (clusters of Xenium) in LUAD No. 16 FF

0	Invasive tumor cell
1	T cell
2	Fibroblast
3	Others
4	Endothelial cell
5	DC
6	Differentiated tumor cell
7	Bronchiolar epithelial cell
8	Macrophage
9	VSMC, myofibroblast
10	CCL22+ immune cell
11	Mastocyte
12	Plasma cell
13	LEC
14	pDC

LUAD No. 17 (FF)

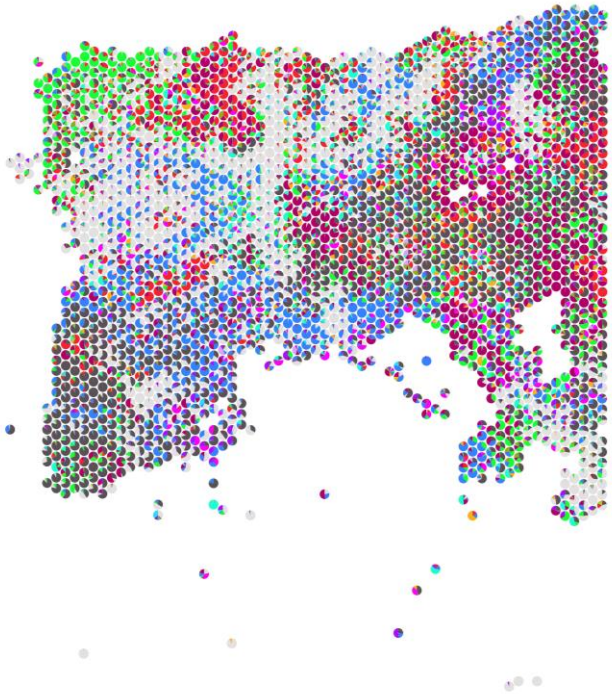

Cell types (clusters of Xenium) in LUAD No. 17 FF

0	Fibroblast
1	Tumor cell
2	Plasma cell
3	Others
4	DC, macrophage
5	SPP1+ macrophage
6	T cell
7	Endothelial cell
8	IDO1+ fibroblast
9	LEC
10	Mastocyte
11	CXCL13+ T cell
12	Invasive tumor cell

d

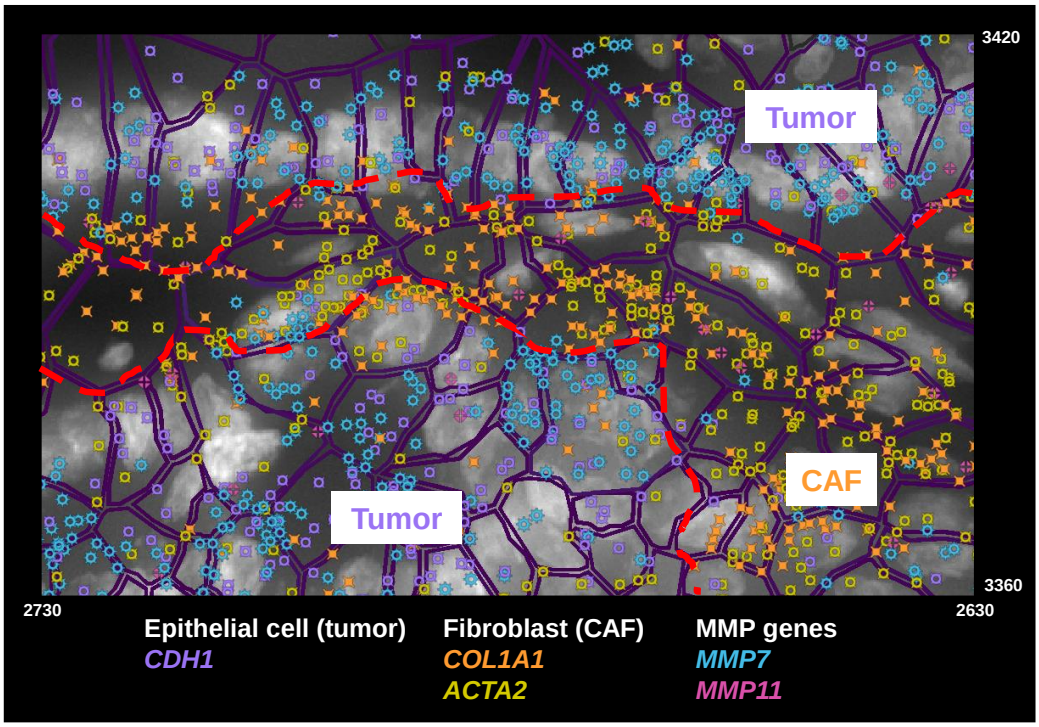
3420
Tumor
CAF
Tumor
3360
2730
2630
Epithelial cell (tumor)
CDH1
Fibroblast (CAF)
COL1A1
ACTA2
MMP genes
MMP7
MMP11

e

(i)

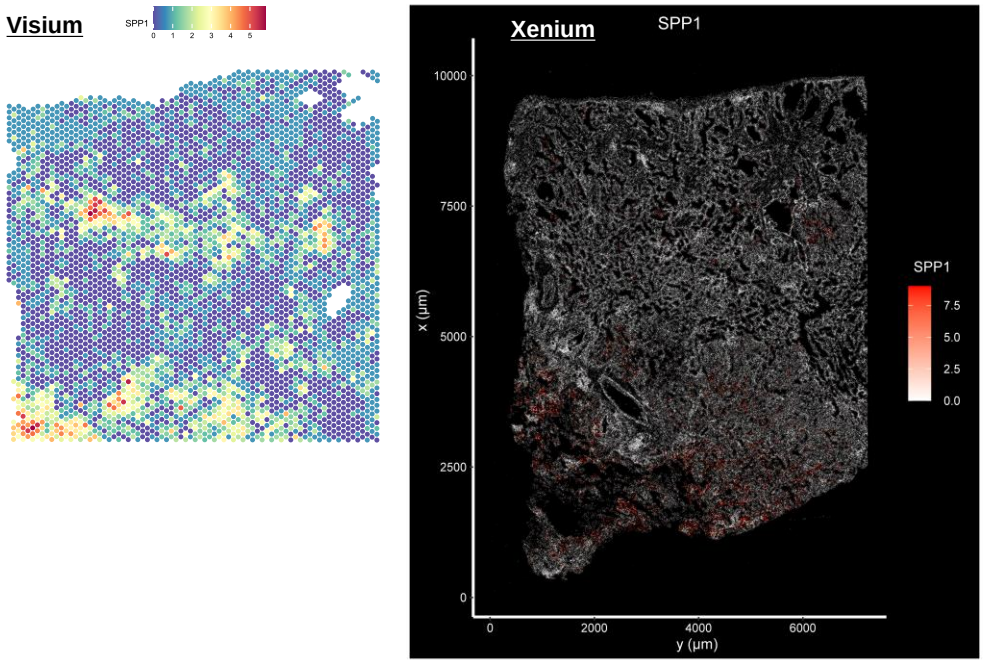
Visium
SPP1
0 1 2 3 4 5
Xenium
SPP1
10000
7500
5000
2500
0
x (µm)
0
2000
4000
6000
y (µm)
SPP1
7.5
5.0
2.5
0.0

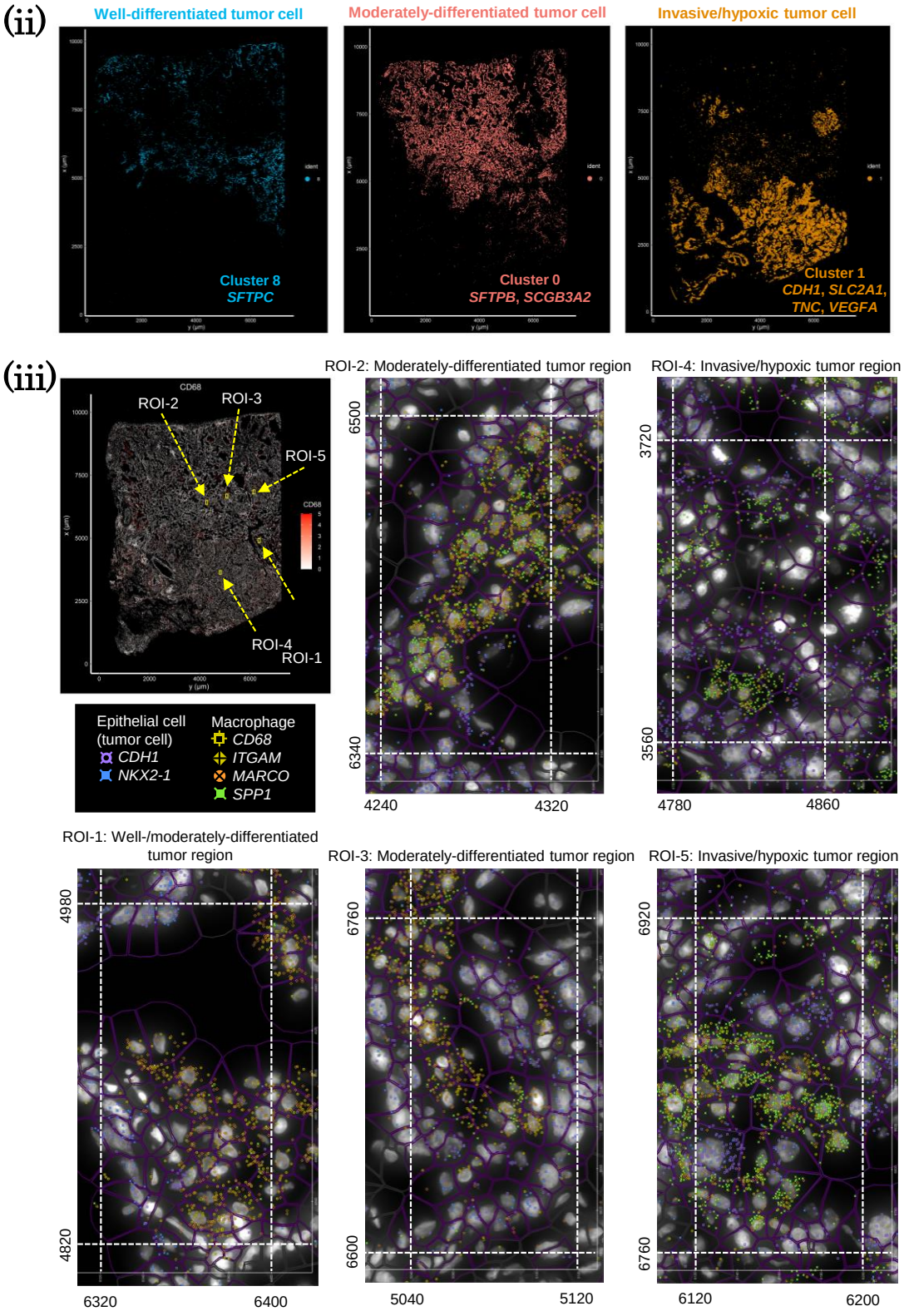
(ii)
Well-differentiated tumor cell
Moderately-differentiated tumor cell
Invasive/hypoxic tumor cell
Cluster 8
SFTPC
Cluster 0
SFTPB, SCGB3A2
Cluster 1
CDH1, SLC2A1,
TNC, VEGFA
(iii)
CD68
ROI-2
ROI-3
ROI-5
ROI-4
ROI-1
Epithelial cell
(tumor cell)
CDH1
NKX2-1
Macrophage
CD68
ITGAM
MARCO
SPP1
ROI-2: Moderately-differentiated tumor region
ROI-4: Invasive/hypoxic tumor region
ROI-1: Well-/moderately-differentiated
tumor region
ROI-3: Moderately-differentiated tumor region
ROI-5: Invasive/hypoxic tumor region

Supplementary Figure S9 Spatial and single-cell expression analysis using Xenium for five IA cases

(**a**) A comparison of expression levels (aggregated bulk) in Visium and Xenium of LUAD No.2 FFPE. Each dot represents one gene. (**b**) Clustering analysis results for Xenium of LUAD No. 3 FFPE, No. 14, 16, and 17 (the result of LUAD No. 2 FFPE is shown in **Figure 6**). The left and middle panels show the UMAP plot with cluster annotations, as well as the spatial plot. The annotation for each cluster is shown in the table in the right panel, respectively. (**c**) Deconvolution of Visium using Xenium data. On the left, the spatial plot of Visium is accompanied by pie charts showing the proportion of cell types. On the right, the table presents information of each cell type (Xenium cluster). (**d**) Association between tumor cells and adjacent CAFs at the single-cell level in the invasive region (as shown in **Figure 6f**). MMP represents matrix metalloproteinase. (**e**) Characterization of macrophages in LUAD No. 14 FF. (i) The expression pattern of *SPP1* is shown in Visium and Xenium data in the left and right panels, respectively. (ii) The spatial distribution of clusters 8 (well-differentiated tumor cell), 0 (moderately-differentiated tumor region), and 1 (invasive/hypoxic tumor region). (iii) The distribution of macrophages is shown by Xenium Explorer. Macrophages expressing high levels of *SPP1* increased in invasive tumor regions.

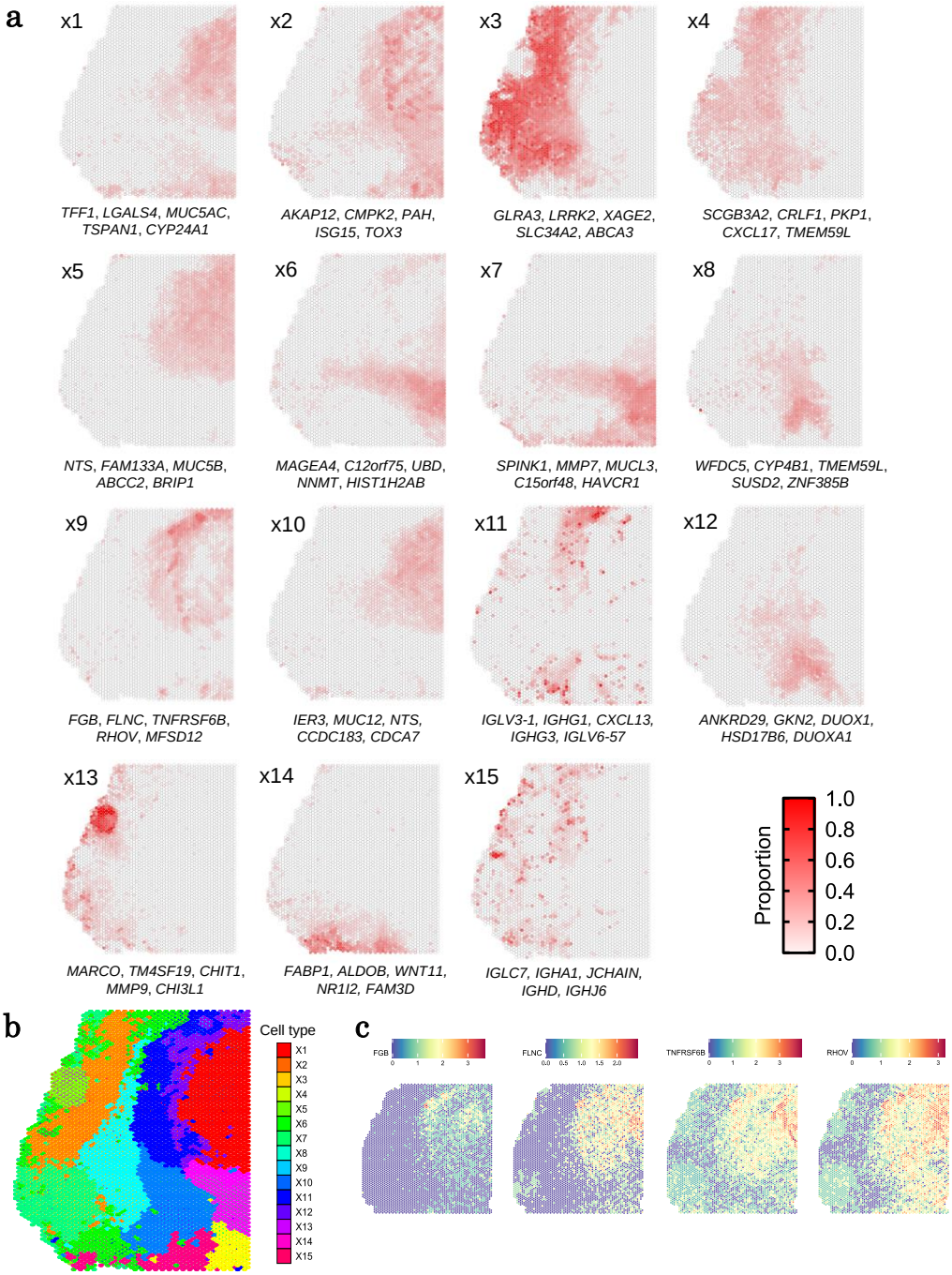

Supplementary Figure S10 Reference-free cell-type deconvolution analysis of Visium

(**a**) Spatial plots of cell proportions for 15 cell-types in LUAD No. 2 FFPE section C, obtained using reference-free cell-type deconvolution analysis[4]. (**b**) The spatial plot of Visium is presented using pie charts showing the proportion of the 15 cell-types. (**c**) Expression patterns of genes specific to the cell-type X9 in Visium data.

Supplementary Figure S11

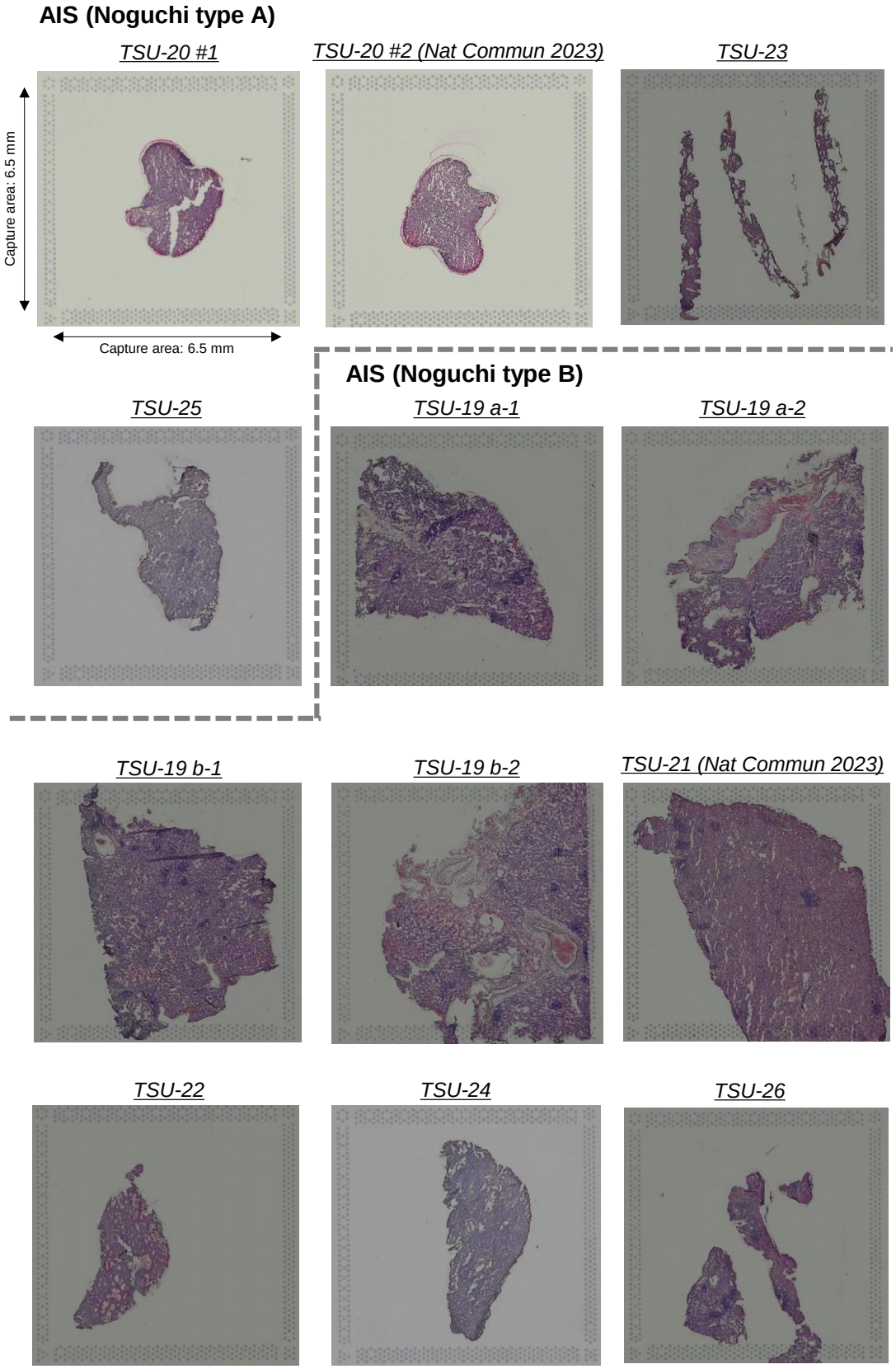

Supplementary Figure S11

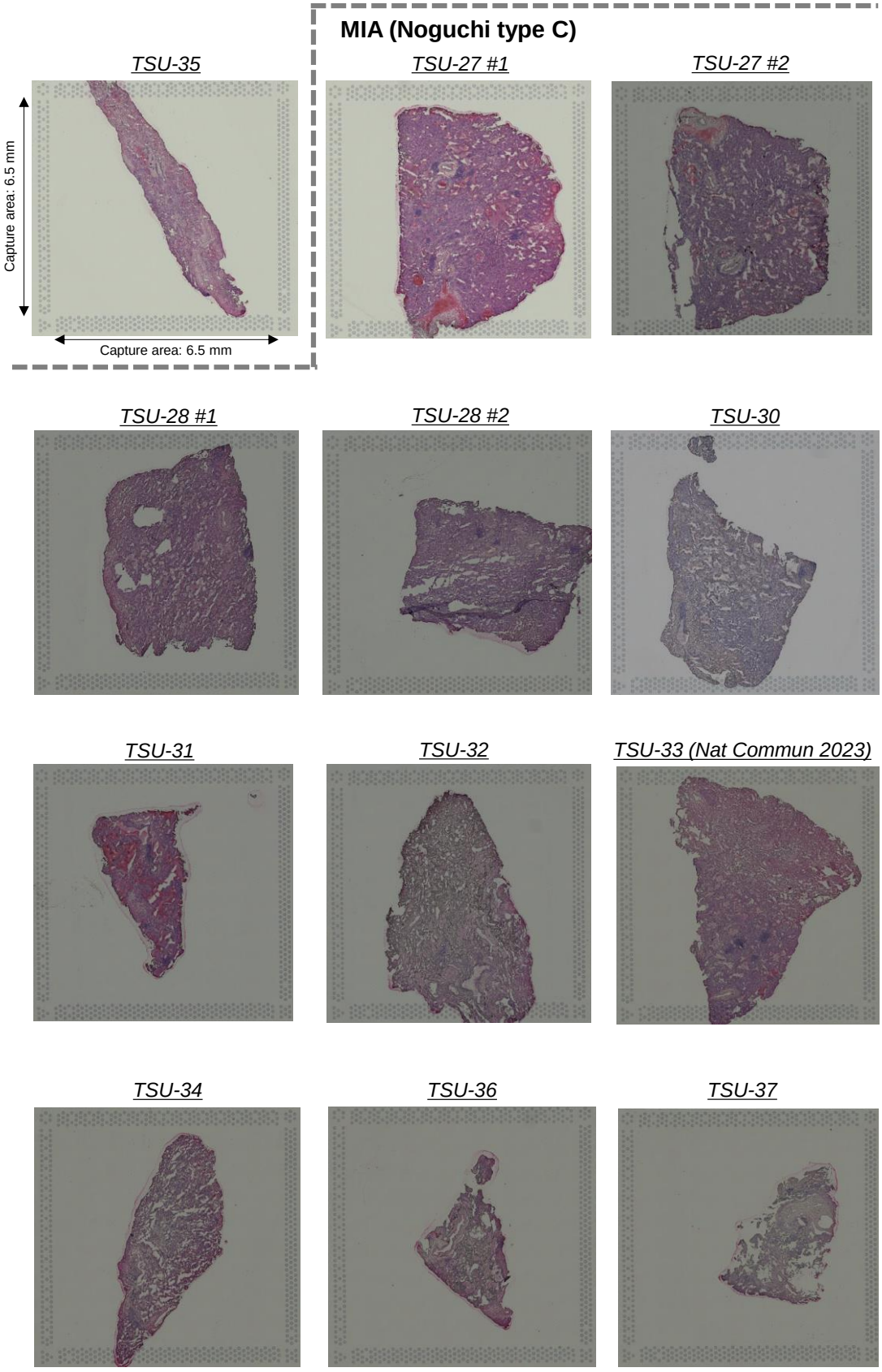

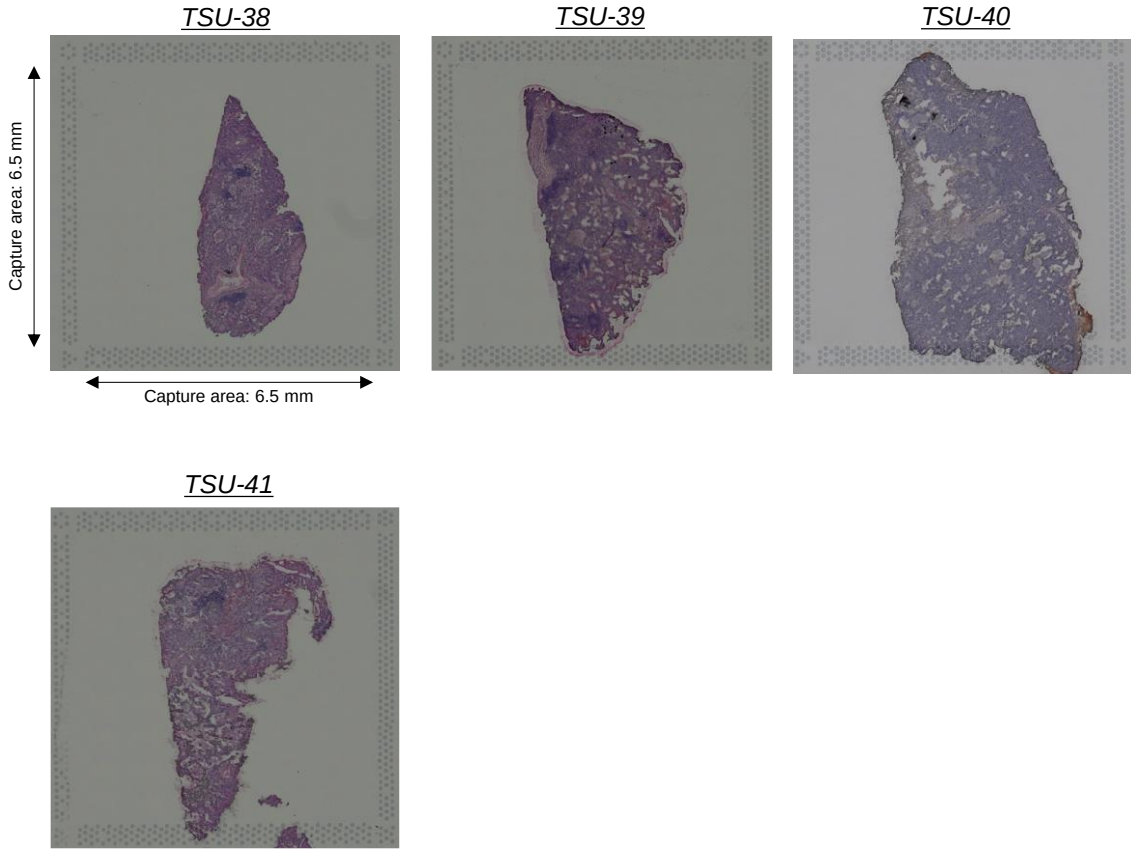

Supplementary Figure S11 H&E images of Visium FF data in 22 early cases

H&E images for Visium analysis. The study presents data from 28 sections taken from patients with adenocarcinoma *in situ* (AIS) and minimally invasive adenocarcinoma (MIA). The capture area that is surrounded by the fiducial frame in the H&E is 6.5 mm × 6.5 mm.

Supplementary Figure S12

AIS (Noguchi type A)

TSU-20 #1 *TSU-20 #2 (Nat Commun 2023)* *TSU-23* *TSU-25*

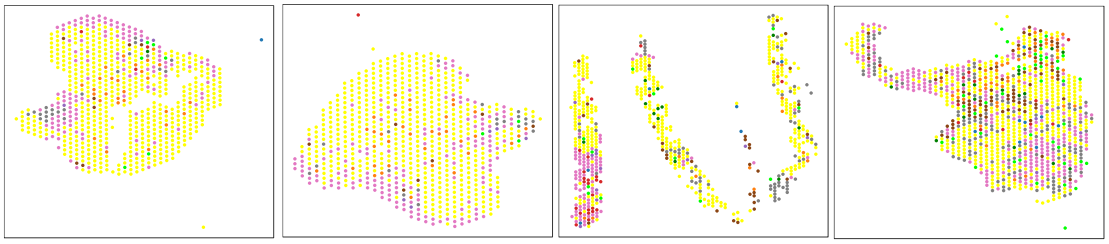

AIS (Noguchi type B)

TSU-19 a-1 *TSU-19 a-2* *TSU-19 b-1* *TSU-19 b-2*

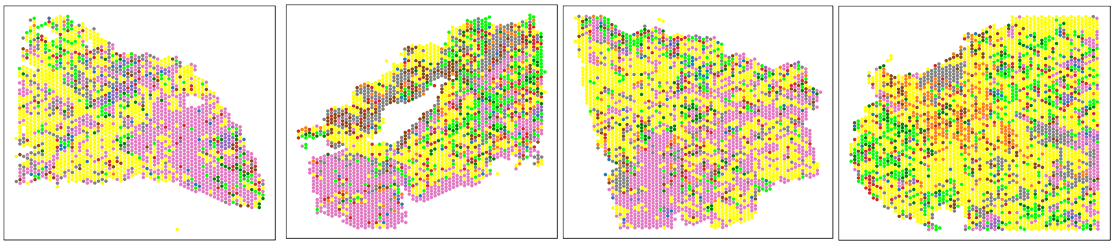

TSU-21 (Nat Commun 2023) *TSU-22* *TSU-24* *TSU-26*

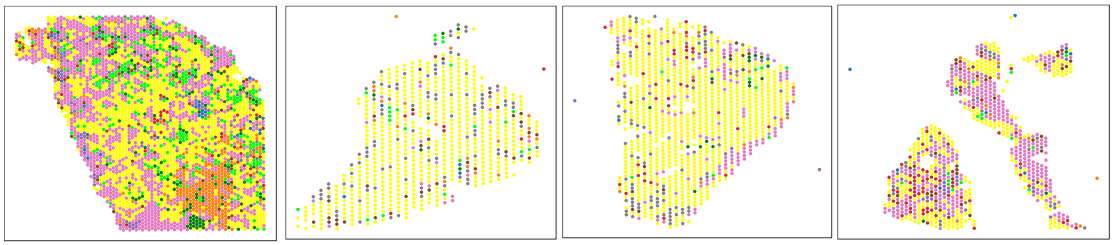

TSU-35

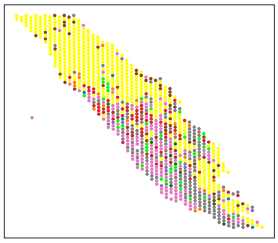

Early-Ad; MIA (Noguchi type C)

TSU-27 #1 *TSU-27 #2* *TSU-28 #1* *TSU-28 #2*

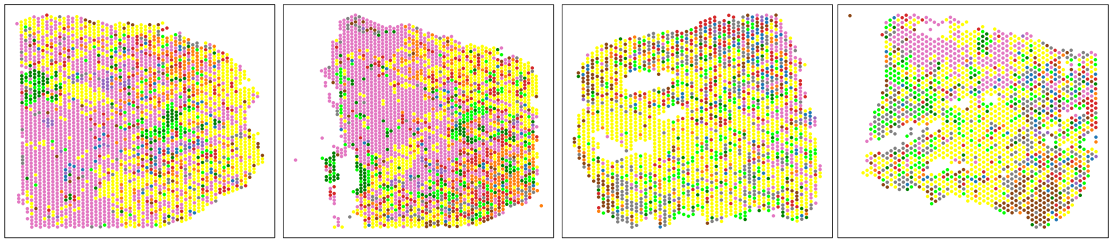

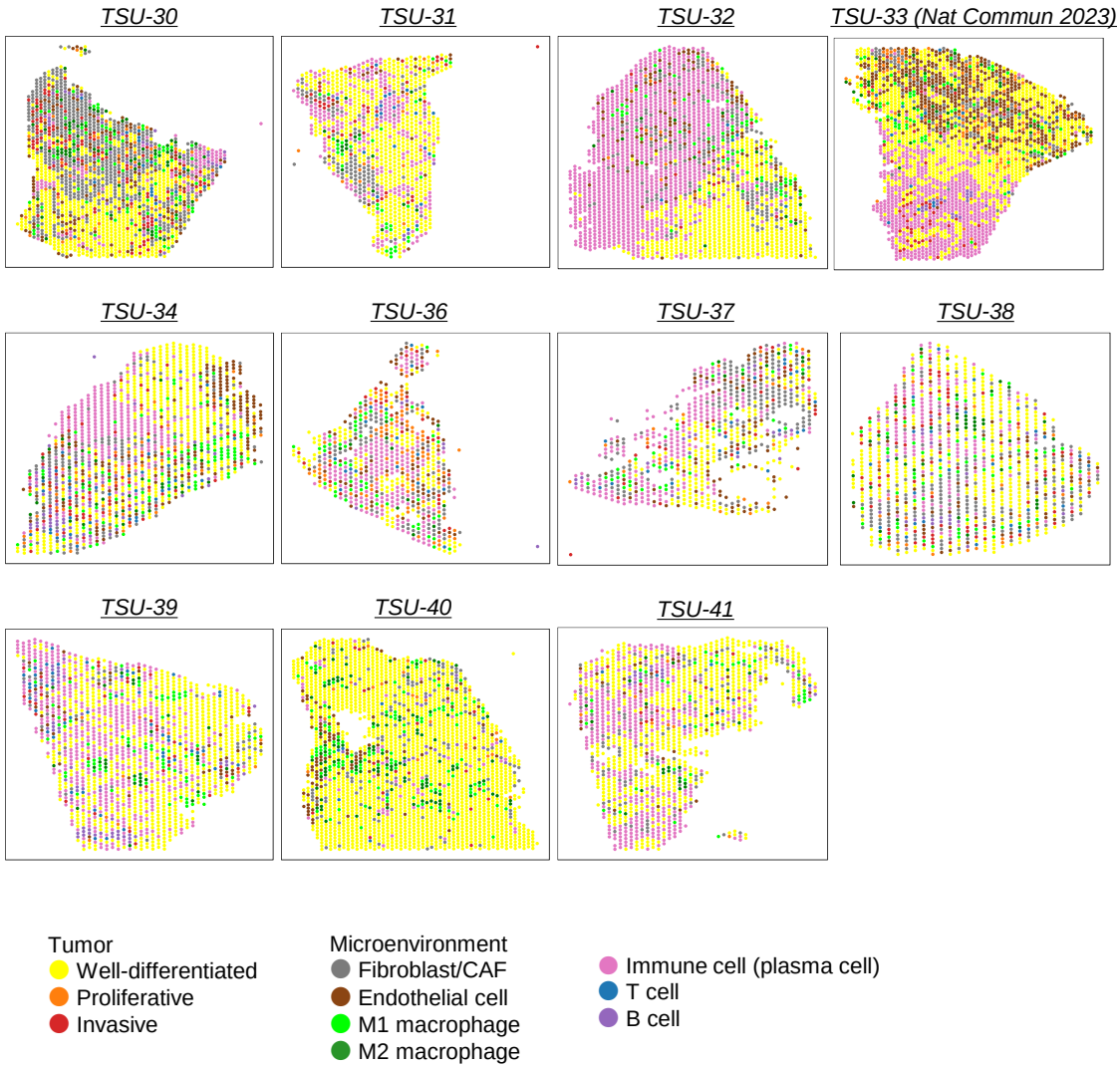

Supplementary Figure S12 TME scoring in AIS/MIA cases

Features are arranged according to TME scoring in AIS and MIA cases. The color legend appears in the margin.

a

Step 1. Weighting proliferative/invasive spots by distance for each spot

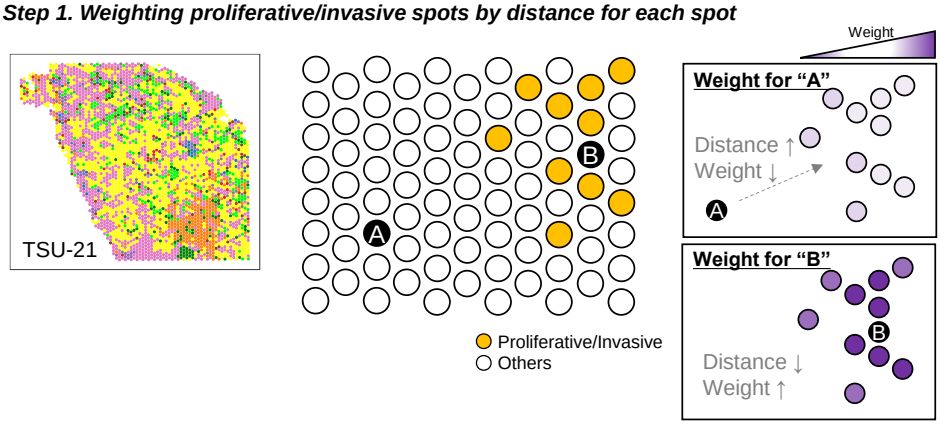

Step 2. Calculating local enrichment score by summing the weighted counts in all spots

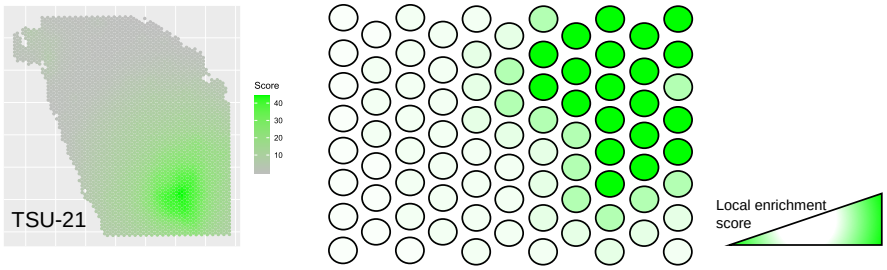

Step 3. Defining "possibly malignant" regions by gathering spots with high local enrichment scores

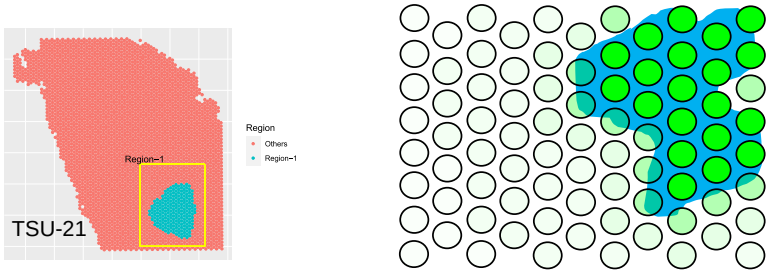

Step 4. Comparing gene expression patterns between spots in the possibly malignant region and others

b

AIS (Noguchi type A)

TSU-20 #1

Local enrichment score of "proliferative"

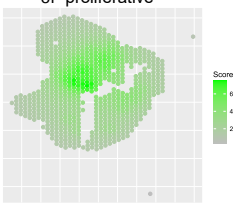

Max: 7.5; Threshold set to 10

Possibly malignant-proliferative region

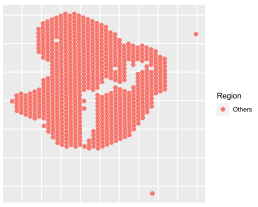

No possibly malignant regions

Local enrichment score of "invasive"

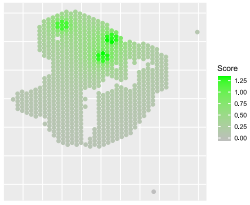

Max: 1.3; Threshold set to 10

Possibly malignant-invasive region

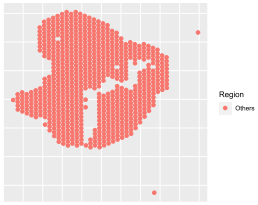

No possibly malignant regions

TSU-20 #2 (Nat Commun 2023)

Local enrichment score of "proliferative"

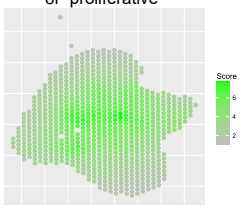

Max: 7.7; Threshold set to 10

Possibly malignant-proliferative region

No possibly malignant regions

Local enrichment score of "invasive"

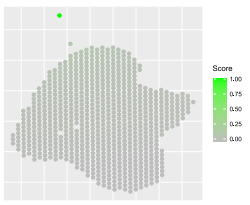

Max: 1.0; Threshold set to 10

Possibly malignant-invasive region

No possibly malignant regions

TSU-23

Local enrichment score of "proliferative"

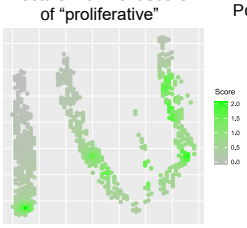

Max: 2.1; Threshold set to 10

Possibly malignant-proliferative region

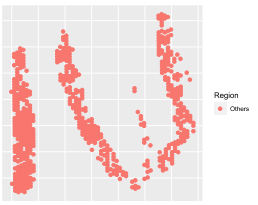

No possibly malignant regions

Local enrichment score of "invasive"

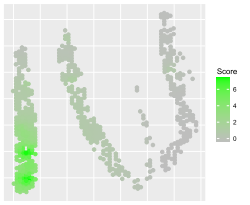

Max: 7.4; Threshold set to 10

Possibly malignant-invasive region

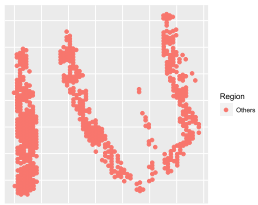

No possibly malignant regions

TSU-25

Local enrichment score of "proliferative"

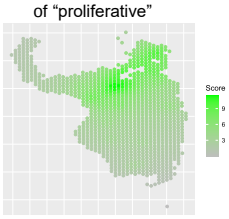

Max: 11.5; Threshold set to 10

Possibly malignant-proliferative region

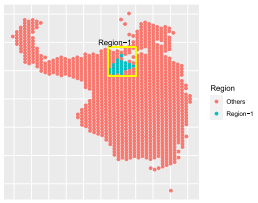

1 possibly malignant region

Local enrichment score of "invasive"

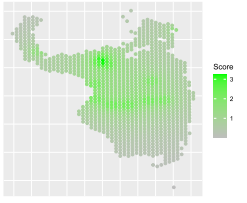

Max: 7.4; Threshold set to 10

Possibly malignant-invasive region

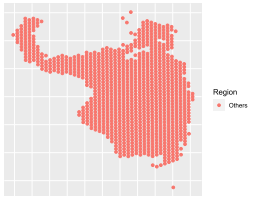

No possibly malignant regions

c

AIS (Noguchi type B)

TSU-19 a-1

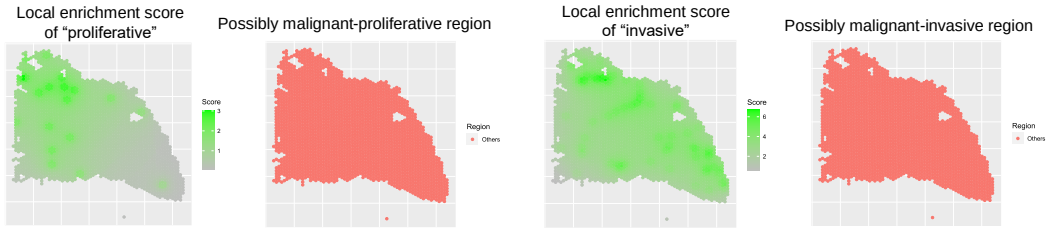

Max: 2.0; Threshold set to 10

No possibly malignant regions

Max: 6.7; Threshold set to 10

No possibly malignant regions

TSU-19 a-2

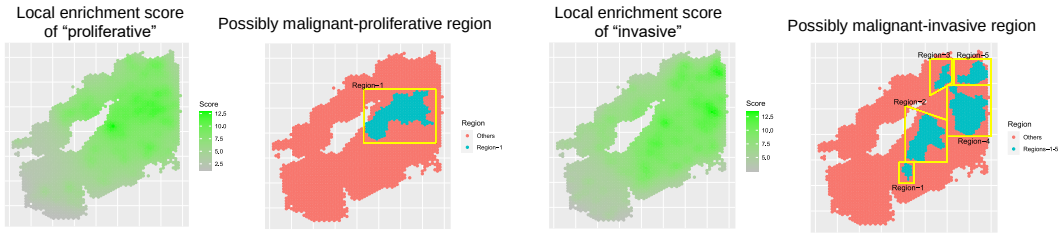

Max: 12.9; Threshold set to 10

1 possibly malignant region

Max: 13.4; Threshold set to 10

5 possibly malignant regions

TSU-19 b-1

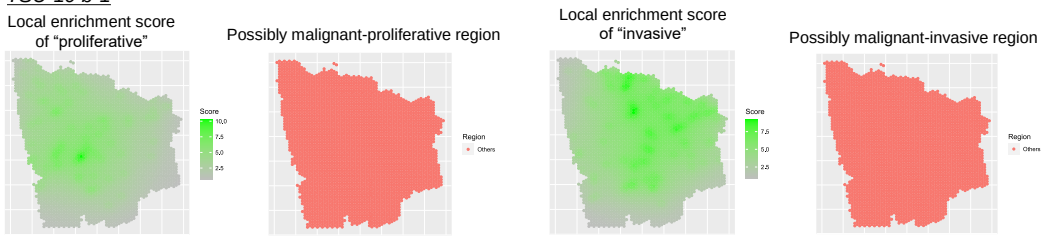

Max: 10.2; Threshold set to 10

No possibly malignant regions

Max: 9.2; Threshold set to 10

No possibly malignant regions

TSU-19 b-2

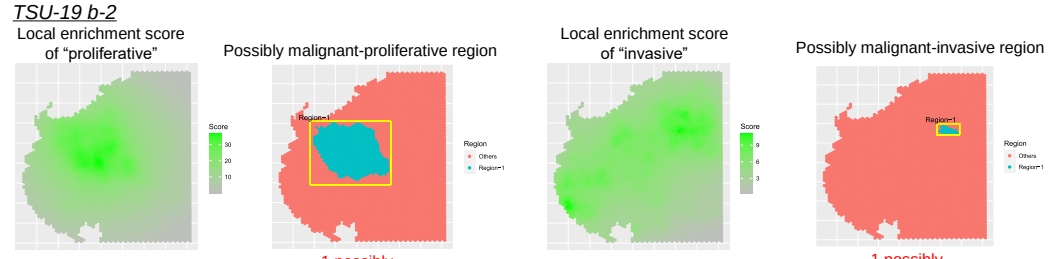

Max: 37.0; Threshold set to 25.9

1 possibly malignant region

Max: 11.1; Threshold set to 10

1 possibly malignant region

TSU-21 (Nat Commun 2023)

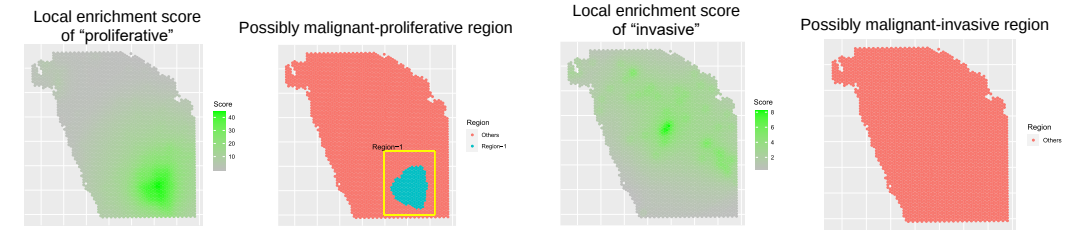

Max: 44.2; Threshold set to 31.0

1 possibly malignant region

Max: 8.2; Threshold set to 10

No possibly malignant regions

TSU-22

Local enrichment score of "proliferative"

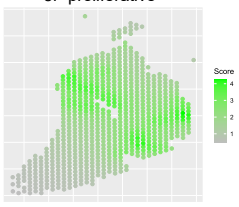

Max: 4.2; Threshold set to 10

Possibly malignant-proliferative region

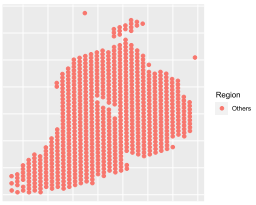

No possibly malignant regions

Local enrichment score of "invasive"

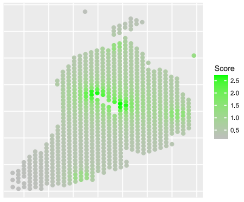

Max: 2.7; Threshold set to 10

Possibly malignant-invasive region

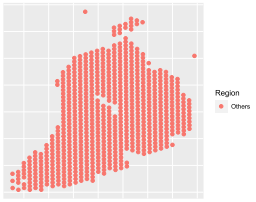

No possibly malignant regions

TSU-24

Local enrichment score of "proliferative"

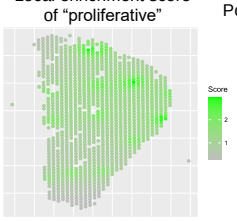

Max: 2.9; Threshold set to 10

Possibly malignant-proliferative region

No possibly malignant regions

Local enrichment score of "invasive"

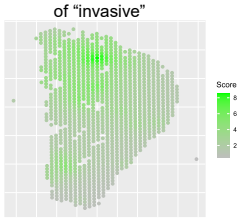

Max: 8.5; Threshold set to 10

Possibly malignant-invasive region

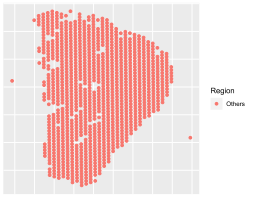

No possibly malignant regions

TSU-26

Local enrichment score of "proliferative"

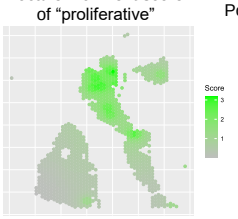

Max: 3.2; Threshold set to 10

Possibly malignant-proliferative region

No possibly malignant regions

Local enrichment score of "invasive"

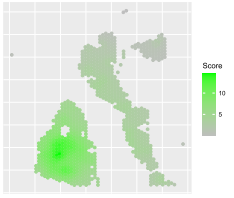

Max: 14.6; Threshold set to 10.2

Possibly malignant-invasive region

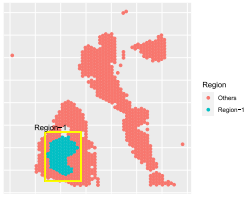

1 possibly malignant region

TSU-35

Local enrichment score of "proliferative"

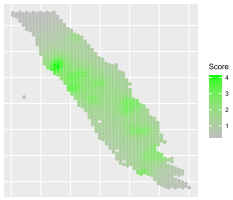

Max: 4.1; Threshold set to 10

Possibly malignant-proliferative region

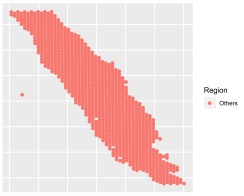

No possibly malignant regions

Local enrichment score of "invasive"

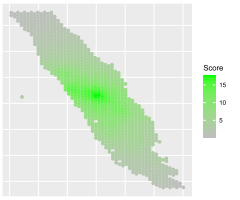

Max: 17.6; Threshold set to 12.3

Possibly malignant-invasive region

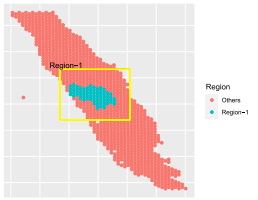

1 possibly malignant region

d

MIA (Noguchi type C)

TSU-27 #1

Local enrichment score of "proliferative"

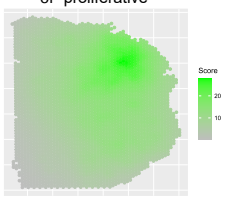

Max: 27.8; Threshold set to 19.5

Possibly malignant-proliferative region

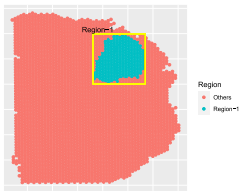

1 possibly malignant region

Local enrichment score of "invasive"

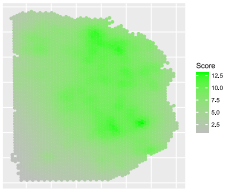

Max: 13.1; Threshold set to 10

Possibly malignant-invasive region

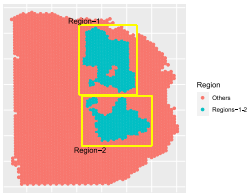

2 possibly malignant regions

TSU-27 #2

Local enrichment score of "proliferative"

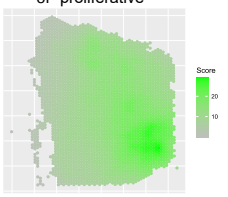

Max: 29.2; Threshold set to 20.5

Possibly malignant-proliferative region

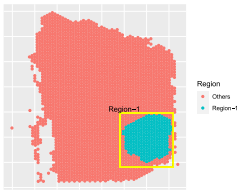

1 possibly malignant region

Local enrichment score of "invasive"

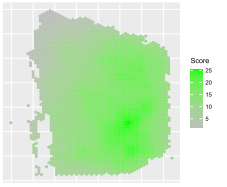

Max: 25.2; Threshold set to 17.7

Possibly malignant-invasive region

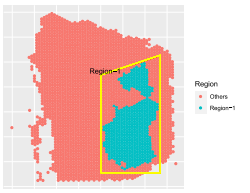

1 possibly malignant region

TSU-28 #1

Local enrichment score of "proliferative"

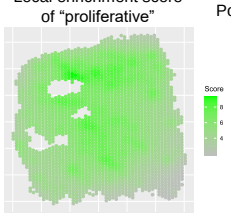

Max: 9.4; Threshold set to 10

Possibly malignant-proliferative region

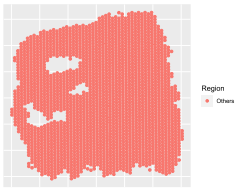

No possibly malignant regions

Local enrichment score of "invasive"

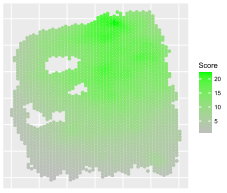

Max: 22.3; Threshold set to 15.6

Possibly malignant-invasive region

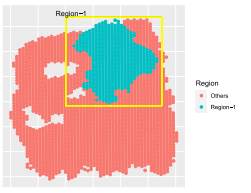

1 possibly malignant region

TSU-28 #2

Local enrichment score of "proliferative"

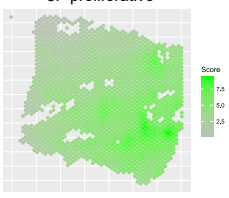

Max: 9.4; Threshold set to 10

Possibly malignant-proliferative region

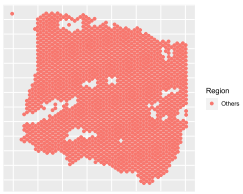

No possibly malignant regions

Local enrichment score of "invasive"

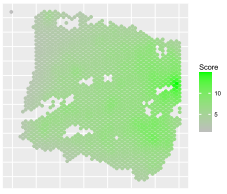

Max: 15.0; Threshold set to 10.5

Possibly malignant-invasive region

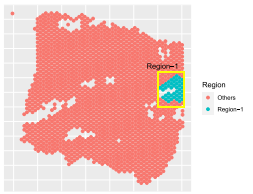

1 possibly malignant region

TSU-30

Local enrichment score of "proliferative"

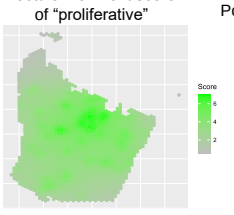

Max: 7.1; Threshold set to 10

Possibly malignant-proliferative region

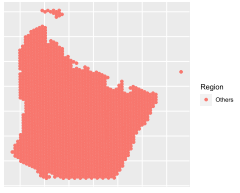

No possibly malignant regions

Local enrichment score of "invasive"

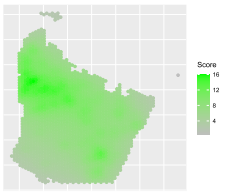

Max: 16.0; Threshold set to 11.2

Possibly malignant-invasive region

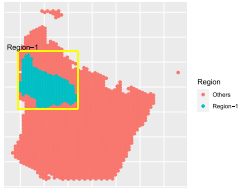

1 possibly malignant region

TSU-31

Local enrichment score of "proliferative"

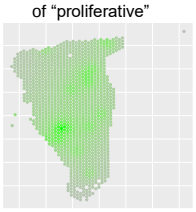

Max: 3.9; Threshold set to 10

Possibly malignant-proliferative region

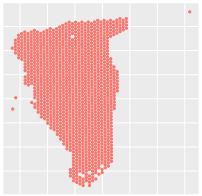

No possibly malignant regions

Local enrichment score of "invasive"

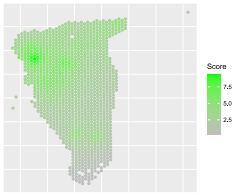

Max: 9.4; Threshold set to 10

Possibly malignant-invasive region

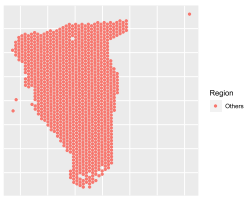

No possibly malignant regions

TSU-32

Local enrichment score of "proliferative"

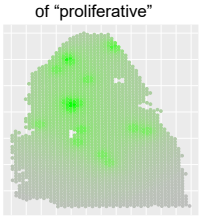

Max: 3.0; Threshold set to 10

Possibly malignant-proliferative region

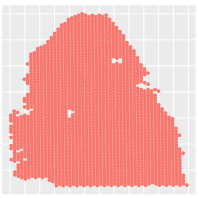

No possibly malignant regions

Local enrichment score of "invasive"

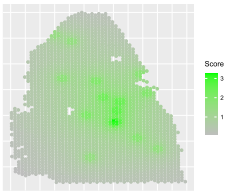

Max: 3.2; Threshold set to 10

Possibly malignant-invasive region

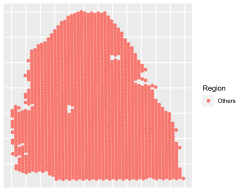

No possibly malignant regions

TSU-33 (Nat Commun 2023)

Local enrichment score of "proliferative"

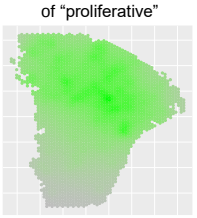

Max: 16.5; Threshold set to 11.6

Possibly malignant-proliferative region

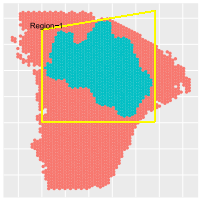

1 possibly malignant region

Local enrichment score of "invasive"

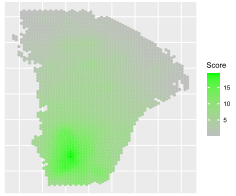

Max: 19.4; Threshold set to 13.6

Possibly malignant-invasive region

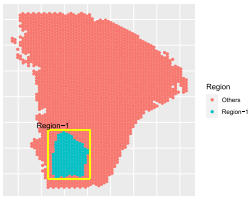

1 possibly malignant region

TSU-34

Local enrichment score of "proliferative"

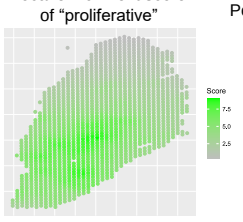

Max: 9.1; Threshold set to 10

Possibly malignant-proliferative region

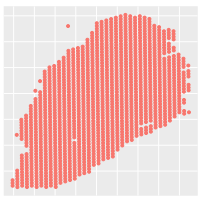

No possibly malignant regions

Local enrichment score of "invasive"

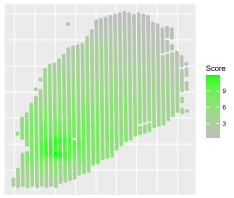

Max: 11.8; Threshold set to 10

Possibly malignant-invasive region

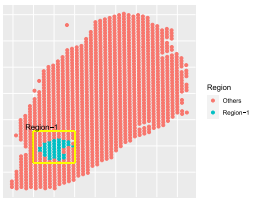

1 possibly malignant region

TSU-36

Local enrichment score of "proliferative"

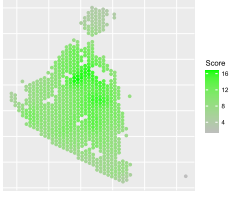

Max: 16.8; Threshold set to 11.8

Possibly malignant-proliferative region

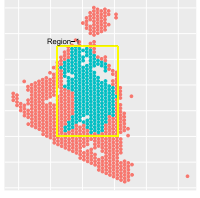

1 possibly malignant region

Local enrichment score of "invasive"

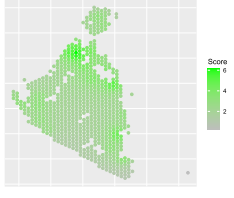

Max: 6.1; Threshold set to 10

Possibly malignant-invasive region

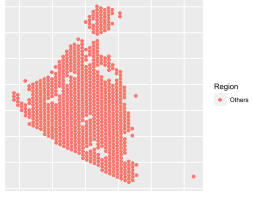

No possibly malignant regions

TSU-37

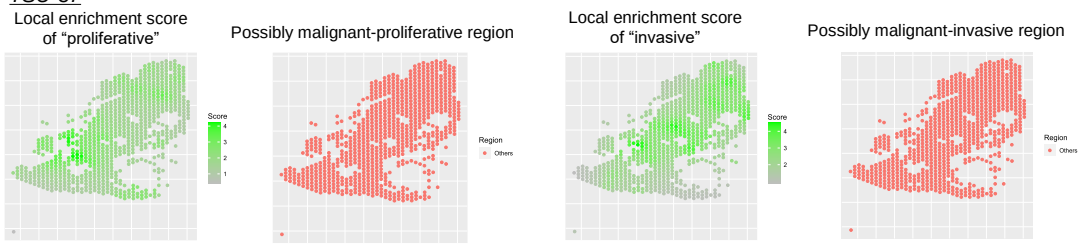

Max: 4.2; Threshold set to 10

No possibly malignant regions

Max: 4.5; Threshold set to 10

No possibly malignant regions

TSU-38

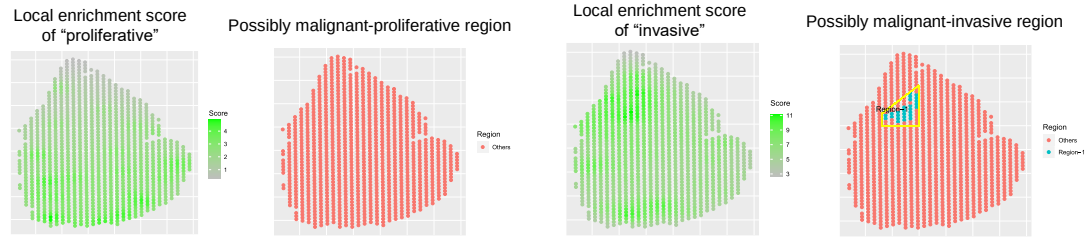

Max: 4.9; Threshold set to 10

No possibly malignant regions

Max: 11.1; Threshold set to 10

1 possibly malignant region

TSU-39

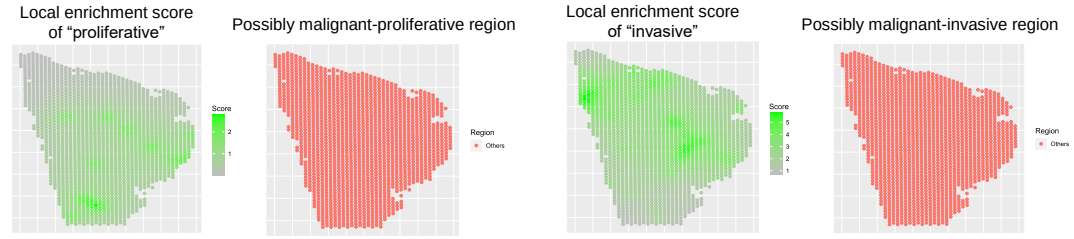

Max: 2.8; Threshold set to 10

No possibly malignant regions

Max: 5.8; Threshold set to 10

No possibly malignant regions

TSU-40

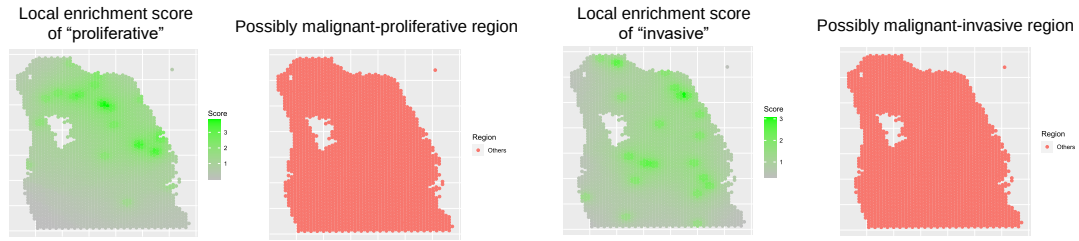

Max: 3.8; Threshold set to 10

No possibly malignant regions

Max: 3.1; Threshold set to 10

No possibly malignant regions

TSU-41

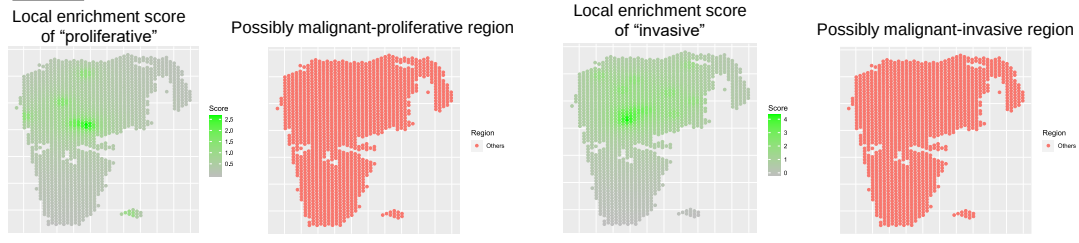

Max: 2.6; Threshold set to 10

No possibly malignant regions

Max: 4.4; Threshold set to 10

No possibly malignant regions

e

IA

LUAD No. 1 FF

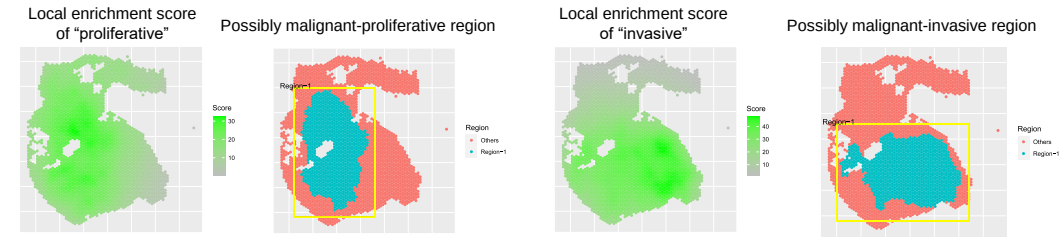

Max: 32.7; Threshold set to 22.9

1 possibly malignant region

Max: 48.1; Threshold set to 33.7

1 possibly malignant region

LUAD No. 2 FF

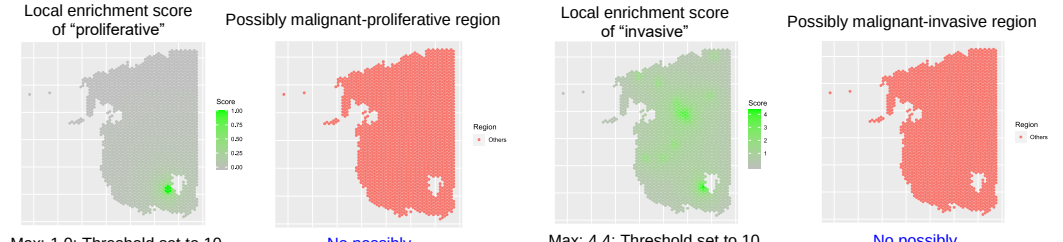

Max: 1.0; Threshold set to 10

No possibly malignant regions

Max: 4.4; Threshold set to 10

No possibly malignant regions

LUAD No. 3 FF

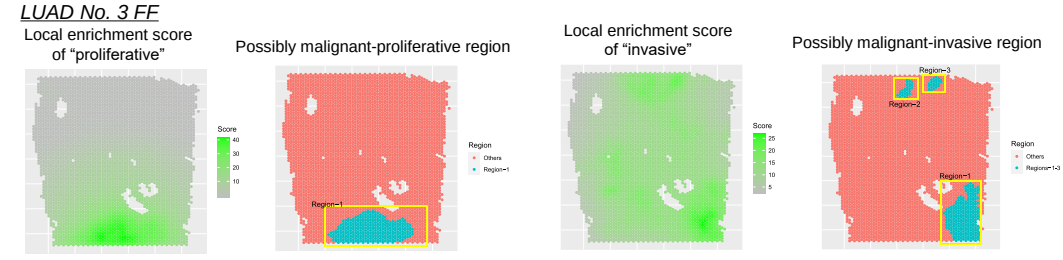

Max: 41.4; Threshold set to 29.0

1 possibly malignant region

Max: 26.8; Threshold set to 18.8

3 possibly malignant regions

LUAD No. 4 FF

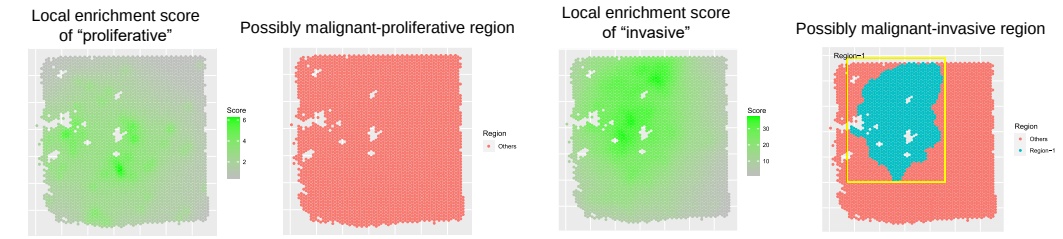

Max: 6.2; Threshold set to 10

No possibly malignant regions

Max: 37.4; Threshold set to 26.2

1 possibly malignant region

LUAD No. 5 FF

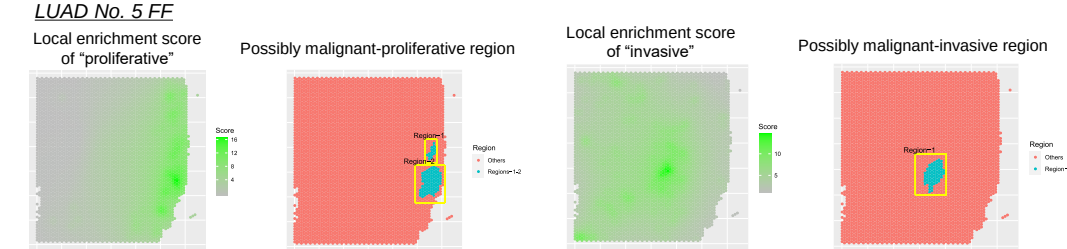

Max: 16.7; Threshold set to 11.7

2 possibly malignant regions

Max: 14.7; Threshold set to 10.3

1 possibly malignant region

LUAD No. 14 FF

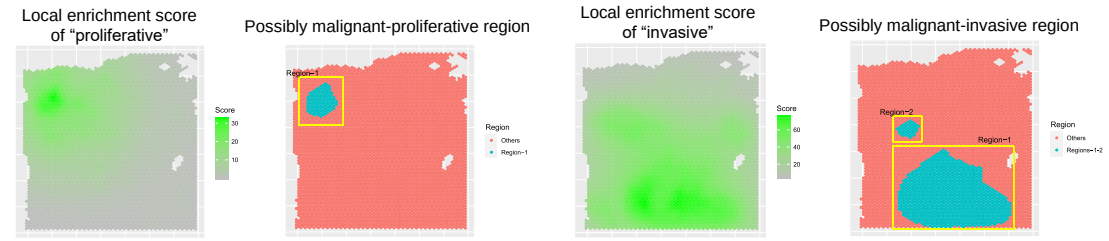

Max: 33.1; Threshold set to 23.2

1 possibly malignant region

Max: 76.1; Threshold set to 53.3

2 possibly malignant regions

LUAD No. 16 FF

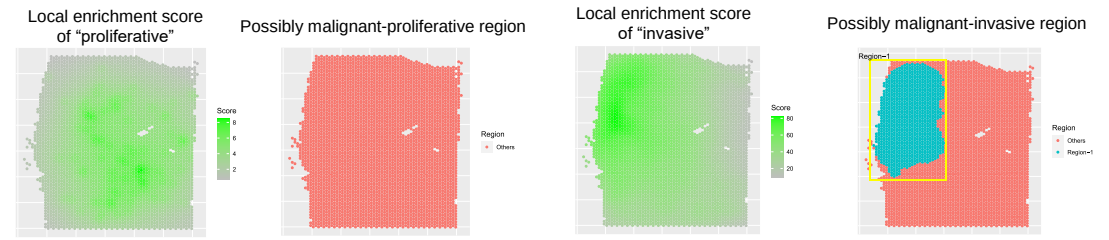

Max: 8.5; Threshold set to 10

No possibly malignant regions

Max: 82.3; Threshold set to 57.6

1 possibly malignant region

LUAD No. 17 FF

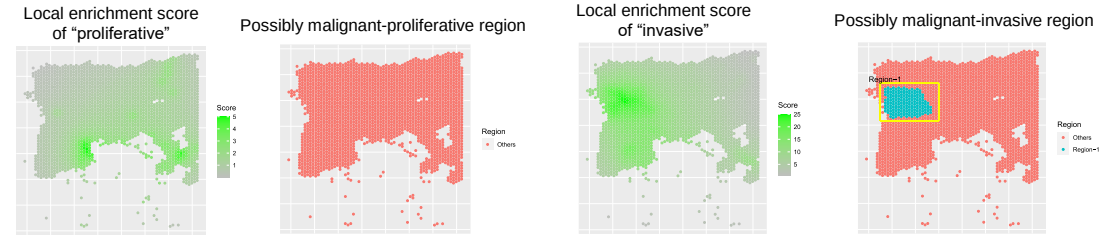

Max: 5.0; Threshold set to 10

No possibly malignant regions

Max: 25.1; Threshold set to 17.6

1 possibly malignant region

LUAD No. 2 FFPE section A

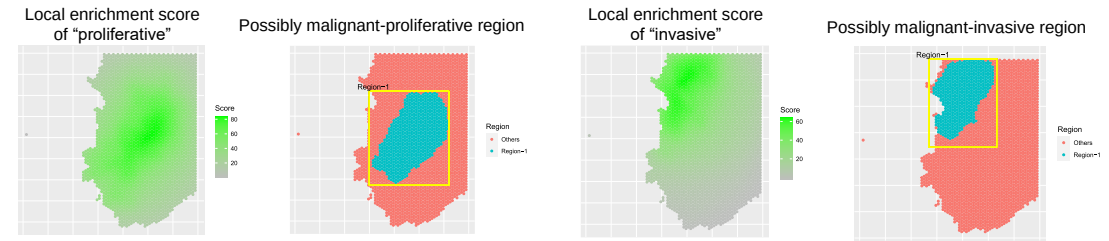

Max: 83.9; Threshold set to 58.7

1 possibly malignant region

Max: 64.6; Threshold set to 45.2

1 possibly malignant region

LUAD No. 2 FFPE section B

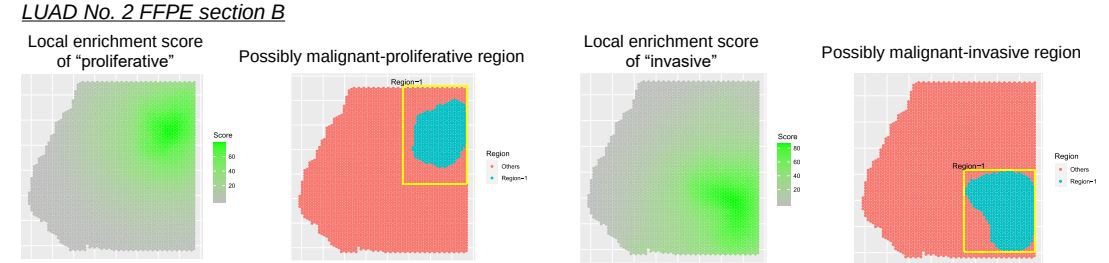

Max: 79.0; Threshold set to 55.3

1 possibly malignant region

Max: 86.1; Threshold set to 60.3

1 possibly malignant region

LUAD No. 2 FFPE section C

Local enrichment score of "proliferative"

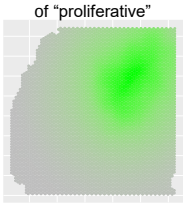

Max: 90.8; Threshold set to 63.5

Possibly malignant-proliferative region

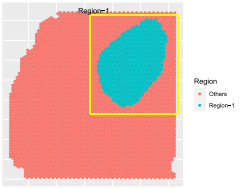

1 possibly malignant region

Local enrichment score of "invasive"

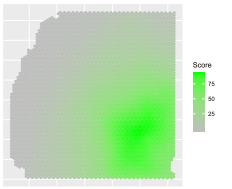

Max: 94.3; Threshold set to 66.0

Possibly malignant-invasive region

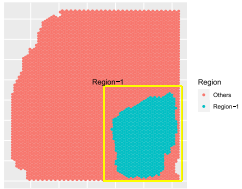

1 possibly malignant region

LUAD No. 2 FFPE section D

Local enrichment score of "proliferative"

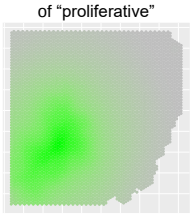

Max: 91.9; Threshold set to 64.4

Possibly malignant-proliferative region

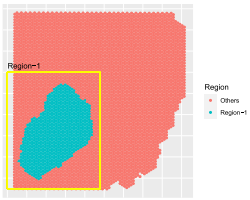

1 possibly malignant region

Local enrichment score of "invasive"

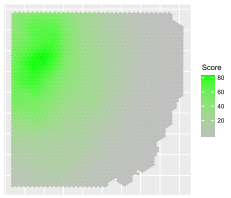

Max: 82.9; Threshold set to 58.1

Possibly malignant-invasive region

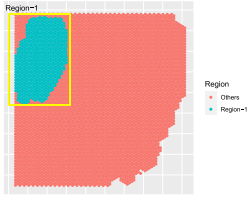

1 possibly malignant region

LUAD No. 3 FFPE section A

Local enrichment score of "proliferative"

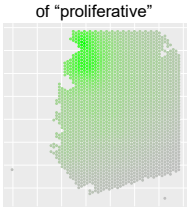

Max: 29.6; Threshold set to 20.7

Possibly malignant-proliferative region

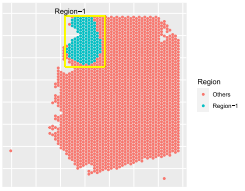

1 possibly malignant region

Local enrichment score of "invasive"

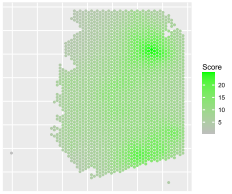

Max: 24.9; Threshold set to 17.5

Possibly malignant-invasive region

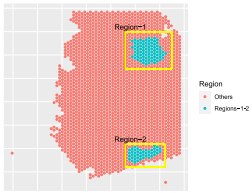

2 possibly malignant regions

LUAD No. 3 FFPE section B

Local enrichment score of "proliferative"

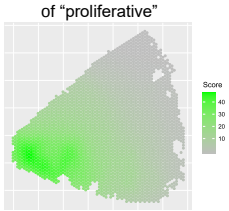

Max: 47.6; Threshold set to 33.3

Possibly malignant-proliferative region

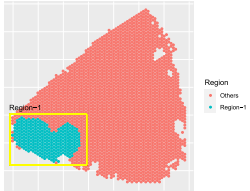

1 possibly malignant region

Local enrichment score of "invasive"

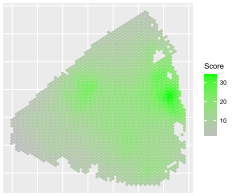

Max: 34.4; Threshold set to 24.1

Possibly malignant-invasive region

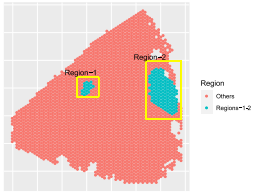

2 possibly malignant regions

LUAD No. 4 FFPE section C

Local enrichment score of "proliferative"

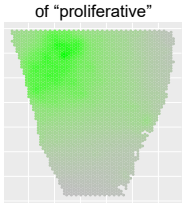

Max: 27.5; Threshold set to 19.2

Possibly malignant-proliferative region

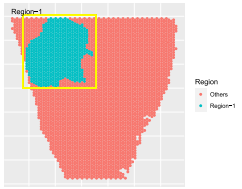

1 possibly malignant region

Local enrichment score of "invasive"

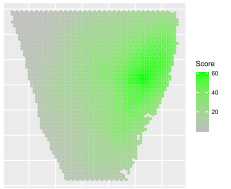

Max: 61.1; Threshold set to 42.7

Possibly malignant-invasive region

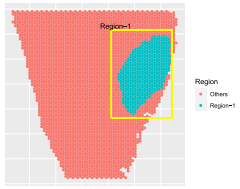

1 possibly malignant region

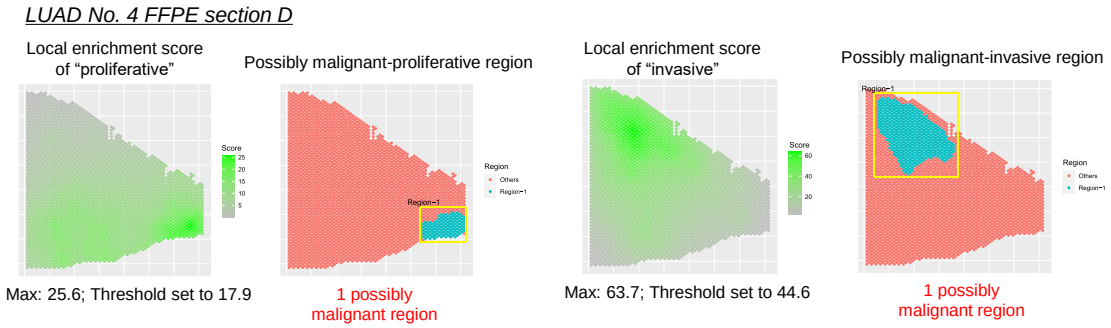

Supplementary Figure S13 Evaluation of changes of TME scores for AIS/MIA cases

(**a**) A workflow for evaluating changes to TME scores. Neighbor scores for "proliferative" and "invasive" spots were calculated, and "possibly malignant" regions ("possibly malignant-proliferative" and "possibly malignant-invasive" regions) were identified. (**b–e**) The spatial distribution of neighbor scores and "possibly malignant" regions is shown for early cases, which include AIS (Noguchi type A), AIS (Noguchi type B), and MIA (Noguchi type C), as well as IA cases. The results for proliferative and invasive spots are shown on the left and right, respectively. The maximum neighbor score, threshold of neighbor scores, and number of "possibly malignant regions" are shown at the bottom of the graphs.

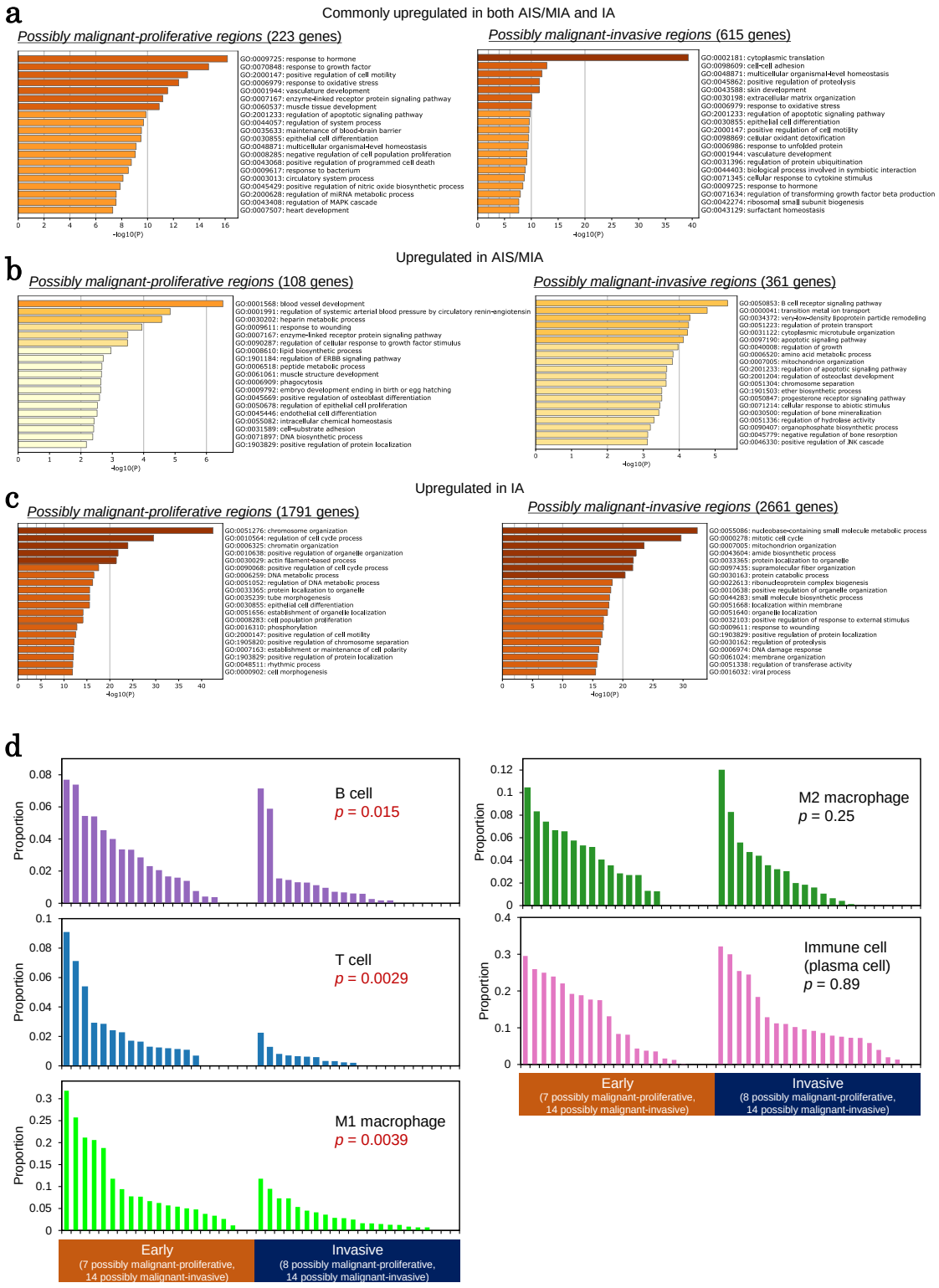
a
Commonly upregulated in both AIS/MIA and IA
Possibly malignant-proliferative regions (223 genes)
GO:0009725: response to hormone
GO:0070848: response to growth factor
GO:2000147: positive regulation of cell motility
GO:0006979: response to oxidative stress
GO:0001944: vasculature development
GO:0007167: enzyme-linked receptor protein signaling pathway
GO:0060537: muscle tissue development
GO:2001233: regulation of apoptotic signaling pathway
GO:0044057: regulation of system process
GO:0035633: maintenance of blood-brain barrier
GO:0030855: epithelial cell differentiation
GO:0048871: multicellular organismal-level homeostasis
GO:0008285: negative regulation of cell population proliferation
GO:0043068: positive regulation of programmed cell death
GO:0009617: response to bacterium
GO:0003013: circulatory system process
GO:0045429: positive regulation of nitric oxide biosynthetic process
GO:2000628: regulation of miRNA metabolic process
GO:0043408: regulation of MAPK cascade
GO:0007507: heart development
0 2 4 6 8 10 12 14 16
-log10(P)
Possibly malignant-invasive regions (615 genes)
GO:0002181: cytoplasmic translation
GO:0098609: cell-cell adhesion
GO:0048871: multicellular organismal-level homeostasis
GO:0045862: positive regulation of proteolysis
GO:0043588: skin development
GO:0030198: extracellular matrix organization
GO:0006979: response to oxidative stress
GO:2001233: regulation of apoptotic signaling pathway
GO:0030855: epithelial cell differentiation
GO:2000147: positive regulation of cell motility
GO:0098869: cellular oxidant detoxification
GO:0006986: response to unfolded protein
GO:0001944: vasculature development
GO:0031396: regulation of protein ubiquitination
GO:0044403: biological process involved in symbiotic interaction
GO:0071345: cellular response to cytokine stimulus
GO:0009725: response to hormone
GO:0071634: regulation of transforming growth factor beta production
GO:0042274: ribosomal small subunit biogenesis
GO:0043129: surfactant homeostasis
0 5 10 15 20 25 30 35 40
-log10(P)
b
Upregulated in AIS/MIA
Possibly malignant-proliferative regions (108 genes)
GO:0001568: blood vessel development
GO:0001991: regulation of systemic arterial blood pressure by circulatory renin-angiotensin
GO:0030202: heparin metabolic process
GO:0009611: response to wounding
GO:0007167: enzyme-linked receptor protein signaling pathway
GO:0090287: regulation of cellular response to growth factor stimulus
GO:0008610: lipid biosynthetic process
GO:1901184: regulation of ERBB signaling pathway
GO:0006518: peptide metabolic process
GO:0061061: muscle structure development
GO:0006909: phagocytosis
GO:0009792: embryo development ending in birth or egg hatching
GO:0045669: positive regulation of osteoblast differentiation
GO:0050678: regulation of epithelial cell proliferation
GO:0045446: endothelial cell differentiation
GO:0055082: intracellular chemical homeostasis
GO:0031589: cell-substrate adhesion
GO:0071897: DNA biosynthetic process
GO:1903829: positive regulation of protein localization
0 1 2 3 4 5 6
-log10(P)
Possibly malignant-invasive regions (361 genes)
GO:0050853: B cell receptor signaling pathway
GO:0000041: transition metal ion transport
GO:0034372: very-low-density lipoprotein particle remodeling
GO:0051223: regulation of protein transport
GO:0031122: cytoplasmic microtubule organization
GO:0097190: apoptotic signaling pathway
GO:0040008: regulation of growth
GO:0006520: amino acid metabolic process
GO:0007005: mitochondrion organization
GO:2001233: regulation of apoptotic signaling pathway
GO:2001204: regulation of osteoclast development
GO:0051304: chromosome separation
GO:1901503: ether biosynthetic process
GO:0050847: progesterone receptor signaling pathway
GO:0071214: cellular response to abiotic stimulus
GO:0030500: regulation of bone mineralization
GO:0051336: regulation of hydrolase activity
GO:0090407: organophosphate biosynthetic process
GO:0045779: negative regulation of bone resorption
GO:0046330: positive regulation of JNK cascade
0 1 2 3 4 5
-log10(P)
c
Upregulated in IA
Possibly malignant-proliferative regions (1791 genes)
GO:0051276: chromosome organization
GO:0010564: regulation of cell cycle process
GO:0006325: chromatin organization
GO:0010638: positive regulation of organelle organization
GO:0030029: actin filament-based process
GO:0090068: positive regulation of cell cycle process
GO:0006259: DNA metabolic process
GO:0051052: regulation of DNA metabolic process
GO:0033365: protein localization to organelle
GO:0035239: tube morphogenesis
GO:0030855: epithelial cell differentiation
GO:0051656: establishment of organelle localization
GO:0008283: cell population proliferation
GO:0016310: phosphorylation
GO:2000147: positive regulation of cell motility
GO:1905820: positive regulation of chromosome separation
GO:0007163: establishment or maintenance of cell polarity
GO:1903829: positive regulation of protein localization
GO:0048511: rhythmic process
GO:0000902: cell morphogenesis
0 5 10 15 20 25 30 35 40
-log10(P)
Possibly malignant-invasive regions (2661 genes)
GO:0055086: nucleobase-containing small molecule metabolic process
GO:0000278: mitotic cell cycle
GO:0007005: mitochondrion organization
GO:0043604: amide biosynthetic process
GO:0033365: protein localization to organelle
GO:0097435: supramolecular fiber organization
GO:0030163: protein catabolic process
GO:0022613: ribonucleoprotein complex biogenesis
GO:0010638: positive regulation of organelle organization
GO:0044283: small molecule biosynthetic process
GO:0051668: localization within membrane
GO:0051640: organelle localization
GO:0032103: positive regulation of response to external stimulus
GO:0009611: response to wounding
GO:1903829: positive regulation of protein localization
GO:0030162: regulation of proteolysis
GO:0006974: DNA damage response
GO:0061024: membrane organization
GO:0051338: regulation of transferase activity
GO:0016032: viral process
0 5 10 15 20 25 30
-log10(P)
d
Proportion
B cell
p = 0.015
T cell
p = 0.0029
M1 macrophage
p = 0.0039
M2 macrophage
p = 0.25
Immune cell
(plasma cell)
p = 0.89
Early
(7 possibly malignant-proliferative,
14 possibly malignant-invasive)
Invasive
(8 possibly malignant-proliferative,
14 possibly malignant-invasive)

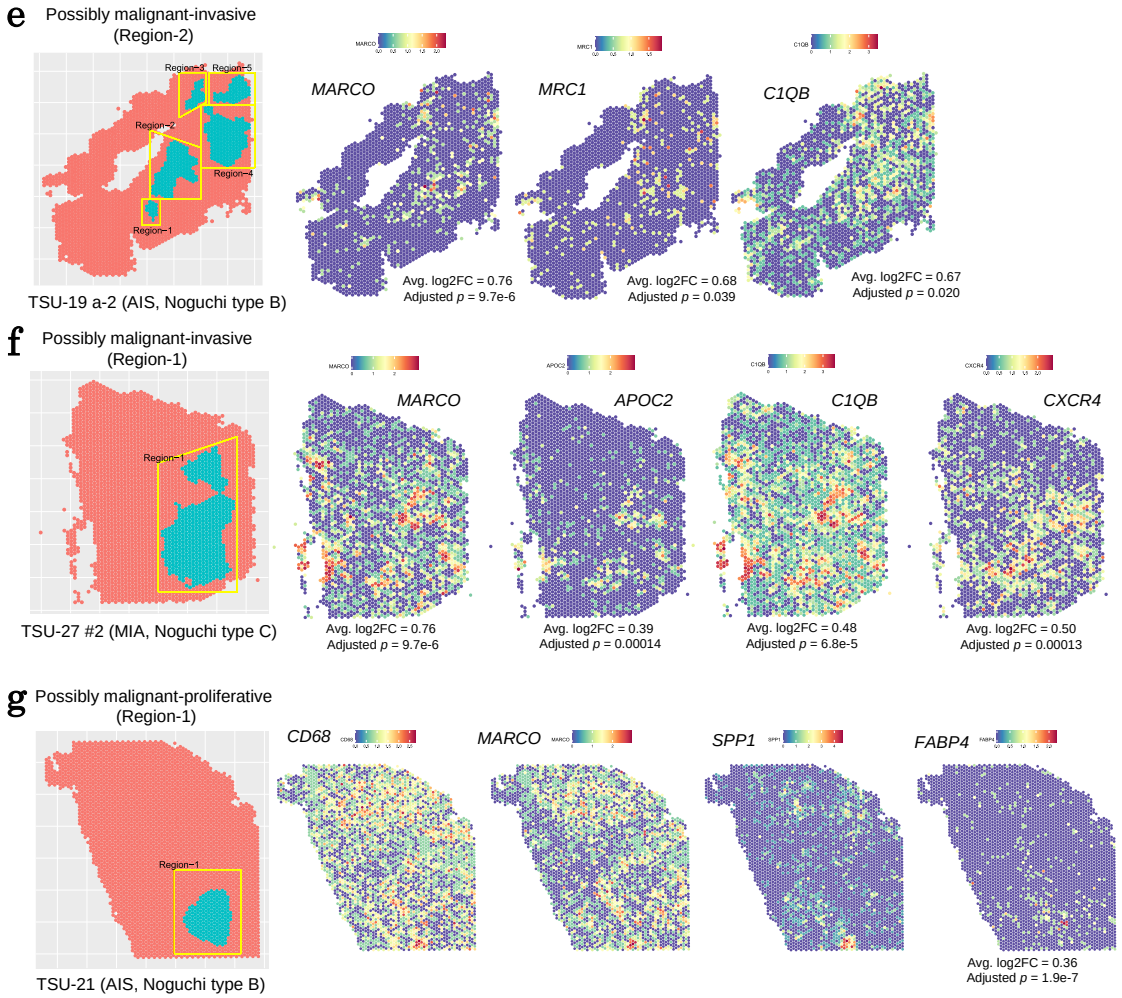

Supplementary Figure S14 Characterization in "possibly malignant" regions

(**a–c**) Results of Gene Ontology (GO) enrichment analysis with Metascape[5] which calculates *p*-values using the hypergeometric test. Genes with significantly higher expression in "possibly malignant-proliferative" or "possibly malignant-invasive" regions were selected for analysis. GO terms associated with highly expressed genes in both AIS/MIA and IA cases are shown in **a**. GO terms associated with only AIS/MIA or IA cases are shown in **b** and **c**, respectively. (**d**) The proportions of spots annotated with immune cells (TME scoring) in "possibly malignant-proliferative" and "possibly malignant-invasive" regions. When "possibly malignant" regions were detected in multiple sequential sections of the same tissue block, we used data from the following sections as a representative: TSU-27 #2, TSU-28 #1, LUAD No. 2 FFPE C, LUAD No. 3

FFPE B, and LUAD No. 4 FFPE C. *P*-value is shown in the inset (Wilcoxon rank sum test). (**e–g**) Representative "possibly malignant" regions. Genes with differential expression from other regions are shown. *P*-values and average log2FC were calculated using the Seurat FindMarkers function based on Wilcoxon rank sum test. (**e**) The "possibly malignant-invasive" region in TSU-19 (left; Region-2 in green); macrophage markers are significantly highly expressed (right). (**f**) The "possibly malignant-invasive" region in TSU-27 (left; Region-1 in blue). Macrophage and immune cell markers represent significantly higher expression (right). (**g**) The "possibly malignant-proliferative" region in TSU-21 (left; Region-1 in blue). Macrophage markers are shown (right). *FABP4* expression is significantly elevated in the "possibly malignant" region.

Supplementary Figure S15

a

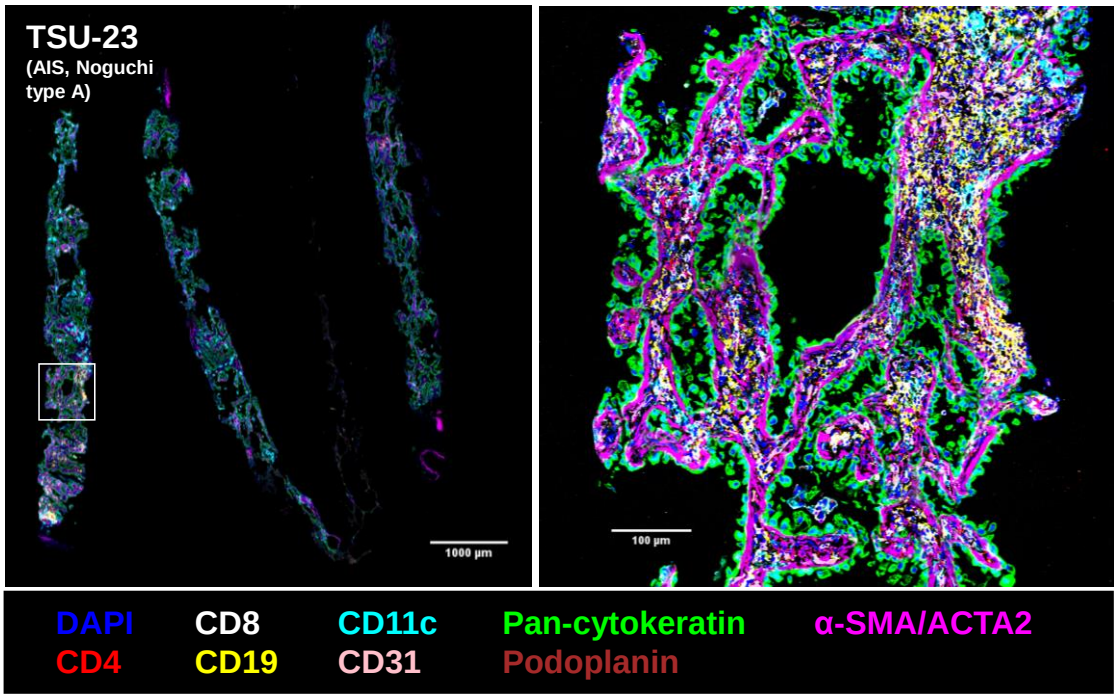

b

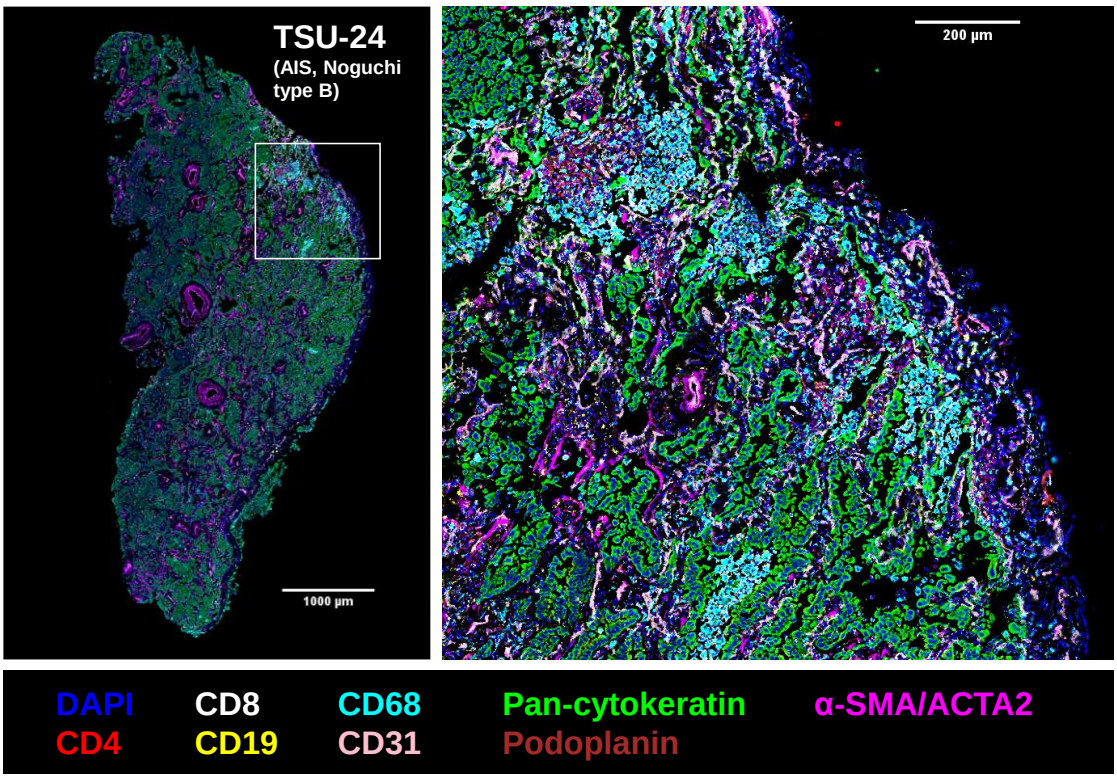

c

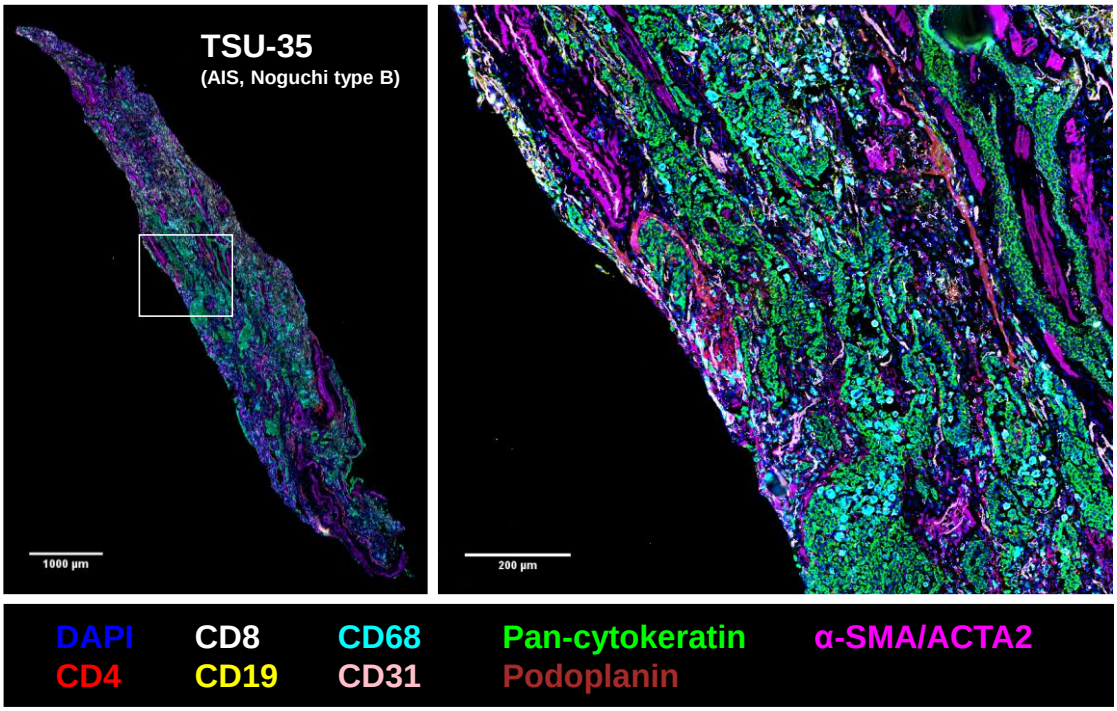
TSU-35
(AIS, Noguchi type B)
1000 μm
200 μm
DAPI CD8 CD68 Pan-cytokeratin α-SMA/ACTA2
CD4 CD19 CD31 Podoplanin

d

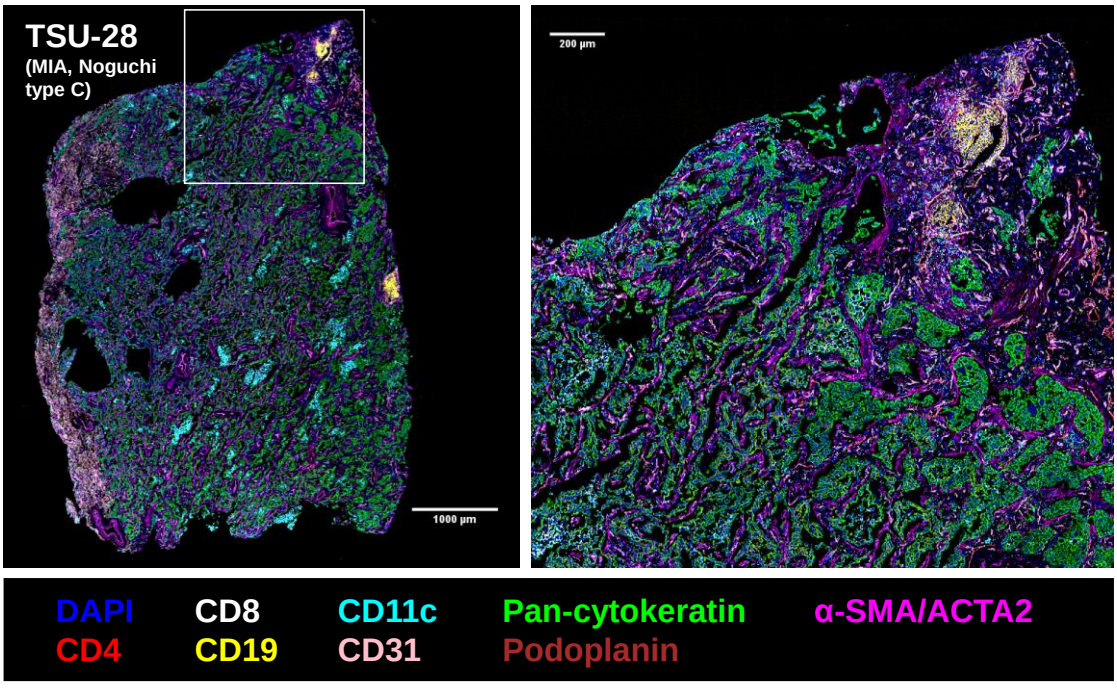
TSU-28
(MIA, Noguchi type C)
1000 μm
200 μm
DAPI CD8 CD11c Pan-cytokeratin α-SMA/ACTA2
CD4 CD19 CD31 Podoplanin

e

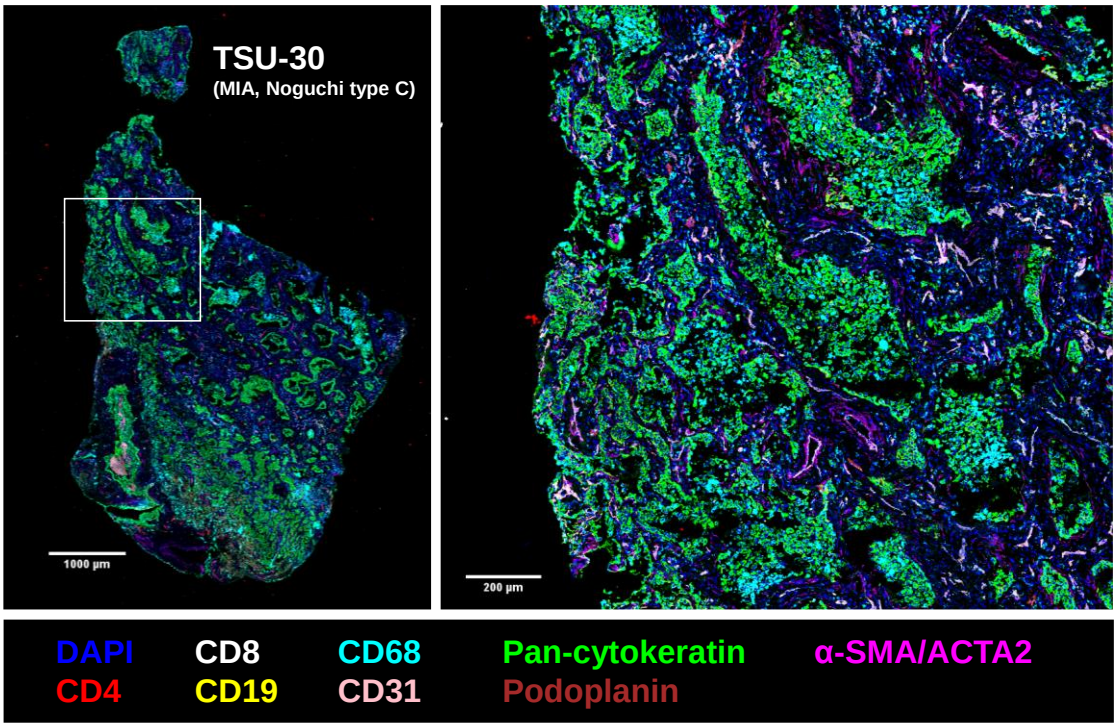
TSU-30
(MIA, Noguchi type C)
1000 μm
200 μm
DAPI
CD8
CD68
Pan-cytokeratin
α-SMA/ACTA2
CD4
CD19
CD31
Podoplanin

f

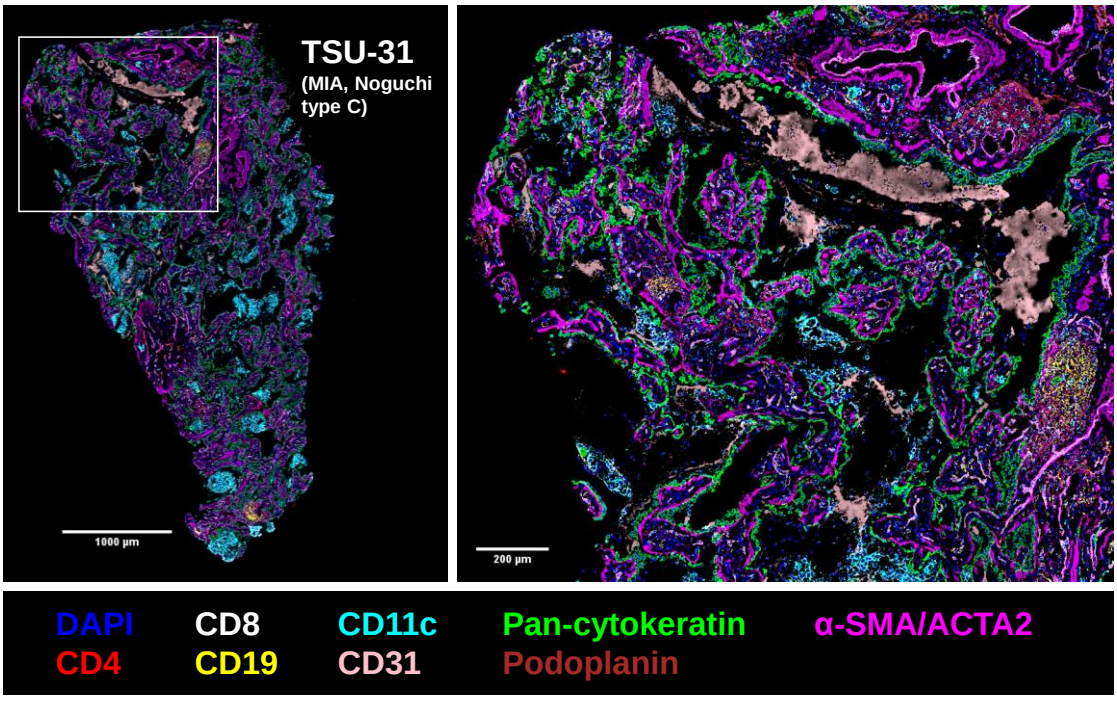
TSU-31
(MIA, Noguchi type C)
1000 μm
200 μm
DAPI
CD8
CD11c
Pan-cytokeratin
α-SMA/ACTA2
CD4
CD19
CD31
Podoplanin

g TSU-20 (AIS, Noguchi type A; *Nat Commun* 2023)

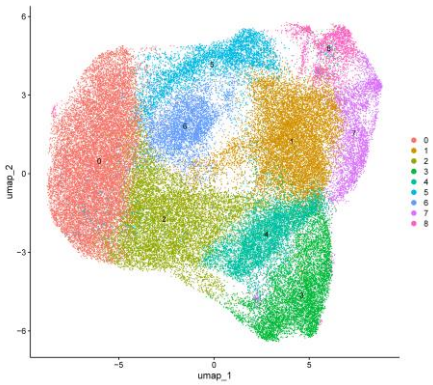

Cluster	Annotation	Feature*
0	High podoplanin tumor cell	NKX2-1, Pan-Cytokeratin, Podoplanin
1	Immune cell	**CD45RO**, **CD4**, CD11c
2	Tumor cell/Stromal cell	α-SMA, Pan-Cytokeratin, β-Catenin1
3	Endothelial cell	CD31, Caveolin, PD-L1
4	Stromal cell/Immune cell	α-SMA, Caveolin, CD163
5	Macrophage/DC	CD11c, CD68
6	High PD-L1 tumor cell	**PD-L1**, NKX2-1, Pan-Cytokeratin
7	B cell	**CD19**, **CXCL13**, CD45RO
8	Proliferating immune cell	**Ki67**, CXCL13, CTLA4

*Top 3 DEGs; log2FC > 0.5; log2FC > 2 in bold

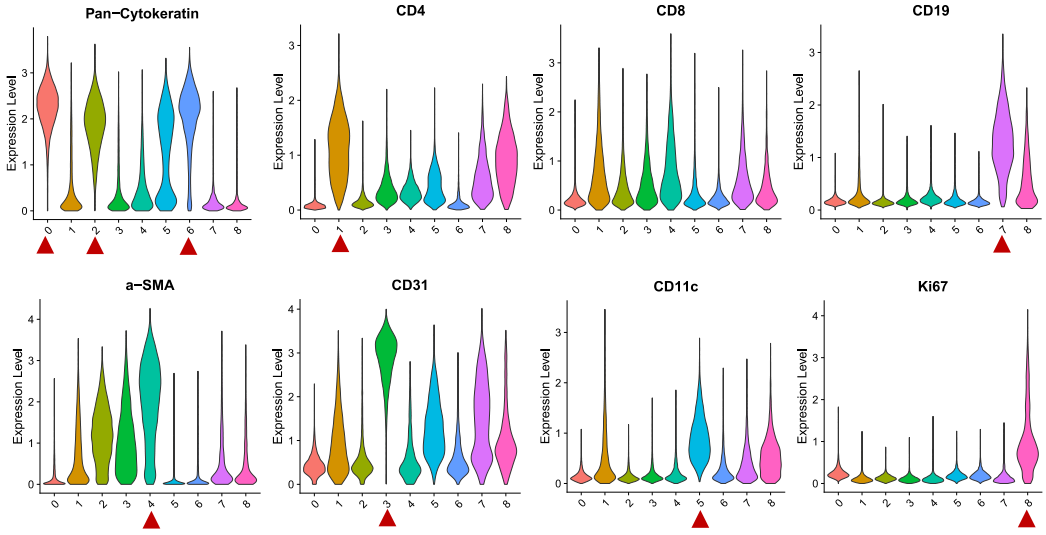

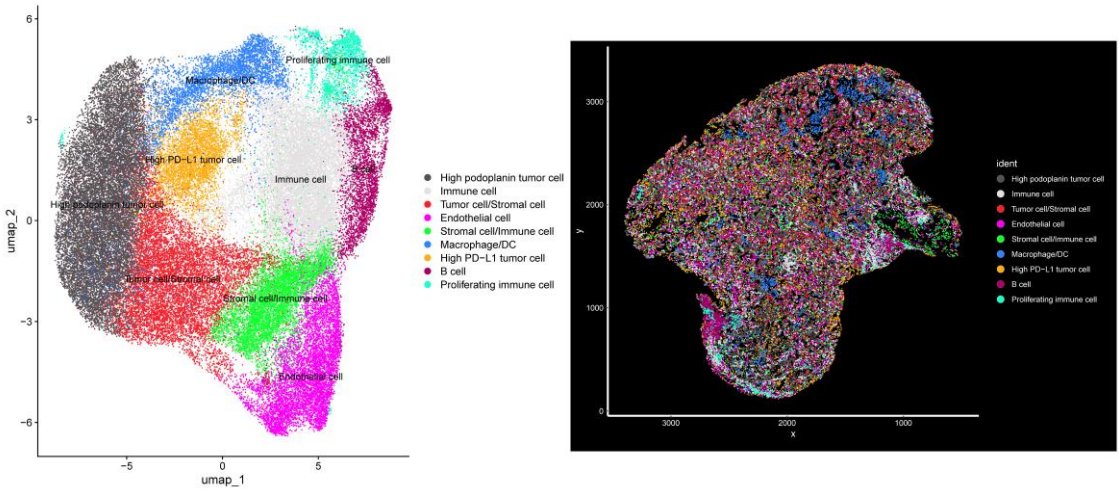

h TSU-23 (AIS, Noguchi type A)

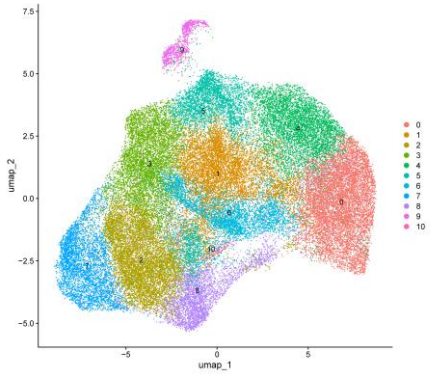

Cluster	Annotation	Feature*
0	Tumor cell	NKX2-1, Pan-Cytokeratin, TP53
1	Stromal cell	CD31, a-SMA
2	T cell	**CD45RO**, CD4, CD8
3	Immune cell	CD163, TP53, CD8
4	Tumor cell/Stromal cell	NKX2-1, Pan-Cytokeratin, α-SMA
5	Proliferating fibroblast/SMC	α-SMA, Ki67
6	Endothelial cell	Podoplanin, CD31
7	B cell	CD19, CD45RO, CD11c
8	Macrophage/DC	**CD11c**, CD4, CD45RO
9	Proliferating cell	**Ki67**, CD11c
10	Stromal cell/Immune cell	**Podoplanin**, CD45RO, CD11c

*Top 3 DEGs; log2FC > 0.5; log2FC > 2 in bold

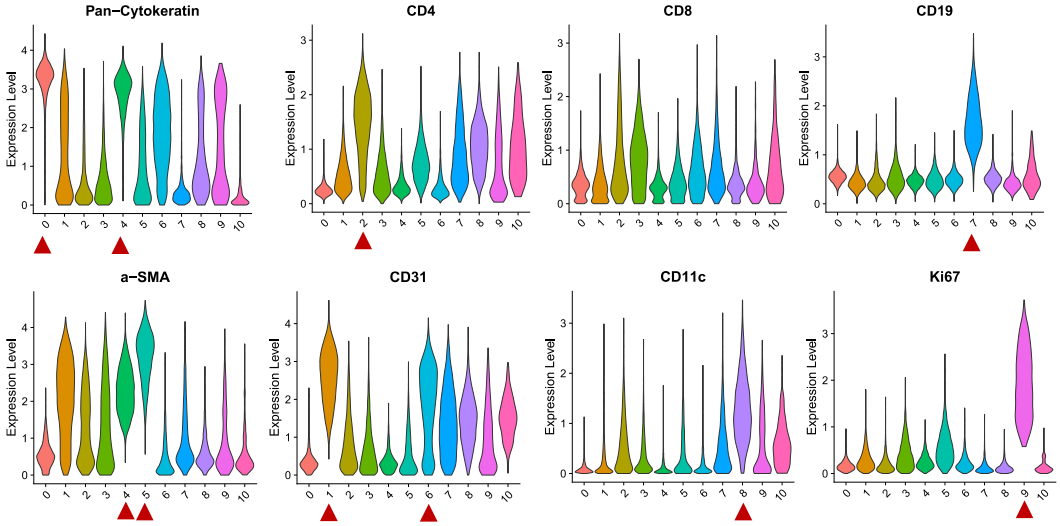

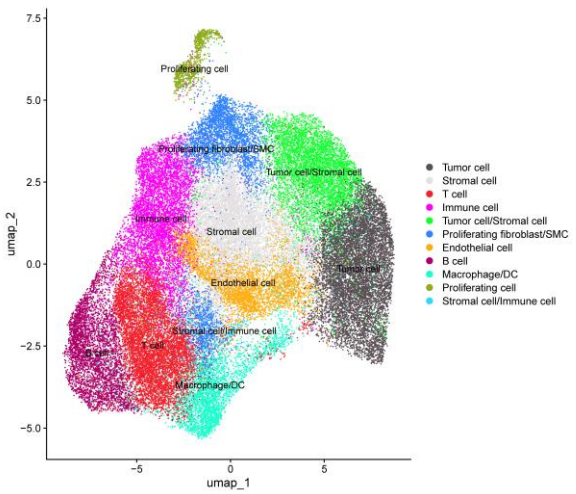

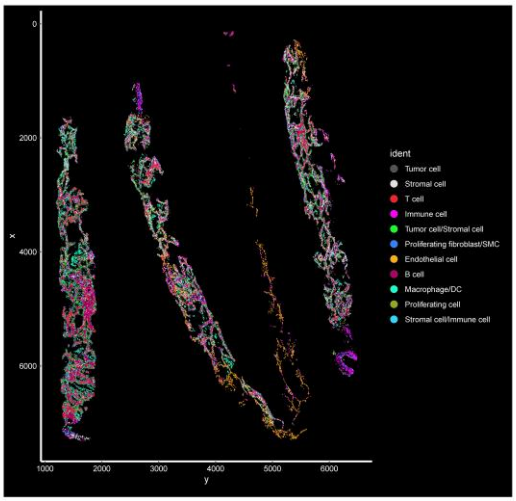

i

TSU-21 (AIS, Noguchi type B; *Nat Commun* 2023)

*Top 3 DEGs; log2FC > 0.5; log2FC > 2 in bold

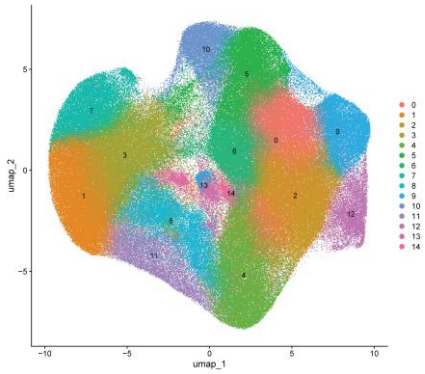

Cluster	Annotation	Feature*
0	Stromal cell/Immune cell	Podoplanin, CD19, Caveolin
1	Tumor cell	Pan-Cytokeratin, NKX2-1, β-Catenin1
2	T cell	CD45RO, CD4, CD8
3	Tumor cell	Pan-Cytokeratin, NKX2-1, β-Catenin1
4	Macrophage/DC	CD11c, CD68, CD4
5	Stromal cell	**α-SMA**, Caveolin, CD31
6	Immune cell	CD163, CD8
7	High LIF tumor cell	NKX2-1, LIF, Pan-Cytokeratin
8	High PD-L1 cell	**PD-L1**, Pan-Cytokeratin, CD11c
9	B cell	**CXCL13**, **CD19**, Podoplanin
10	High PD-L1 stromal cell	**PD-L1**, Caveolin, CD31
11	Tumor cell/Immune cell	CD11c, Pan-Cytokeratin
12	Treg	**FOXP3**, CD45RO, CD4
13	Proliferating cell	**Ki67**
14	Proliferating B cell	**CXCL13**, CD19, Ki67

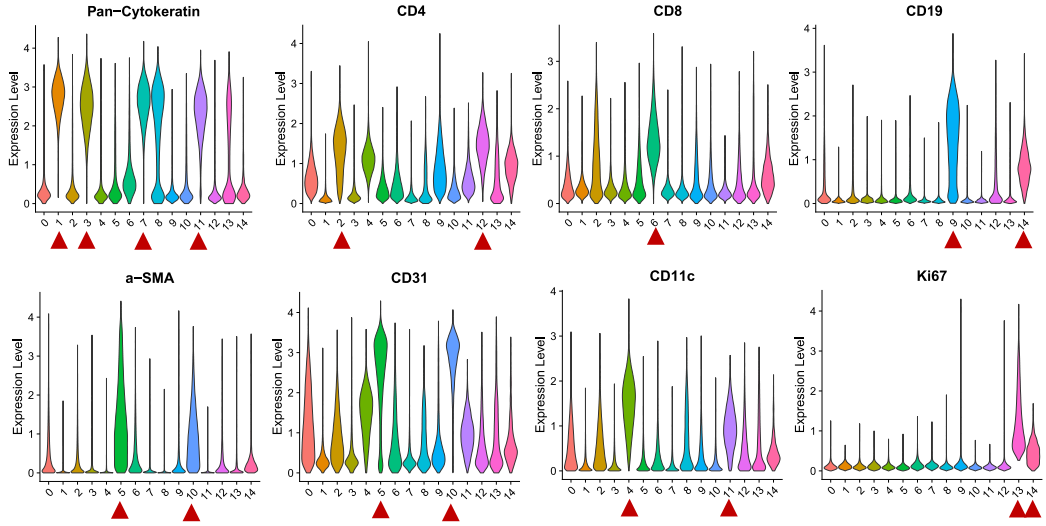

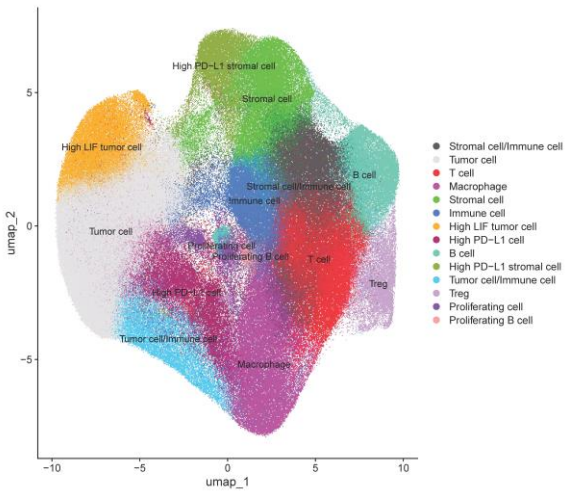

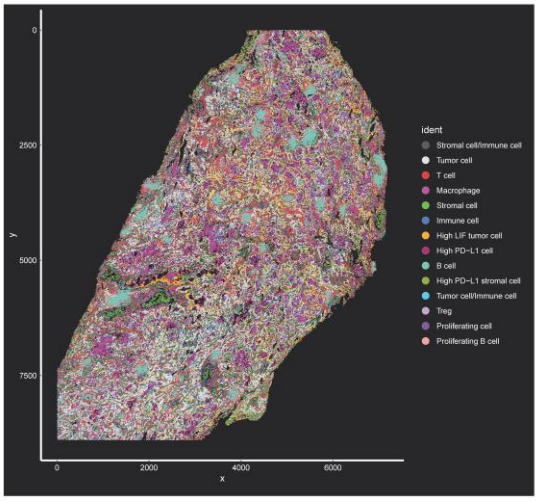

j TSU-24 (AIS, Noguchi type B)

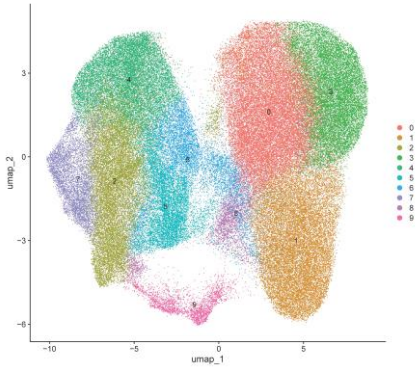

Cluster	Annotation	Feature*
0	Tumor cell	NKX2-1, Pan-Cytokeratin
1	High podoplanin tumor cell	Podoplanin, Pan-Cytokeratin, NKX2-1
2	Macrophage/DC	**CD11c**, CD68, CD45RO
3	Tumor cell	NKX2-1, PD-1, Pan-Cytokeratin
4	Immune cell	CD163, CD19, CD8
5	Stromal cell	**CD31**, α-SMA
6	Fibroblast/SMC	**α-SMA**
7	CD4+ T cell	**CD45RO**, **CD4**, CTLA4
8	Others	CD11c, Pan-Cytokeratin
9	Proliferating cell	**Ki67**, CD11c

*Top 3 DEGs; log2FC > 0.5; log2FC > 2 in bold

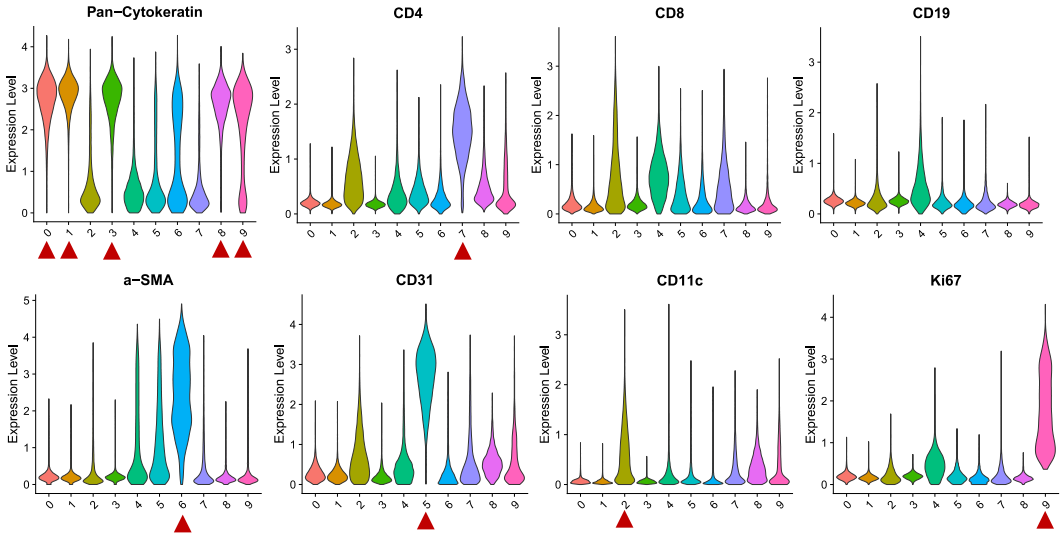

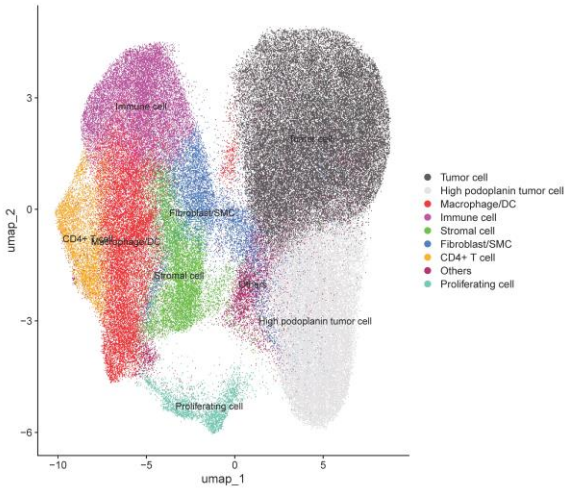

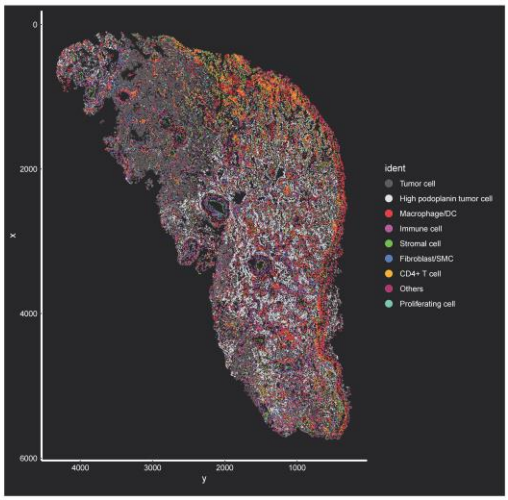

k TSU-35 (AIS, Noguchi type B)

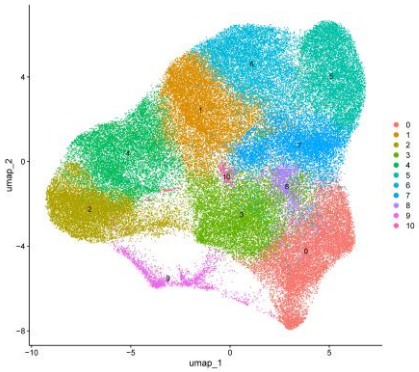

Cluster	Annotation	Feature*
0	T cell	**CD45RO**, CD4, CD8
1	Endothelial cell	Podoplanin, CD31
2	Tumor cell	**NKX2-1**, Pan-Cytokeratin
3	Macrophage/DC	CD11c, CD68, CD4
4	High podoplanin tumor cell	NKX2-1, Pan-Cytokeratin, Podoplanin
5	Fibroblast/SMC	α-SMA, FOXP3, CD56
6	Endothelial cell	CD31, α-SMA
7	Immune cell	CD163, TP53, CD8
8	B cell	**CD19**, CD45RO, CD4
9	Proliferating tumor cell	**Ki67**, NKX2-1
10	Proliferating immune cell	Ki67, PD-L1, CXCL13

*Top 3 DEGs; log2FC > 0.5; log2FC > 2 in bold

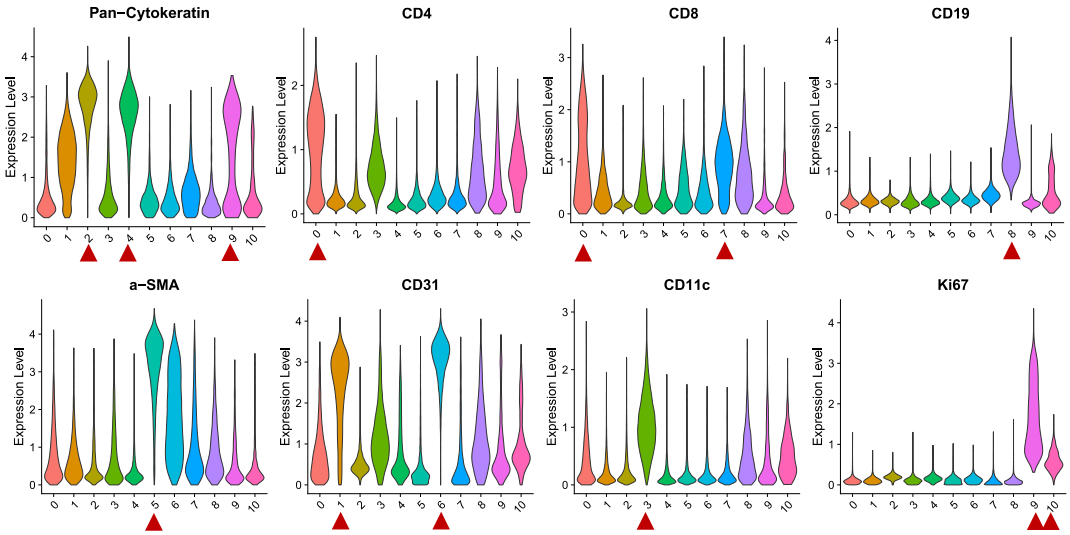

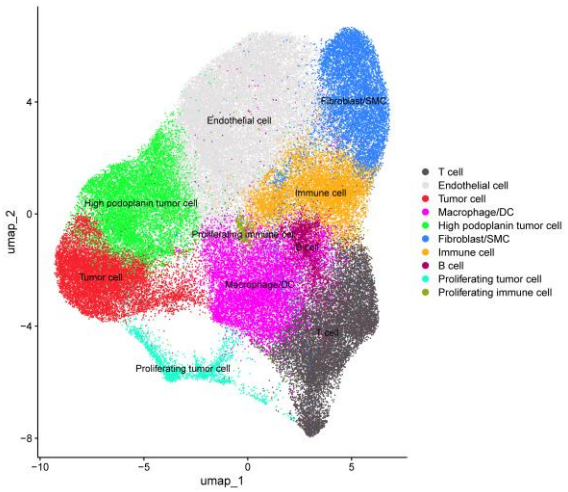

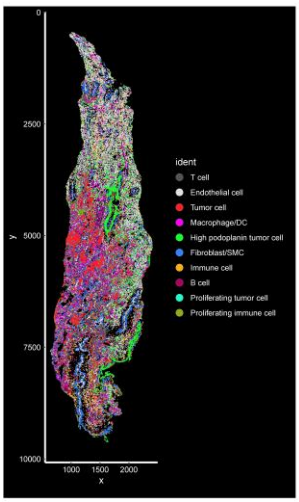

1

TSU-28 (MIA, Noguchi type C)

*Top 3 DEGs; log2FC > 0.5; log2FC > 2 in bold

Cluster	Annotation	Feature*
0	High podoplanin tumor cell	NKX2-1, Pan-Cytokeratin, Podoplanin
1	Tumor cell	NKX2-1, Pan-Cytokeratin
2	Proliferating fibroblast/SMC	**α-SMA**, Ki67
3	Immune cell	CD163, CD8, TP53
4	Endothelial cell	**CD31**, α-SMA
5	Macrophage/DC	**CD11c**, CD45RO, CD4
6	CD4+ T cell	**CD45RO**, **CD4**
7	Endothelial cell	CD31, Podoplanin
8	Tumor cell/Immune cell	CD11c, Pan-Cytokeratin, NKX2-1
9	Proliferating tumor cell	**Ki67**, NKX2-1
10	B cell	CD19, CD45RO, CD4
11	CD8+ T cell	CD8, CD45RO, PD-1
12	Tumor cell/Stromal cell	α-SMA, NKX2-1, Pan-Cytokeratin
13	Proliferating immune cell	**Ki67**, CD163, CD45RO

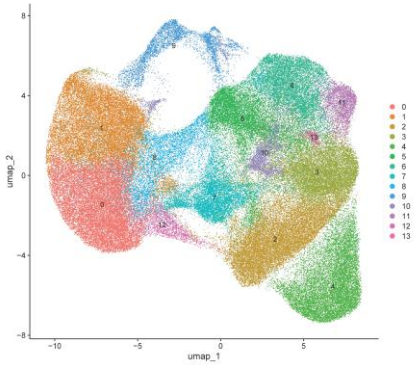

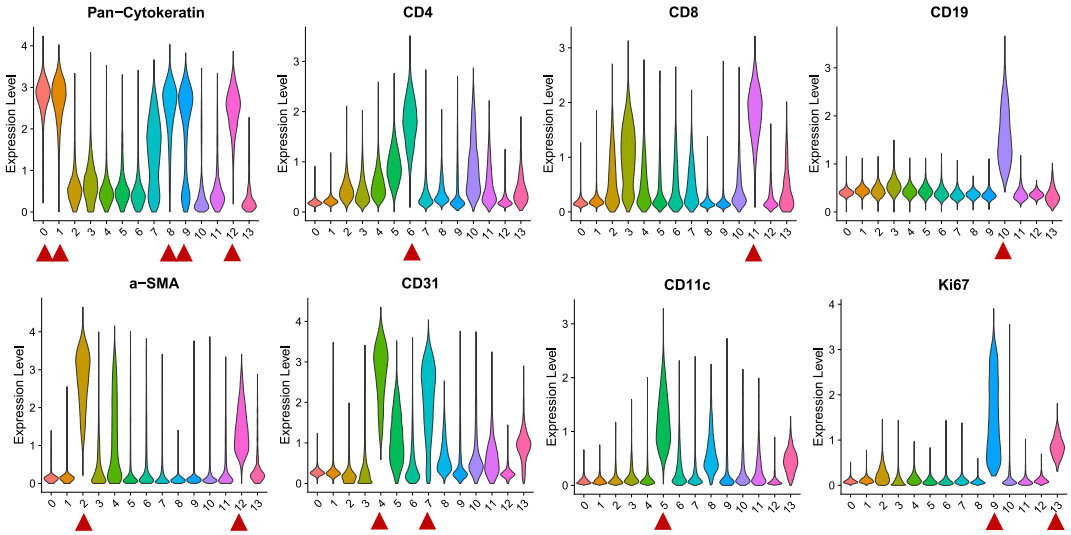

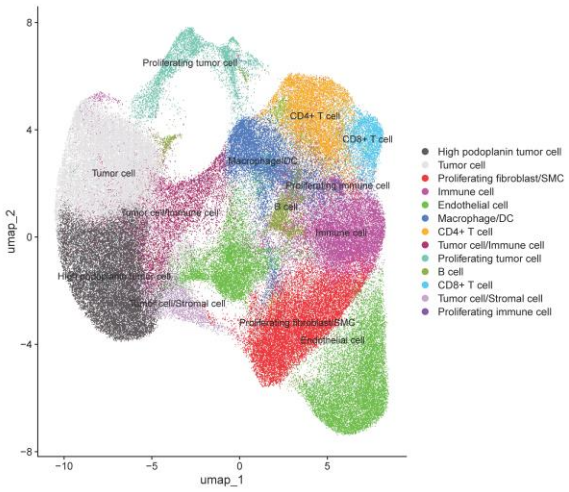

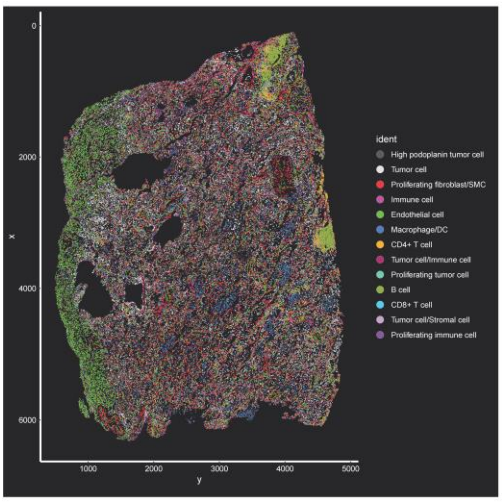

m TSU-30 (MIA, Noguchi type C)

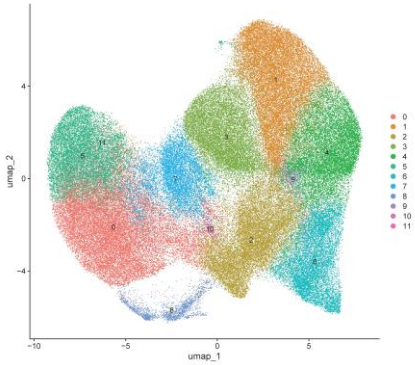

Cluster	Annotation	Feature*
0	Tumor cell	NKX2-1, Pan-Cytokeratin
1	Fibroblast/SMC	α-SMA, CD56
2	Macrophage/DC	**CD11c**, CD68, CD4
3	Endothelial cell	**CD31**, α-SMA
4	Immune cell	CD163, CD8, TP53
5	High podoplanin tumor cell	NKX2-1, Podoplanin, Pan-Cytokeratin
6	T cell	**CD45RO**, **CD4**, **CD8**
7	Endothelial cell	Podoplanin, CD31, PD-L1
8	Proliferating cell	**Ki67**, CD11c, NKX2-1
9	B cell	CD19, CD45RO, CD4
10	Proliferating immune cell	**Ki67**, PD-L1, CXCL13
11	Tumor cell/Immune cell	**CTLA4**, NKX2-1, Podoplanin

*Top 3 DEGs; log2FC > 0.5; log2FC > 2 in bold

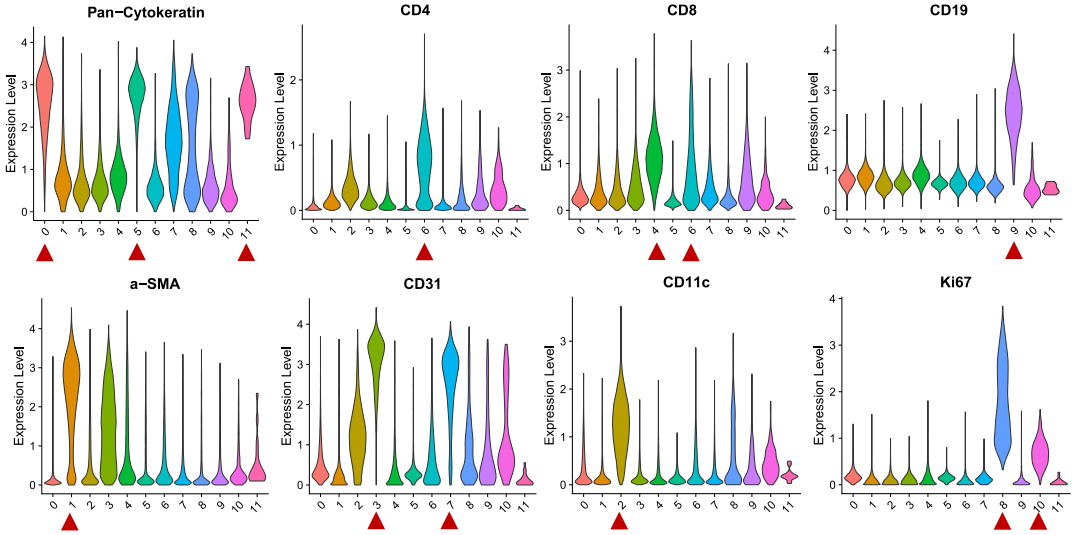

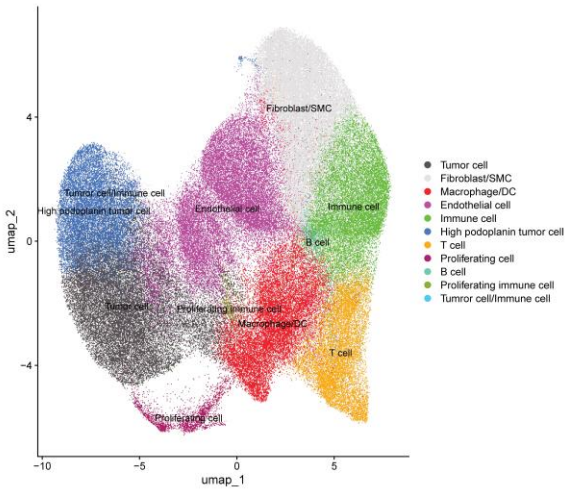

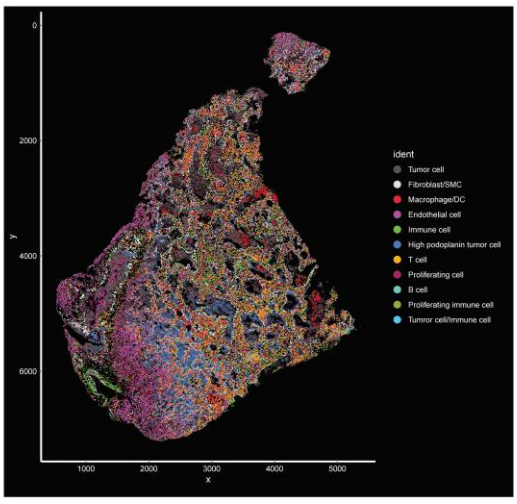

n TSU-31 (MIA, Noguchi type C)

*Top 3 DEGs; log2FC > 0.5; log2FC > 2 in bold

Cluster	Annotation	Feature*
0	Tumor cell	**NKX2-1**, **Pan-Cytokeratin**
1	Macrophage/DC	**CD11c**, CD31, CD4
2	Proliferating fibroblast/SMC	**α-SMA**, Ki67, Podoplanin
3	CD4+ T cell	CD4, CD45RO, PD-1
4	Immune cell	CD163, TP53, CD8
5	Endothelial cell	CD31, α-SMA
6	B cell	**CD19**, Podoplanin
7	CD8+ T cell	**CD8**, CD45RO, PD-1
8	Tumor cell/Stromal cell	Pan-Cytokeratin, NKX2-1, a-SMA
9	Treg	FOXP3, CD45RO, CD4
10	Proliferating immune cell	**Ki67**, CD11c, CD4
11	Endothelial cell	**Podoplanin**, CD31
12	Proliferating tumor cell	**Ki67**, NKX2-1, Pan-Cytokeratin

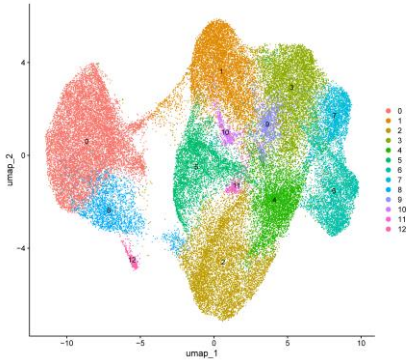

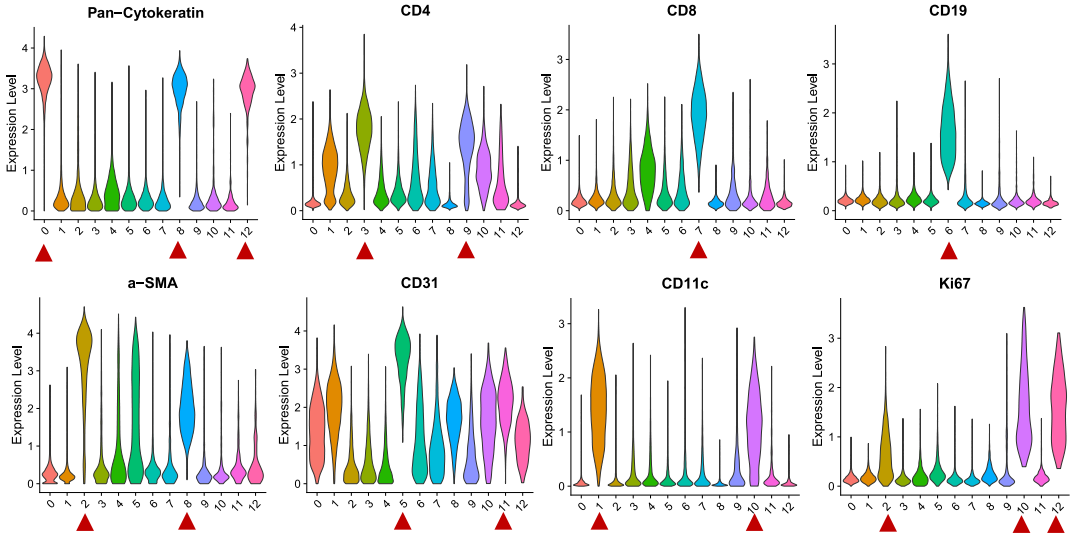

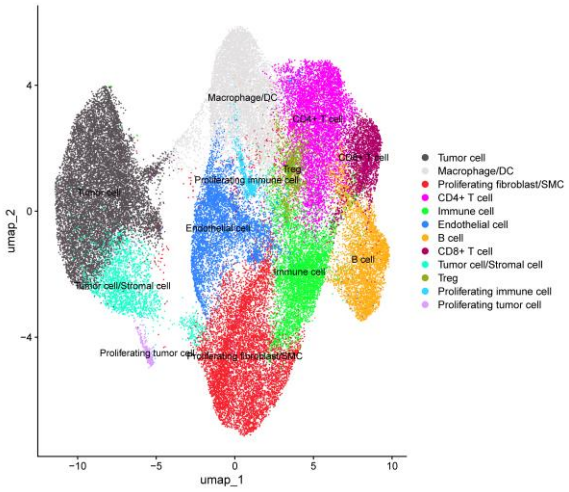

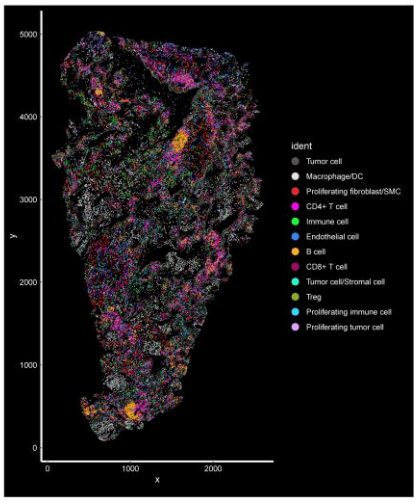

o TSU-33 (MIA, Noguchi type C; *Nat Commun* 2023)

*Top 3 DEGs; log2FC > 0.5; log2FC > 2 in bold

Cluster	Annotation	Feature*
0	Endothelial cell	Caveolin, CD31, Podoplanin
1	Proliferating immune cell	CD163, CD8, Ki67
2	Tumor cell	NKX2-1, Pan-Cytokeratin, Galectin3
3	Macrophage/DC	CD11c, CD68, CD4
4	Fibroblast/SMC	**α-SMA**, Caveolin
5	High podoplanin tumor cell	NKX2-1, Podoplanin, Pan-Cytokeratin
6	T cell	CD45RO, CD4, CD8
7	High PD-L1 endothelial cell	**PD-L1**, CD31, Caveolin
8	B cell	**CXCL13**, CD19, CD4
9	Macrophage/DC/Endothelial cell	CD11c, CD31, CD68
10	Proliferating immune cell	Ki67, PD-L1, CD45RO
11	Others	CD31, CD45RO, Podoplanin
12	Proliferating tumor cell	**Ki67**, NKX2-1, Pan-Cytokeratin

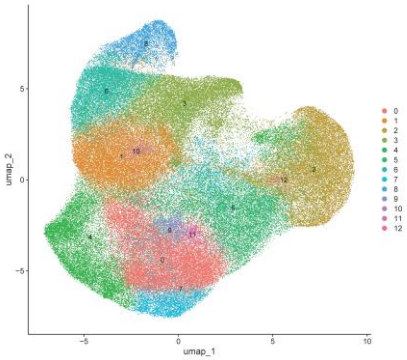

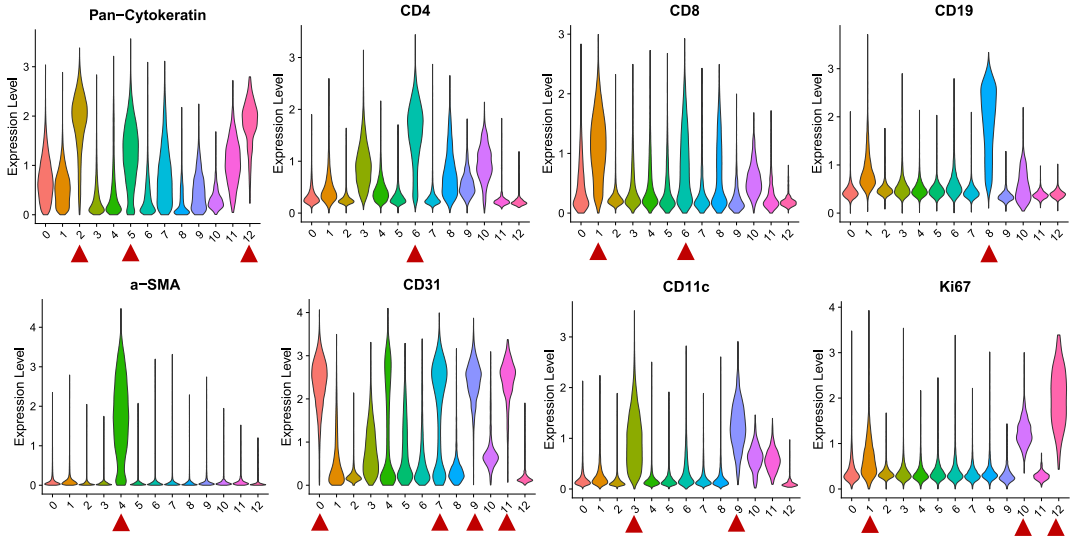

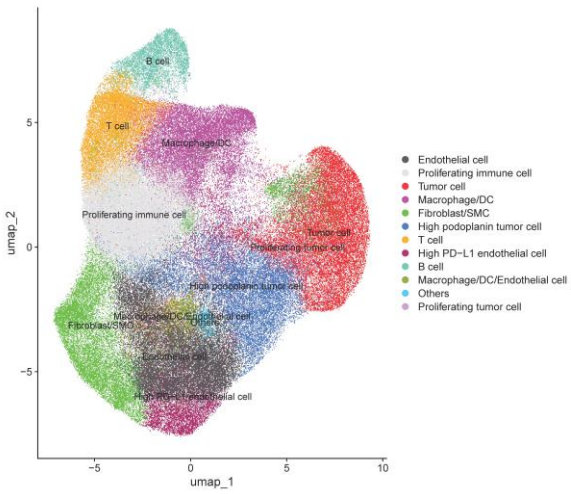

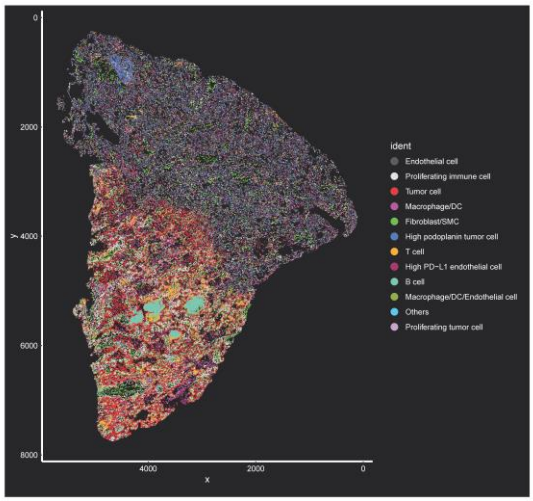

Supplementary Figure S15 Representative images and cell phenotyping results of PhenoCycler data in AIS/MIA cases

(**a–f**) Representative images of PhenoCycler results in the FF sections of AIS and MIA cases: TSU-23, TSU-24, TSU-35, TSU-28, TSU-30, and TSU-31. PhenoCycler signals of DAPI and eight proteins are shown. ROIs were chosen based on their proximity to the "possibly malignant" region or their abundance of proliferative or invasive spots. Each section includes the entire image as well as the ROIs. (**g–o**) Clustering and annotation of PhenoCycler data for cell phenotyping of AIS/MIA cases (TSU-20, TSU-23, TSU-21, TSU-24, TSU-35, TSU-28, TSU-30, TSU-31 and TSU-33). The data from the previous study[6] was used in three cases (TSU-20, TSU-21 and TSU-33). The top panel displays a UMAP plot of the clustering results as well as a table with cell phenotype annotations for each cluster. The table includes the differentially expressed proteins of each cluster (top 3 with log2FC > 0.5; proteins with log2FC > 2 are bold). The middle panel shows violin plots of representative cell type markers. The UMAP and spatial plot with cell phenotyping information are shown in the bottom panel.

TSU-23 (AIS, Noguchi type A)

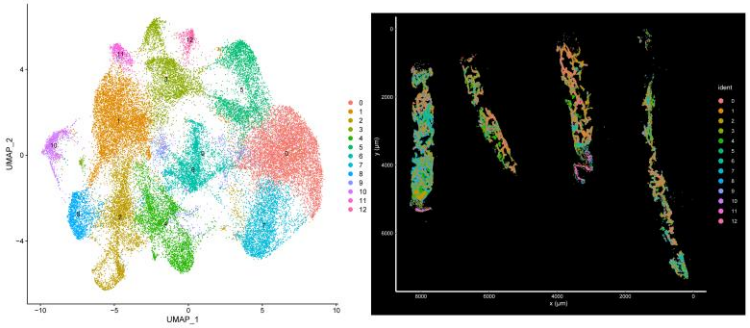

Cluster	Annotation
0	Differentiated tumor cell
1	Fibroblast
2	T cell, B cell
3	Endothelial cell
4	Macrophage
5	Differentiated tumor cell
6	Others
7	Differentiated tumor cell
8	Plasma cell
9	Others
10	Mastocyte
11	VMSC, myofibroblast
12	Artery endothelial cell

TSU-25 (AIS, Noguchi type A)

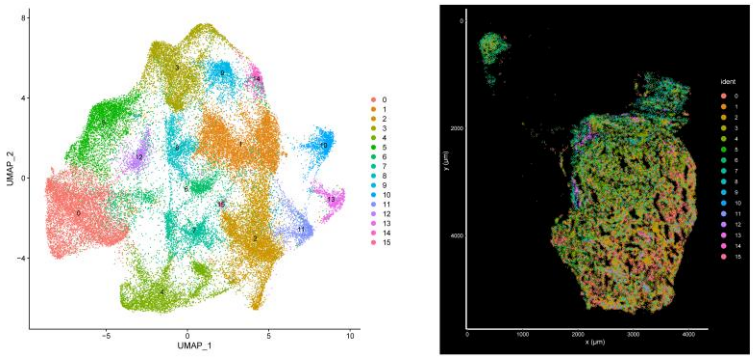

Cluster	Annotation
0	Differentiated tumor cell
1	Fibroblast
2	T cell
3	Endothelial cell
4	Macrophage
5	Differentiated tumor cell
6	Others
7	DC
8	Others (IL6-high)
9	Pericyte
10	Mastocyte
11	Plasma cell
12	Others (AT1, VEGFA-high)
13	LEC
14	VMSC, myofibroblast
15	pDC

TSU-24 (AIS, Noguchi type B)

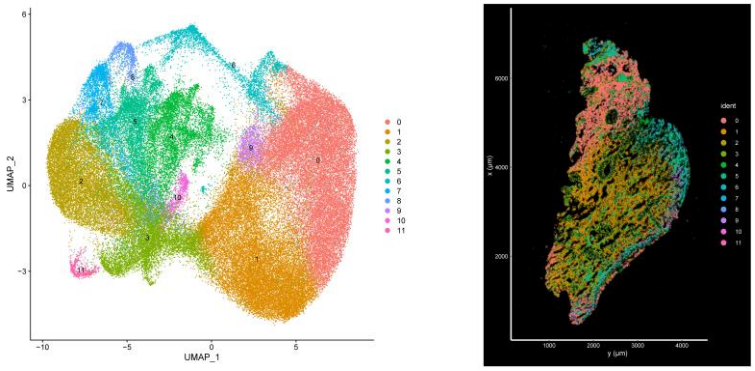

Cluster	Annotation
0	Differentiated tumor cell
1	Differentiated tumor cell
2	Fibroblast
3	Others
4	Macrophage
5	T cell
6	Differentiated tumor cell
7	Endothelial cell
8	Others (IL6-high)
9	IDO1-expressing tumor cell
10	Mastocyte
11	LEC

TSU-35 (AIS, Noguchi type B)

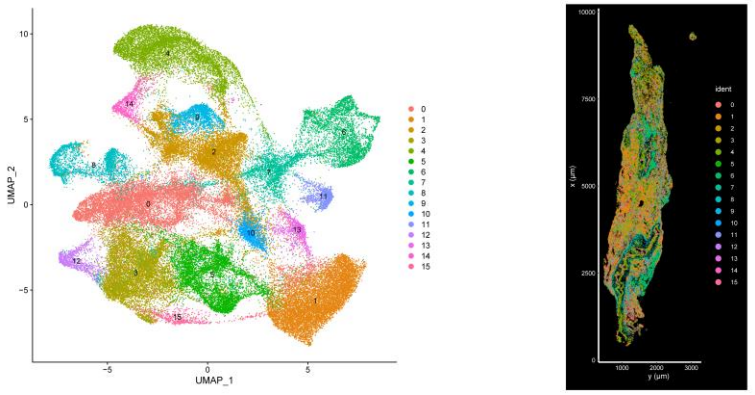

Cluster	Annotation
0	Fibroblast
1	Differentiated tumor cell
2	Endothelial cell
3	T cell
4	VMSC, myofibroblast
5	Macrophage
6	Bronchiolar epithelial cell
7	Bronchiolar epithelial cell
8	LEC
9	Pericyte
10	Differentiated tumor cell
11	Mastocyte
12	Plasma cell
13	Others (AT1, VEGFA-high)
14	Artery endothelial cell
15	CCL22+ DC

TSU-27 (MIA, Noguchi type C)

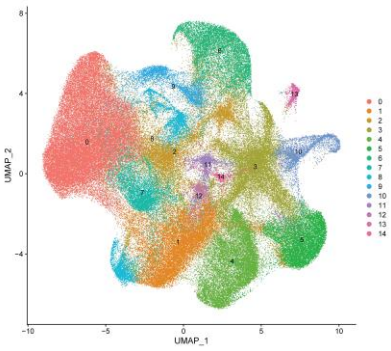

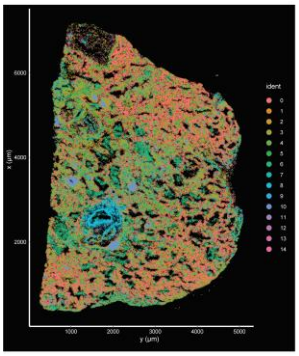

Cluster	Annotation
0	IDO1 expressing tumor cell
1	Fibroblast
2	Others (tumor cell, macrophage)
3	T cell
4	Endothelial cell
5	Plasma cell
6	Macrophage
7	Differentiated tumor cell
8	Bronchiolar epithelial cell
9	CCL22+ DC
10	CXCL13+ B cell
11	Mastocyte
12	Others (IL6 high, iCAF)
13	Fibroblast
14	LEC

TSU-28 (MIA, Noguchi type C)

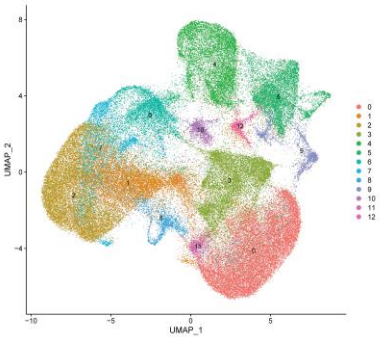

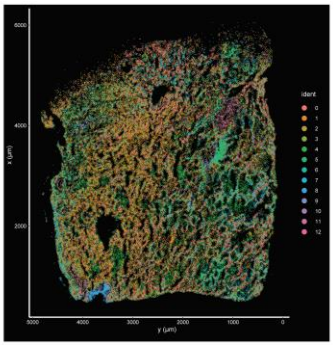

Cluster	Annotation
0	Fibroblast
1	Differentiated tumor cell
2	Differentiated tumor cell
3	Endothelial cell
4	Macrophage
5	T cell
6	Differentiated tumor cell
7	Differentiated tumor cell
8	Bronchiolar epithelial cell
9	LEC
10	Mastocyte
11	VMSC, myofibroblast
12	Plasma cell

TSU-30 (MIA, Noguchi type C)

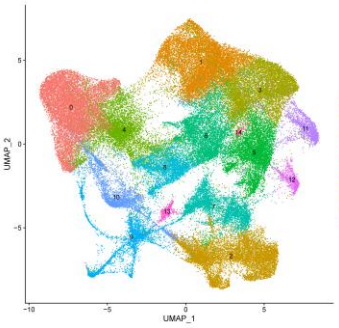

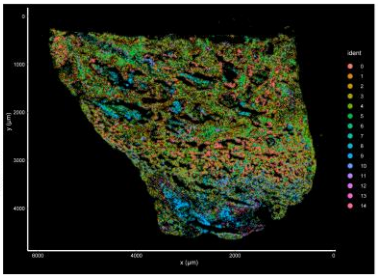

Cluster	Annotation
0	Differentiated tumor cell
1	Fibroblast
2	Endothelial cell
3	Fibroblast
4	Differentiated tumor cell
5	T cell
6	DC, macrophage
7	VMSC, myofibroblast
8	SPP1+ macrophage
9	Bronchiolar epithelial cell
10	Differentiated tumor cell
11	Mastocyte
12	LEC
13	Fibroblast
14	Plasma cell

TSU-33 (MIA, Noguchi type C)

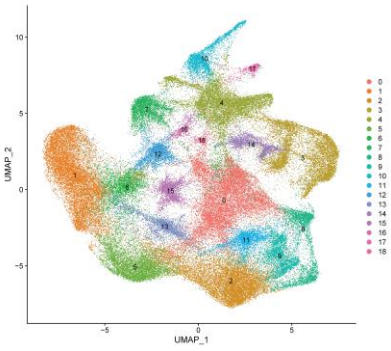

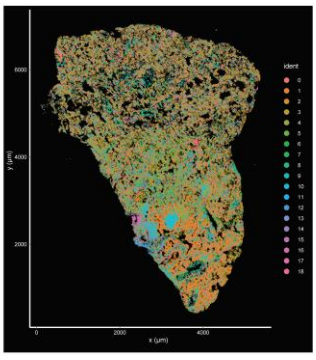

Cluster	Annotation
0	Fibroblast
1	Differentiated tumor cell
2	Endothelial cell
3	Macrophage
4	T cell
5	Differentiated tumor cell
6	Differentiated tumor cell
7	Plasma cell
8	VMSC, myofibroblast
9	Endothelial cell
10	CXCL13+ B cell
11	Pericyte
12	Others
13	Others (AT1, VEGFA-high)
14	DC
15	Mastocyte
16	Bronchiolar epithelial cell
17	LEC
18	pDC

TSU-36 (MIA, Noguchi type C)

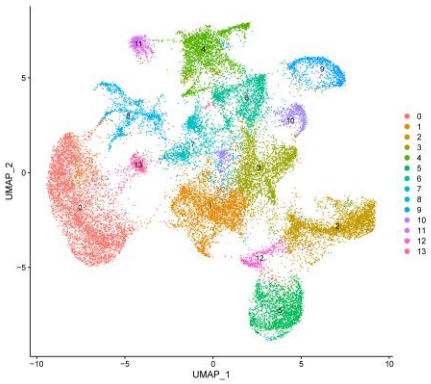

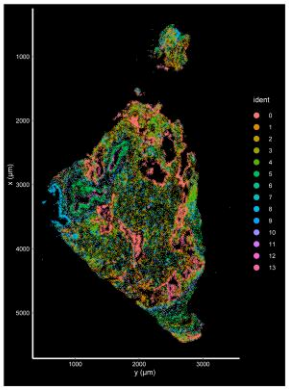

Cluster	Annotation
0	Differentiated tumor cell
1	Fibroblast
2	Endothelial cell
3	Fibroblast
4	T cell
5	VMSC, myofibroblast
6	Macrophage
7	Plasma cell
8	Bronchiolar epithelial cell
9	LEC
10	Fibroblast
11	Mastocyte
12	Artery endothelial cell
13	Macrophage

TSU-41 (MIA, Noguchi type C)

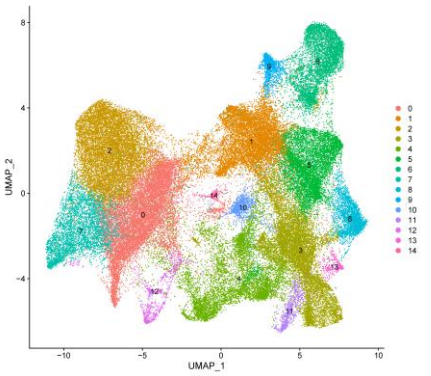

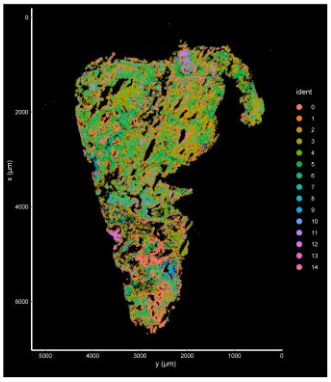

Cluster	Annotation
0	Differentiated tumor cell
1	Fibroblast
2	Differentiated tumor cell
3	T cell
4	Macrophage
5	Fibroblast
6	Endothelial cell
7	Differentiated tumor cell
8	Plasma cell
9	VMSC, myofibroblast
10	Mastocyte
11	CCL22+ immune cell
12	Bronchiolar epithelial cell
13	LEC
14	Fibroblast

Supplementary Figure S16 Spatial and single-cell expression analysis using Xenium for 10 AIS/MIA cases

Clustering results for Xenium of early adenocarcinoma cases. The left and middle panels show the UMAP plot with cluster annotations and the spatial plot, respectively. The annotation for each cluster is shown in the table to the right.

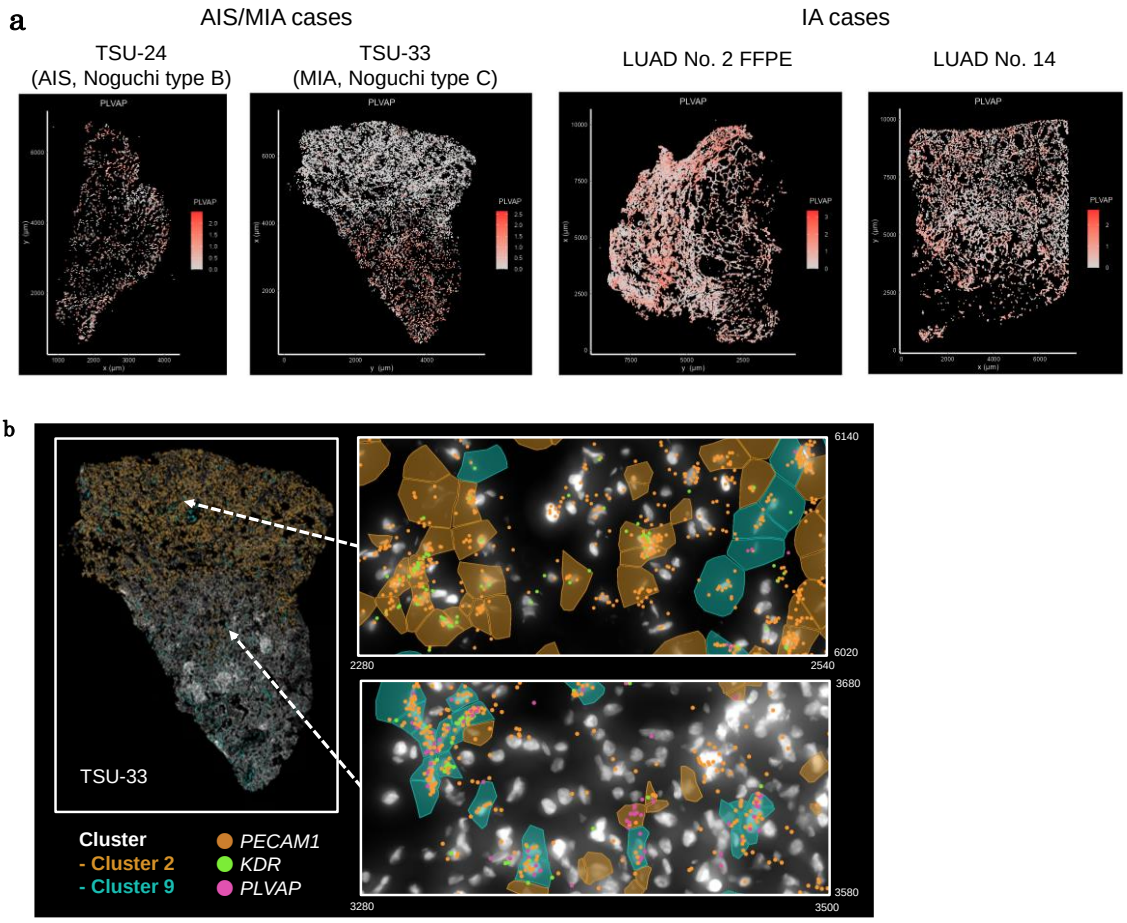

Supplementary Figure S17 Characterization of endothelial cells in Xenium data

(**a**) *PLVAP* expression profiles in Xenium data. Endothelial cell clusters are cluster 7 (TSU-24), clusters 2 and 9 (TSU-33), cluster 3 (LUAD No. 2 FFPE), and cluster 5 (LUAD No. 14), as shown in **Supplementary Figures S9** and **S16**. (**b**) The cluster distribution (left) and spatial expression patterns of endothelial cell markers (right) in Xenium are shown for TSU-33. Plots of RNA molecules of two representative regions are enlarged. The plots were rotated and horizontally flipped to match the orientation of Visium.

Note:

To characterize stromal cell features in AIS/MIA and IA cases in addition to immune cells, we focused on endothelial cell phenotypes. It is reported that endothelial cells would differentiate into three types, in response to angiogenic signals: migratory tip cells for the guide of vessel sprouts, proliferating stalk cells for extending sprouts, and quiescent phalanx cells which are need to line new vessels[7,8]. We focused on expression

patterns of *PLVAP*, which is a common marker of tumor endothelial cells and expressed in immature stalk cells[9]. In TSU-33 which harbors two endothelial cell clusters, cluster 9 showed differentially higher expression of *PLVAP* than cluster 2. Cluster 9 cells are located in more invasive regions (lower parts of the tissue section, including the "possibly malignant-invasive" region) while most of cluster 2 cells are in the top part of the tissue where tumors represented transcriptionally/histologically less malignant features, which indicate that cluster 9 cells might be tumor endothelial cells associated with angiogenesis. However, in other cases, endothelial cells widely expressed *PLVAP*. The results indicate that angiogenesis would occur with tumor endothelial cells and begin from early phases of lung cancer cases. Further evaluation will be needed to extend characterization of endothelial signaling in lung cancer progression.

Supplementary Tables

Supplementary Table S1 Number of spatial omics datasets used in this study

Case	Pathological stage	Smoking history	Driver gene	FF/FFPE	Spatial omics analysis		
					Visium	PhenoCycler	Xenium
IA							
LUAD No. 1	IA3	n	*EGFR*	FF	1	0	0
LUAD No. 2	IIB	y	*KRAS*	FF	1	0	0
				FFPE	4	1	1
LUAD No. 3	IA3	n	*EGFR*	FF	1	0	0
				FFPE	2	1	1
LUAD No. 4	IB	n	*EGFR*	FF	1	0	0
				FFPE	2	1	1
LUAD No. 5	IIB	n	*EGFR*	FF	1	0	0
LUAD No. 14	IVA	y	*KRAS*	FF	1	0	1
LUAD No. 16	IA3	y	*EGFR*	FF	1	0	1
LUAD No. 17	IIIA	n	*EGFR*	FF	1	0	1
AIS, Noguchi type A							
TSU-20	0	n	*MAP2K1*	FF	1 (1)*	(1)*	(1)*
TSU-23	0	n	*EGFR*	FF	1	1	1
TSU-25	0	y	*EGFR*	FF	1	0	1
AIS, Noguchi type B							
TSU-19	0	y	*EGFR*	FF	4	0	0
TSU-21	0	n	*EGFR*	FF	(1)*	(1)*	(1)*
TSU-22	0	y	*EGFR*	FF	1	0	0
TSU-24	0	y	*EGFR*	FF	1	1	1
TSU-26	0	n	*EGFR*	FF	1	0	0
TSU-35	0	n	*EGFR*	FF	1	1	1
MIA, Noguchi type C							
TSU-27	IA1	n	*EGFR*	FF	2	0	1
TSU-28	IA1	n	*EGFR*	FF	2	1	1
TSU-30	IA1	n	*EGFR*	FF	1	1	1
TSU-31	IA1	y	*EGFR*	FF	1	1	0

TSU-32	IA1	y	*EGFR*	FF	1	0	0
TSU-33	IA1	y	*EGFR*	FF	(1)*	(1)*	1
TSU-34	IA1	n	-	FF	1	0	0
TSU-36	IA1	n	*EGFR*	FF	1	0	1
TSU-37	IA1	n	*EGFR*	FF	1	0	0
TSU-38	IA1	n	*EGFR*	FF	1	0	0
TSU-39	IA1	y	*MET*	FF	1	0	0
TSU-40	IA1	n	*EGFR*	FF	1	0	0
TSU-41	IA1	n	*EGFR*	FF	1	0	1

Visium data of LUAD No. 2 FFPE were obtained from four serial sections. Visium data of LUAD No. 3 FFPE, LUAD No. 4 FFPE, TSU-20, TSU-27 and TSU-28 were obtained from two serial sections. Four Visium data of TSU-19 were obtained from the different regions.

*These datasets were previously reported[6].

Note:

For LUAD No. 2, we planned to compare the results of FF and FFPE samples. In some cases, specimens were collected only when either preparation was available. In fact, in Visium analysis, the experimental protocols for FF and FFPE differ significantly. Both procedures have advantages and disadvantages. FFPE has better tissue morphology and histology than FF. However, when it comes to biochemical assays, such as full-length RNA sequencing and epigenome analyses, FF samples are far more suitable. In FFPE samples, RNA is generally degraded, so a probe-based approach is used to capture transcriptome profiles. For another example of the study design, for some specimens, several sections were prepared to test the reproducibility of data collection (using consecutive sections) and the horizontal spread of the profiles (using adjacent sections).

LUAD No. 2 and 3 were initially selected because they have typical driver mutations (*KRAS* and *EGFR*, respectively) and exhibit diverse local expression profiles. Those specimens were then chosen for the PhenoCycler and Xenium analyses because we believed that the interactions between the presumed cell types, based on the marker expression patterns in the Visium analysis, should be confirmed at the single-cell level. For other cases, we prioritized cases with both well-differentiated and malignant expression features that were more heterogeneous. It is also true that, in some cases, we could not conduct a thorough analysis because the remaining tissues had been exhausted (e.g., we had no remaining tissues of LUAD No. 4 FFPE for performing Xenium analysis).

Supplementary Table S2 General statistics of Visium in IA cases

Case	FF/FFPE	Number of spots	Number of reads	Mean reads per spot	Median genes per spot	Median UMI counts per spot	Sequencing saturation
LUAD No. 1	FF	2,649	474,827,182	179,248	4,394	11,803	0.87
LUAD No. 2	FF	2,226	486,607,210	218,602	5,530	18,788	0.87
LUAD No. 3	FF	3,804	472,542,245	124,222	2,579	6,597	0.90
LUAD No. 4	FF	3,854	455,530,400	118,197	2,461	5,174	0.91
LUAD No. 5	FF	4,143	382,522,043	92,330	3,144	7,728	0.84
LUAD No. 14	FF	4,630	417,203,997	90,109	3,263	7,738	0.85
LUAD No. 16	FF	3,640	426,493,578	117,169	2,031	3,937	0.91
LUAD No. 17	FF	2,179	455,397,893	208,994	2,050	5,019	0.94
LUAD No. 2, A	FFPE	2,575	315,922,331	122,688	9,975	59,403	0.48
LUAD No. 2, B	FFPE	3,854	355,786,830	92,316	9,192	42,861	0.49
LUAD No. 2, C	FFPE	4,666	243,622,025	52,212	8,168	31,746	0.32
LUAD No. 2, D	FFPE	4,596	336,240,758	73,159	8,289	32,632	0.37
LUAD No. 3, A	FFPE	2,099	282,276,626	134,481	4,895	10,892	0.88
LUAD No. 3, B	FFPE	2,876	266,006,934	92,492	4,104	8,391	0.84
LUAD No. 4, C	FFPE	3,243	165,416,495	51,007	6,246	17,624	0.54
LUAD No. 4, D	FFPE	2,941	193,834,742	65,908	7,570	25,442	0.54

Supplementary Table S3 General statistics of Visium in AIS/MIA cases

Case	Number of spots	Number of reads	Mean reads per spot	Median genes per spot	Median UMI counts per spot	Sequencing saturation
AIS, Noguchi type A						
TSU-20 #1	737	467,436,361	634,242	3,833	10,021	0.96
TSU-23	638	569,456,998	892,566	3,536	9,510	0.96
TSU-25	1,069	531,049,007	496,772	2,018	3,457	0.98
AIS, Noguchi type B						
TSU-19 a-1	2,256	623,161,699	276,224	2,277	4,355	0.97
TSU-19 a-2	2,526	768,602,464	304,277	1,547	2,597	0.98
TSU-19 b-1	3,083	636,194,448	206,356	1,577	2,872	0.98
TSU-19 b-2	3,519	651,275,192	185,074	1,654	2,852	0.97
TSU-22	764	826,932,037	1,082,372	3,422	10,011	0.99
TSU-24	1,161	599,708,658	516,545	3,587	8,324	0.97
TSU-26	871	666,957,994	765,738	2,389	5,843	0.98
TSU-35	1,024	403,958,649	394,491	2,520	4,687	0.97
MIA, Noguchi type C						
TSU-27 #1	3,046	271,416,110	89,106	2,182	3,977	0.87
TSU-27 #2	2,839	225,147,862	79,305	2,514	5,268	0.86
TSU-28 #1	2,441	405,565,409	166,147	2,627	4,541	0.91
TSU-28 #2	1,834	188,769,395	102,928	2,446	4,315	0.88
TSU-30	1,853	885,669,797	477,965	2,071	4,068	0.98
TSU-31	1,140	553,622,646	485,634	2,886	6,593	0.97
TSU-32	2,288	542,335,550	237,035	1,722	3,380	0.97
TSU-34	1,449	295,738,028	204,098	1,042	1,519	0.97
TSU-36	748	414,866,084	554,634	1,329	2,362	0.99
TSU-37	813	533,601,580	656,337	1,777	3,123	0.99
TSU-38	1,093	726,121,219	664,338	2,009	3,833	0.98
TSU-39	1,662	223,231,157	134,315	2,199	4,086	0.93
TSU-40	2,613	699,359,814	267,646	2,905	6,254	0.96
TSU-41	1,458	753,321,845	516,682	2,358	5,201	0.98

All datasets were obtained from FF samples. Datasets #1 and #2 were derived from serial sections of the same block. Data a-1, a-2, b-1, and b-2 of TSU-19 were obtained from

different tissue regions. The quality of TSU-23 (needle biopsy) data apperars to be lower, as only 49.2% of reads were assigned to tissue-covered spots.
Data from three sections, TSU-20 (#2), TSU-21, and TSU-33, were previously published[6].

Supplementary Table S4 General information of PhenoCycler for FFPE samples of IA cases

(a) List of antibodies, barcodes, and reporters

PhenoCycler inventories

Molecule	Conjugated-antibody catalog number	Clone	Barcode	Fluorescence
CD31	4450017	EP3095	BX001	AF750
CD20	4450018	L26	BX007	AF750
beta-actin	4450040	W16197A	BX010	AF750
Pan-Cytokeratin	4450020	AE-1/AE-3	BX019	AF750
CD44	4450041	IM7	BX005	Atto 550
E-cadherin	4250021	4A2C7	BX014	Atto 550
CD45RO	4250023	UCHL1	BX017	Atto 550
ß-catenin1	4450036	12F7	BX020	Atto 550
Podoplanin	4250004	NC-08	BX023	Atto 550
CD8	4250012	C8/144B	BX026	Atto 550
Mac2/Galectin-3	4450034	M3/38	BX035	Atto 550
Ki67	4250019	B56	BX047	Atto 550
CD4	4550112	EPR6855	BX003	Cy5 / AF647
LIF	4550120	M1506B09	BX006	Cy5 / AF647
CD68	4550113	KP1	BX015	Cy5 / AF647
CD11c	4550114	118/A5	BX024	Cy5 / AF647
IDO1	4550123	V1NC3IDO	BX027	Cy5 / AF647
CD3e	4550119	EP449E	BX045	Cy5 / AF647

Custom conjugated

Molecule	Antibody catalog number	Clone	Barcode	Fluorescence
α-SMA/ACTA2	ab7817 (Abcam)	1A4	BX004	AF750
Collagen-IV	ab226485 (Abcam)	EPR20966	BX013	AF750
HLA-A	ab216653 (Abcam)	EP1395Y	BX016	AF750
HLA-DPB1	ab215973 (Abcam)	EPR11226	BX022	AF750
TP53	554169 (BD Pharmingen)	Pab 1801	BX025	AF750
CD163	ab213612 (Abcam)	EPR19518	BX028	AF750
CD278/ICOS	ab236226 (Abcam)	SP98	BX031	AF750
TIGIT	ab243903 (Abcam)	BLR047F	BX037	AF750
DC-LAMP	DDX0191P-100 (Eurobio)	1010E1.01	BX029	Atto 550

CD274/PD-L1	ab228413 (Abcam)	28-8	BX041	Atto 550
FOXP3	14-4777-82 (Invitrogen)	236A/E7	BX052	Atto 550
CD56	ab214435 (Abcam)	EP2567Y	BX055	Atto 550
CD223/LAG3	#15372 (CST)	D2G4O	BX021	Cy5 / AF647
BCA1/CXCL13	ab270408 (Abcam)	EPR23400-92	BX030	Cy5 / AF647
CTLA4	NB100-64849 (Novus)	BNI3	BX033	Cy5 / AF647
TTF-1/NKX2-1	ab212886 (Abcam)	8G7G3/1	BX042	Cy5 / AF647
CD279/PD-1	ab186928 (Abcam)	EPR4877(2)	BX054	Cy5 / AF647

(b) Run design

Cycle	DAPI	Atto 550		Cy5/AF647		AF750	
		Reporter No.	Molecule	Reporter No.	Molecule	Reporter No.	Molecule
1	DAPI	Blank	—	Blank	—	Blank	—
2	DAPI	RX005	CD44	RX003	CD4	RX001	CD31
3	DAPI	RX014	E-cadherin	RX006	LIF	RX004	α-SMA/ACTA2
4	DAPI	RX017	CD45RO	RX015	CD68	RX007	CD20
5	DAPI	RX020	ß-Catenin1	RX021	CD223/LAG3	RX010	Beta-actin
6	DAPI	RX023	Podoplanin	RX024	CD11c	RX013	Collagen-IV
7	DAPI	RX026	CD8	RX027	IDO1	RX016	HLA-A
8	DAPI	RX029	DC-LAMP	RX030	BCA1/CXCL13	RX019	Pan-Cytokeratin
9	DAPI	RX035	Mac2/Galectin-3	RX033	CTLA4	RX022	HLA-DPB1
10	DAPI	RX041	CD274/PD-L1	RX042	TTF-1/NKX2-1	RX025	TP53
11	DAPI	RX047	Ki67	RX045	CD3e	RX028	CD163
12	DAPI	RX052	FOXP3	RX054	CD279/PD-1	RX031	CD278/ICOS
13	DAPI	RX055	CD56	Empty	—	RX037	TIGIT
14	DAPI	Blank	—	Blank	—	Blank	—

Supplementary Table S5 General information of PhenoCycler for FF samples of AIS/MIA cases

(a) List of antibodies, barcodes, and reporters

PhenoCycler inventoried					Run set*	
Molecule	Conjugated-antibody catalog number	Clone	Barcode	Florescence	Set #1	Set #2
CD19	4550099	HIB19	BX003	AF647	y	y
CD8	4150004	SK1	BX004	AF488	y	y
CD279/PD-1	4250010	EH12.2H7	BX014	Atto 550	y	y
CD68	4350019	KP1	BX015	Cy5		y
CD45RO	4250023	UCHL1	BX017	Atto 550	y	y
Pan-Cytokeratin	4150020	AE-1/AE-3	BX019	AF488	y	y
CD4	4350010	SK3	BX021	Cy5	y	y
Podoplanin	4250004	NC-08	BX023	Atto 550	y	y
CD11c	4550107	S-HCL-3	BX027	AF647	y	y
CD31	4250009	WM59	BX032	Atto 550	y	y
Mac2/Galectin-3	4450034	M3/38	BX035	Atto 550		y
Ki67	4250019	B56	BX047	Atto 550	y	y
Custom					Run set	
Molecule	Antibody catalog number	Clone	Barcode	Florescence	Set #1	Set #2
TP53	554169 (BD Pharmingen)	Pab 1801	BX025	AF488	y	y
CD163	ab213612 (Abcam)	EPR19518	BX028	AF488	y	y
BCA1/CXCL13	ab270408 (Abcam)	EPR23400-92	BX030	Cy5		y
CTLA4	NB100-64849 (Novus Biologicals)	BNI3	BX033	Cy5		y
CD274/PD-L1	ab228413 (Abcam)	28-8	BX041	Atto 550		y
TTF-1/NKX2-1	ab242428 (Abcam)	SP141	BX050	AF647	y	y
FOXP3	#14-4777-82 (Invitrogen)	236A/E7	BX052	Atto 550	y	y
α-SMA/ACTA2	ab7817 (Abcam)	1A4	BX054	Cy5	y	y
CD56/NCAM1	ab214435 (Abcam)	EP2567Y	BX055	Atto 550		y

Run set #1 was used for TSU-23, TSU-28, and TSU-31. Run set #2 was used for TSU-24, TSU-30, and TSU-35.

(b) Run design for set #1

Cycle	DAPI	Atto 550		Cy5/AF647		AF488	
		Reporter No.	Molecule	Reporter No.	Molecule	Reporter No.	Molecule
1	DAPI	Blank	---	Blank	---	Blank	---
2	DAPI	RX014	CD279/PD-1	RX003	CD19	RX004	CD8
3	DAPI	RX017	CD45RO	RX021	CD4	RX019	Pan-Cytokeratin
4	DAPI	RX023	Podoplanin	RX027	CD11c	RX025	TP53
5	DAPI	RX032	CD31	RX050	TTF-1/NKX2-1	BX028	CD163
6	DAPI	RX047	Ki67	RX054	α-SMA/ACTA2	Empty	---
7	DAPI	RX052	FOXP3	Empty	---	Empty	---
8	DAPI	Blank	---	Blank	---	Blank	---

(c) Run design for set #2

Cycle	DAPI	Atto 550		Cy5/AF647		AF488	
		Reporter No.	Molecule	Reporter No.	Molecule	Reporter No.	Molecule
1	DAPI	Blank	---	Blank	---	Blank	---
2	DAPI	RX014	CD279/PD-1	RX003	CD19	RX004	CD8
3	DAPI	RX017	CD45RO	BX015	CD68	RX019	Pan-Cytokeratin
4	DAPI	RX023	Podoplanin	RX021	CD4	RX025	TP53
5	DAPI	RX032	CD31	RX027	CD11c	BX028	CD163
6	DAPI	BX035	Mac2/Galectin-3	BX030	BCA1/CXCL13	Empty	---
7	DAPI	BX041	CD274/PD-L1	BX033	CTLA4	Empty	---
8	DAPI	RX047	Ki67	RX050	TTF-1/NKX2-1	Empty	---
9	DAPI	RX052	FOXP3	RX054	α-SMA/ACTA2	Empty	---
10	DAPI	BX055	CD56/NCAM1	Empty	---	Empty	---
11	DAPI	Blank	---	Blank	---	Blank	---

Supplementary Table S6 General statistics of Xenium in IA cases

Case	Region area (μm²)	Total cell area (μm²)	Fraction of transcripts decoded q20	Decoded transcripts per 100 μm²	Number of cells detected	Median genes per cell	Median transcripts per cell
LUAD No. 2 (FFPE)	74,526,696	51,690,317	0.87	161.6	472,420	53	152
LUAD No. 3 (FFPE)	40,266,013	22,894,703	0.81	53.1	150,055	31	50
LUAD No. 14 (FF)	69,333,431	48,584,499	0.75	89.7	309,940	45	102
LUAD No. 16 (FF)	46,729,502	35,272,599	0.85	96	294,386	36	75
LUAD No. 17 (FF)	32,817,217	17,305,433	0.79	79.1	96,749	41	107

Supplementary Table S7 General statistics of Xenium in AIS/MIA cases

	Region area (μm²)	Total cell area (μm²)	Fraction of transcripts decoded q20	Decoded transcripts per 100 μm²	Number of cells detected	Median genes per cell	Median transcripts per cell
AIS, Noguchi type A							
TSU-23	27,551,678	5,836,253	0.80	92.9	38,219	45	112
TSU-25	17,612,095	8,171,814	0.79	108.5	48,942	52	148
AIS, Noguchi type B							
TSU-24	22,792,052	11,220,056	0.80	91.1	91,457	37	87
TSU-35	20,302,622	9,640,210	0.82	108.7	67,699	50	136
MIA, Noguchi type C							
TSU-27	33,728,086	23,518,171	0.79	159.3	173,219	61	180
TSU-28	28,900,204	19,153,553	0.85	68.8	104,968	39	88
TSU-30	23,686,133	14,794,324	0.83	89.3	84,611	46	132
TSU-33	30,232,430	18,764,465	0.81	62.2	100,199	43	97
TSU-36	13,673,489	5,616,139	0.83	48.0	26,817	33	82
TSU-41	21,550,217	11,274,866	0.82	114.9	74,186	52	146

All datasets were obtained from FF samples.

Data from two sections, TSU-20 and TSU-21, were previously reported[6].

Supplementary Table S8 List of genes and parameters for calculating TME scores and evaluation of their changes

(a) Signature genes for tumor cells

Cell type (epithelial/tumor)	Gene
Well-differentiated	*CAPS*, *SNTN*, *HOPX*, *SFTPC*, *SFTPB*, *SCGB3A2*, *NAPSA*, *SCGB1A1*, *SCGB3A1*, *SFTPA1*, *CLDN18*
Proliferative	*WEE1, FOS*, *FOSB*
Invasive	*SPINK1*, *MMP7*, *CXCL14*, *S100A6*, *TGFBI*, *TNC*

(b) Signature genes for the microenvironment

Cell type	Gene
Immune-rich (plasma cell)	*IGKC, IGHG1, IGHA1, JCHAIN*, *IGHG2*, *IGLC1*, *CRISPLD2*, *IGKV4-1*, *IGHM*, *IGHG3*, *IGHD*, *IGKV4-1*, *IGLC1*, *IGHG4*
B cell	*CD79A, CD79B*, *MS4A1*, *CXCR4*
T cell	*CD2*, *CD3D*, *CD3E*, *CD3G*, *CD8A*, *CD4*
Fibroblast/CAF	*DCN, COL1A1*, *COL1A2*, *ACTA2*, *MYH11*
Endothelial cell	*CLDN5, PECAM1*, *VWF*, *AQP1*
M1 Macrophage	*CD68, CXCL9*, *APOE*
M2 Macrophage (anti-inflammatory)	*CD163*, *C1QC*, *SPP1*

(c) Parameters for extracting the regions with TME changes

Trajectory path	Cluster path	Slope threshold	Regions with TME change	
			All	Overlap
LUAD No. 2, B (FFPE)	8 -> 1 -> 2 -> 3 -> 0 -> 10 -> 4	0.02	10	5
LUAD No. 2, C (FFPE)	8 -> 1 -> 2 -> 3 -> 0 -> 10 -> 4	0.02	10	5
LUAD No. 3, B (FFPE) P1	9 -> 6 -> 3	0.04	4	4
LUAD No. 3, B (FFPE) P2	9 -> 10	0.03	3	3
LUAD No. 14 P1	4 -> 5 -> 8 -> 10 -> 13 -> 0 -> 15	0.02	10	5
LUAD No. 14 P2	4 -> 5 -> 0 -> 15	0.02	10	5
LUAD No. 14 P3	14 -> 11 -> 2 -> 12 -> 6	0.045	5	5
LUAD No. 16	9 -> 7 -> 10	0.035	5	5

Supplementary References

1. Gu, Z., Eils, R. & Schlesner, M. Complex heatmaps reveal patterns and correlations in multidimensional genomic data. *Bioinformatics* **32**, 2847–2849 (2016).
2. Jin, S. *et al.* Inference and analysis of cell-cell communication using CellChat. *Nat. Commun.* **12**, 1088 (2021).
3. Dries, R. *et al.* Giotto: a toolbox for integrative analysis and visualization of spatial expression data. *Genome Biol.* **22**, 78 (2021).
4. Miller, B. F., Huang, F., Atta, L., Sahoo, A. & Fan, J. Reference-free cell type deconvolution of multi-cellular pixel-resolution spatially resolved transcriptomics data. *Nat. Commun.* **13**, 2339 (2022).
5. Zhou, Y. *et al.* Metascape provides a biologist-oriented resource for the analysis of systems-level datasets. *Nat. Commun.* **10**, 1523 (2019).
6. Haga, Y. *et al.* Whole-genome sequencing reveals the molecular implications of the stepwise progression of lung adenocarcinoma. *Nat. Commun.* **14**, 8375 (2023).
7. Zeng, Q. *et al.* Understanding tumour endothelial cell heterogeneity and function from single-cell omics. *Nat. Rev. Cancer* **23**, 544–564 (2023).
8. Korn, C. & Augustin, H. G. Mechanisms of Vessel Pruning and Regression. *Dev. Cell* **34**, 5–17 (2015).
9. Goveia, J. *et al.* An Integrated Gene Expression Landscape Profiling Approach to Identify Lung Tumor Endothelial Cell Heterogeneity and Angiogenic Candidates. *Cancer Cell* **37**, 21-36.e13 (2020).